

**Interactions between soil-water dynamics and hardwood  
floodplain forest in the lower middle Elbe river – Germany**

Dissertation

with the aim of achieving a doctoral degree

at the Faculty of Mathematics, Informatics and Natural Sciences

Department of Earth System Sciences

at Universität Hamburg

submitted by

Lizeth K. Vásconez Navas

Hamburg, 2023

Department of Earth System Sciences

Date of Oral Defense:

12.07.2023

Reviewers:

Prof. Dr. Annette Eschenbach

Prof. Dr. Kai Jensen

Members of the examination commission:

Prof. Dr. Annette Eschenbach

Prof. Dr. Kai Jensen

Dr. Joscha Becker

Prof. Dr. Gerhard Schmiedl

Prof. Dr. Uwe Schneider

Chair of the Subject Doctoral Committee

Earth System Sciences:

Prof. Dr. Herman Held

Dean of MIN Faculty:

Prof. Dr.-Ing. Norbert Ritter

# Table of Contents

List of Figures .....	v
List of Tables .....	vii
Journal Articles and Manuscripts under review / in preparation.....	viii
Summary .....	10
Zusammenfassung .....	13
Chapter 1 .....	17
1.1 Introduction.....	17
1.2 Background .....	18
1.2.1 Floodplains and floodplain forests in Germany and in the Elbe Catchment. .....	18
1.2.2 Floodplain geomorphology and soil properties, relevance for restoration.	19
1.2.3 Soil hydrology, drought and forest interactions .....	21
1.3 Objectives, research questions and study significance .....	22
Chapter 2.....	24
Article 1: Are active and former floodplain soils of the lower middle Elbe similar? A study of soil characteristics and possible implications for forest restoration .....	24
2.1 Abstract .....	24
2.2 Introduction.....	25
2.3 Methodology .....	28
2.3.1 Research area and plot selection.....	28
2.3.2 Lateral distance to the and river and flooding days per year .....	30
2.3.3 Soil survey and sampling .....	31
2.3.4 Soil laboratory analyses .....	31
2.3.5 Statistical analyses.....	33
2.4 Results .....	34
2.4.1 Soil classification and soil forming processes .....	34
2.4.2 Variability of topsoil physicochemical properties among HGUs.....	36
2.4.3 Correlation analyses between physicochemical variables .....	40
2.4.4 Physicochemical interactions within the hydrological gradient .....	41
2.5 Discussion .....	43
2.5.1 Distribution of soil types, formation processes and properties per HGU ...	43
2.5.2 Influence of the hydrological processes (e.g. flooding days, lateral distance to the river) on soil physicochemical properties. ....	47
2.5.3 Interactions between soils physicochemical properties .....	49
2.5.4 Implications for hardwood floodplain forest restoration and potential for replicability at the regional scale. ....	50

2.6 Conclusions.....	51
Chapter 3.....	53
Article 2: Sap flow velocity under drought and high evaporative demand: A comparison of two hardwood floodplain forest species under different soil conditions .....	53
3.1 Abstract .....	53
3.2 Introduction.....	55
3.3 Methodology .....	58
3.3.1 Research area and forest selection.....	58
3.3.2 Soil sampling and instrumentation. ....	59
3.3.3 Soil water data analyses .....	60
3.3.4 Meteorological data and study period selection .....	61
3.3.5 Tree selection, tree xylem instrumentation and sap velocity calculation ...	61
3.3.6 Jarvis - Potential sap flow velocity model.....	64
3.3.7 Statistical analyses and data processing .....	65
3.4 Results .....	66
3.4.1 Meteorological data and soil hydrology data .....	66
3.4.2 Differences of mean daytime sap flow velocity, the influence of site conditions, month and species .....	67
3.4.3 Modeled hourly sap flow velocity.....	69
3.4.4 Ratio between measured and modeled $V_h$ and the relation to $\Psi$ .....	71
3.5 Discussion.....	73
3.5.1 Differences of daytime sap flow velocity between species daytime sap velocity of <i>U. laevis</i> higher than <i>Q. robur</i> . ....	73
4.2 Effect of site conditions (soil substrate) and soil water potential .....	75
3.6 Conclusions.....	76
Chapter 4.....	78
Synthesis, conclusions and outlook.....	78
4.1 Synthesis and summary of results.....	78
4.2 Conclusions and Outlook .....	83
References .....	85
Appendix.....	94
5.1 Appendix Article I .....	94
5.2 Appendix Article II .....	101
Acknowledgements .....	111

## List of Figures

- Figure 1. Active floodplain forest site in Wittenberge, Brandenburg. .... 19
- Figure 2. Scheme of the lateral gradient of the floodplain including four hydrogeomorphic units: Active floodplain low (AL), Active floodplain high (AH), Former floodplain seepage (FS) and, Former floodplain disconnected (FD)..... 21
- Figure 3. Study area and selected study plots. AL active floodplain, low; AH active floodplain, high; FS former floodplain, seepage influence; FD former floodplain, disconnected from the river hydrology. Longitude-Latitude coordinates of every plot can be found in Appendix E..... 29
- Figure 4. Dominating soil reference group per HGU and soil texture distribution per horizon. AL active floodplain, low; AH active floodplain, high; FS former floodplain, seepage influence; FD former floodplain, disconnected from the river hydrology..... 34
- Figure 5. First depth of appearance of hydromorphic characteristics (HCD) in every hydrogeomorphic unit (HGU). Boxplots that do not share the same letter have significant different means ( $p < 0.05$ ). Active floodplain -Low (AL), Active floodplain-High (AH), Former floodplain- seepage influenced (FS), Former floodplain – disconnected from the river hydrology (FD). Boxes and whiskers represent the 1x and 1.5x interquartile range, black strips median, and rhombus the mean. Black dots denote potential extreme values. White and yellow dots denote single observations, soil drillings and soil pits, respectively..... 36
- Figure 6. NMDS ordination plot including all studied parameters in the topsoil mineral layer. Points denote plots and the polygons the respective HGU. Vectors denote each physicochemical property and how it is tending to a HGU. Distance= Bray Curtis,  $k=2$ , stress = 0.062. HGU- hydrogeomorphic unit: Active floodplain -Low (AL), Active floodplain-High (AH), Former floodplain- seepage influenced (FS), Former floodplain – disconnected from the river hydrology (FD). TN (total Nitrogen), TC (total Carbon), CEC (cation exchange capacity), C/N (C/N ratio),  $Mg^{2+} - K^+ - Ca^{2+} - Na^+$  (Magnesium, Potassium, Calcium and Sodium base cations, respectively),  $K_{sol}$  (soluble Potassium),  $P_{sol}$  (soluble Phosphorus), BS (Base saturation). LDR (lateral distance to the river), HCD (hydromorphic characteristics starting depth) ..... 37
- Figure 8. Correlation network plot (spearman correlation), minimum correlation =0.3, p level  $\leq 0.05$  for all measured physicochemical and hydrological variables in the mineral topsoil (blue positive correlations; red negative correlations). TN (total Nitrogen), TC (total Carbon), CEC (cation exchange capacity), C/N (C/N ratio),  $Mg^{2+} - K^+ - Ca^{2+} - Na^+$  (Magnesium, Potassium, Calcium and Sodium base cations, respectively),  $K_{sol}$  (soluble Potassium),  $P_{sol}$  (soluble Phosphorus), BS (Base saturation). LDR (lateral distance to the river), HCD (hydromorphic characteristics starting depth) ..... 40
- Figure 9. Regression analysis between the starting depth of appearance of hydromorphic characteristics (HCD) and (a) C/N ratio, (b)  $P_{sol}$ , (c) pH and the effect of

pH on (d)  $P_{\text{sol}}$  Linear regression line and R2 is only showed for significant regressions ( $p < 0.05$ ). HGU-Hydrogeomorphic Unit: Active floodplain-Low (AL), Active floodplain-High (AH), Former floodplain- seepage influenced (FS), Former floodplain – disconnected from the river hydrology (FD)..... 41

Figure 11. Location of the sandy (Lat=53.1796°, Long=11.0087°, Elbe km 526) and loamy (Lat=53.0877°, Long=11.2945°, Elbe km 498) study sites in the active floodplain of the lower middle Elbe. .... 59

Figure 12. Proposed curves of sap velocity with increasing sapwood depth for *Quercus robur* (oak) and *Ulmus Laevis* (elm). .... 63

Figure 13 Differences between mean daytime sap flow velocities ( $V_h$ ) of *Quercus robur* and *Ulmus laevis* in loamy and sandy soils under periods of high and low water availability. Boxes and whiskers represent the 1x and 1.5x interquartile range, strips median. Letters represent significant differences between groups ( $p < 0.05$ ). The table result of the Imem is presented in Appendix E..... 67

Figure 14 Daily mean of daytime sap flow velocity ( $V_h$ ) of *Quercus robur* and *Ulmus laevis* under periods of high and low water availability in a loamy (upper row) and sandy (lower row) site. Boxes and whiskers represent the 1x and 1.5x interquartile range, black strips median. Every box ( $n \approx 15$  working sensors per species in hourly intervals between 4 am and 9 pm)..... 68

Figure 15. Modeled  $V_h$  (black lines) and measured  $V_h$  for *Quercus robur* (blue lines, left column) and *Ulmus laevis* (green lines, right colum) in the loamy site under periods of high water availability (above row) and low water availability (below row)..... 69

Figure 16. Modeled  $V_h$  (black lines) and measured  $V_h$  for *Quercus robur* (blue lines, left column) and *Ulmus laevis* (green lines, right colum) in the sandy site under periods of high water availability (above row) and low water availability (below row)..... 70

Figure 17. Relationship between the daily means of measured and modeled daytime sap flow velocities ( $V_{h_{\text{measured}}}/V_{h_{\text{modeled}}}$ ) of *Quercus robur* and *Ulmus laevis* and the daily weighted mean soil water potentials under periods of high and low water availability in the a) loamy site and b) sandy site..... 71

## List of Tables

Table 1. Characteristics of the hydrogeomorphic units (HGUs).....	30
Table 2. Statistical summary of daytime micrometeorology and weighted means (160 cm – 3 soil profiles) of soil volumetric water content $\Theta$ and water tension $\Psi$ during 7 days in June (21.-27.) and 7 days in August (6.-12.), representing periods of high and low water availability respectively. ....	66
Table 3. Multiple linear regression model, summary results for the best-fit model explaining Sap flow velocity of the Elms. ....	73

## Journal Articles and Manuscripts under review / in preparation

**Vásconez Navas, L.K.**, Becker, J.N., Heger, A., Gröngröft, A. Eschenbach, A., (2023) *Are active and former floodplain soils of the lower middle Elbe similar? A study of soil characteristics and possible implications for forest restoration.* *Catena*, 222. <https://doi.org/10.1016/j.catena.2022.106814>

Author contributions: Lizeth K. Vásconez: Conceptualization; Field work; Methodology; Software; Data curation; Formal analysis; Validation; Visualization; Investigation; Writing – original draft. Joscha N. Becker: Supervision; Conceptualization; Methodology; Validation; Formal analysis; Writing – review and editing. Adrian Heger: Conceptualization; field work; data curation; review and editing. Alex Gröngröft: Conceptualization; review and editing; Annette Eschenbach: Supervision; Conceptualization; Writing – review and editing; Validation.

**Vásconez Navas, L.K.**, Busch, H., Thomsen, S., Becker, J.N., Kleinschmidt, V., Gröngröft, A. Eschenbach, A., (under review) *Sap flow velocity under drought and high evaporative demand: a comparison of two hardwood floodplain forest species under different soil conditions.* Under review at *Journal Science of the Total Environment*

Author contributions: Lizeth K. Vásconez: Conceptualization; Field work; Methodology; Software; Data curation; Formal analyses; Validation; Visualization; Investigation; Writing – original draft. Henrik Busch: Field work; Software; Data curation; Formal analysis; Visualization; Investigation; Writing. Simon Thomsen: Conceptualization; Field work; Methodology; Sensor design; Software; Data curation; review and editing. Joscha N. Becker: Supervision; Validation; Formal analyses; Writing – review and editing. Volker Kleinschmidt: Field work; Software; review and editing. Alex Gröngröft: Conceptualization; review and editing; Annette Eschenbach: Supervision; Conceptualization; Writing – review and editing; Validation.

### *Co-authorships within the MediAN project:*

Heger, A., Becker, J. N., **Vásconez Navas, L. K.**, Eschenbach, A. (2021). *Factors controlling soil organic carbon stocks in hardwood floodplain forests of the lower middle Elbe River.* *Geoderma*, 404. <https://doi.org/10.1016/j.geoderma.2021.115389>.

Author contributions: Adrian Heger: Conceptualization; Methodology; Software; Data curation; Formal analysis; Validation; Visualization; Investigation; Writing – original draft. Joscha N. Becker: Conceptualization; Methodology; Validation; Formal analysis; Writing – review and editing. Lizeth K. Vásconez: Conceptualization; Writing – review and editing; Methodology; Formal analysis; Investigation. Annette Eschenbach: Supervision; Conceptualization; Writing – review and editing; Validation.

Heger, A., Becker, J. N., **Vásconez Navas, L. K.**, Eschenbach, A. (under review). *Drivers for soil organic carbon stabilization in Elbe River floodplains.* Under review at *Journal of Plant Nutrition and Soil Science*



Author contributions: Adrian Heger: Conceptualization; Methodology; Software; Data curation; Formal analysis; Validation; Visualization; Investigation; Writing – original draft. Joscha N. Becker: Conceptualization; Methodology; Validation; Formal analysis; Writing – review and editing. Lizeth K. Vásconez: Writing – review and editing. Annette Eschenbach: Supervision; Conceptualization; Writing – review and editing; Validation.

Leonova, A., Heger, A., **Vásconez Navas, L.K.**, Jensen, K., Reisdorff, C., (2022) Fine root mortality under severe drought reflects different root distribution of *Quercus robur* and *Ulmus laevis* trees in hardwood floodplain forests. *Trees* 36, 1105–1115 (2022). <https://doi.org/10.1007/s00468-022-02275-3>

- Author contributions: Anastasia Leonova: Field work; Fine root analysis; Writing original draft; Adrian Heger and Lizeth K.Vásconez: Soil hydrology analyses; Kai Jensen and Christoph Reisdorff provided the conceptual framework of the study; supervised the data analysis and worked on the manuscript.

Heger, A., Becker, J. N., **Vásconez Navas, L. K.**, Holl, D., Eschenbach, A. (2022). *Soil texture and pH affect soil CO<sub>2</sub> efflux in hardwood floodplain forests of the lower middle Elbe River*. *Eur J Soil Sci*, 74(1). <https://doi.org/10.1016/74.10.1111/ejss.13331>.

Author contributions: Adrian Heger: Conceptualization; Methodology; Software; Data curation; Formal analysis; Validation; Visualization; Investigation; Writing – original draft. Joscha N. Becker: Conceptualization; Methodology; Validation; Formal analysis; Writing – review and editing. Lizeth K. Vásconez: Writing – review and editing; Methodology; Formal analysis; Data curation. David Holl: Writing – review and editing. Annette Eschenbach: Supervision; Conceptualization; Writing – review and editing; Validation.

## Summary

Hardwood floodplain forests are one of the most biodiverse and productive ecosystems in Central Europe. They provide important ecosystem services as nature habitat, flood retention, runoff regulation, carbon storage, recreation and others. At the same time, they have been under threat since hundreds of years due to anthropogenic activities such as river channelization, diking and land use change to agricultural and grazing lands. Furthermore, recent and future effects of climate change comprise increased and more frequent droughts. They interfere with regular hydrologic fluctuations in hardwood floodplain forests, which are highly sensitive and dependent on the connection to the river hydrology. Processes specific to floodplains, like active sedimentation and groundwater fluctuations contribute to topographic and soil heterogeneity in this ecosystem. Soils play a pivotal role for the functioning and productivity of hardwood floodplain forests, as they regulate nutrient and water availability and contribute to the storage and stabilization of soil organic carbon. The overarching aim of this thesis is to understand how the heterogeneity of the floodplain landscape influences soil nutrient distribution and soil water availability, and analyze how these factors influence forest processes and productivity. Two different studies were conducted to achieve this aim.

In the first study, I investigated the influence of diking on the distribution of nutrients and soil formation processes in four defined hydrogeomorphic units (HGUs) that account for landscape heterogeneity (high and low sites) and hydrological connection (active and former floodplain). For this, mixed topsoil samples (0-10 cm of mineral soil) were collected in 44 hardwood floodplain forest sites (2500m<sup>2</sup> each) along 150 km of the lower middle Elbe and 18 soil profiles were studied. Soil parameters as grain size

distribution, pH, total carbon (TC), total nitrogen (TN), plant available phosphorous ( $P_{sol}$ ), cation exchange capacity (CEC) and base saturation (BS) were determined in the laboratory. Main results show that diking had a strong influence on floodplain nutrient availability. The active floodplain presented higher availability of  $P_{sol}$ , which was related to higher soil pH values and most probably to the active sedimentation of riverine particulate matter and the input of soluble nutrients from the flooding water. Former floodplain soils acidified significantly and showed lower nutrient availability. This occurs in the absence of flooding that allows litter accumulation, decomposition and further soil development.

In the second one, I studied the sap flow velocity of five oaks (*Quercus robur*) and five elms (*Ulmus laevis*) under high evaporative demand and different soil water availability (high and low) in two active floodplain forest sites (sandy and loamy). In this study, continuous monitoring of soil water parameters as volumetric water content and water tension (at defined depths up to 1.6 m below ground), as well as micrometeorological parameters and tree sap flow velocity were performed during the vegetation period of 2020. The sap flow velocity of the trees was measured with self-built heat-ratio method devices at three positions per tree. This data was averaged for the five trees per species per site. Based on measured values of vapor pressure deficit and global radiation, I model potential sap flow under non-water-limited conditions by using the Jarvis-type model. The ratio between modeled and measured sap flow, under high and low water availability and for the sandy and loamy site, was analyzed against measured soil water tension to define the relevance of soil water on the sap flow velocity dynamics. Sap flow velocity in Elms was up to 100% higher than in oaks. However, under low water availability, high evaporative demand, and sandy texture, *Ulmus laevis* reduced sap flow velocity considerably. In comparison to *Ulmus laevis*, the *Quercus*

*robur* displayed lower, but less variable sap flow velocities, and sensitivity to soil substrate and associated soil water storage by presenting 50% lower sap flow velocity in the sandy site compared to the loamy site. For *Ulmus laevis*, the ratio of measured and modeled sap flow against soil water potential showed that in the sandy site under low water availability, the measured sap flow deviates from potential sap flow, implying a reduction of sap flow velocity. In linear regressions, I show that soil water potential explains the sap flow velocity variability of *Ulmus laevis*.

Both studies point to the importance of considering the spatial complexity of soil properties and processes in floodplains for floodplain restoration measures, in particular concerning reforestation with hardwood species. I show that the nutrient distribution in the floodplain soils is driven by the connection to the river hydrology and that those sites that were disconnected do not display similar nutrient contents as those in the active floodplain. The active floodplain provides higher potential for hardwood floodplain forest restoration in terms of nutrient availability. In the active floodplain, soil water potential explains sap flow variability under periods of drought and in sand-dominated sites. Regarding species, *Quercus robur* appears to be more tolerant to drought stress and shows a higher adaptation to site conditions by lowering sap flow velocity under periods of water stress. Thus, this species may be better equipped to avoid problems like cavitation under the expected increase of drought events.

## Zusammenfassung

Hartholzauenwälder gehören zu den artenreichsten und produktivsten Ökosystemen in Mitteleuropa und erbringen wichtige Ökosystemleistungen als Lebensraum, Hochwasserrückhalt, Abflussregulierung, Kohlenstoffspeicherung, Erholungsraum, weitere. Gleichzeitig sind sie seit Jahrhunderten durch anthropogene Aktivitäten wie die Kanalisierung und Eindeichung von Flüssen sowie die Umnutzung von Wald in Agrar- und Weideland bedroht. Darüber hinaus beeinträchtigen aktuelle sowie zukünftige Auswirkungen des Klimawandels wie zunehmende und häufigere Dürreperioden die regelmäßigen hydrologischen Schwankungen die Hartholzauenwälder, die sehr empfindlich und abhängig von der Anbindung an die Flusshydrologie sind. Auenspezifische Prozesse wie aktive Sedimentation und Grundwasserschwankungen tragen zur topografischen und pedologischen Heterogenität in diesem Ökosystem bei. Die Böden spielen eine zentrale Rolle für die Funktion des Ökosystems und die Produktivität von Hartholzauenwäldern, da sie die Verfügbarkeit von Nährstoffen und Wasser regulieren und zur Speicherung und Stabilisierung des organischen Kohlenstoffs beitragen. In dieser Arbeit soll untersucht werden, wie sich die Heterogenität der Auenlandschaft auf die Nährstoffverteilung und die Wasserverfügbarkeit im Boden auswirkt und wie diese Faktoren die Prozesse im Wald und dessen Produktivität beeinflussen. Um dieses Ziel zu erreichen, wurden zwei verschiedene Studien durchgeführt.

Die erste Studie behandelt den Einfluss der Eindeichung auf die Nährstoffverteilung und die Bodenbildungsprozesse in vier definierten hydrogeomorphen Einheiten (HGUs), die die landschaftliche Heterogenität (Hoch- und Tieflagen) und den hydrologischen Zusammenhang (aktive und ehemalige Aue) berücksichtigen. Dazu wurden gemischte Oberbodenproben (0-10 cm Mineralboden) an 44

Hartholzauwaldstandorten (2500m<sup>2</sup>) entlang 150 km der unteren Mittelelbe gesammelt und 18 Bodenprofile untersucht. Bodenparameter wie Korngrößenverteilung, pH-Wert, Gesamtkohlenstoff (TC), Gesamtstickstoff (TN), pflanzenverfügbare Phosphor (P<sub>sol</sub>), Kationenaustauschkapazität (KAK) und Basensättigung (BS) wurden im Labor bestimmt. Die wichtigsten Ergebnisse zeigen, dass die Eindeichung einen starken Einfluss auf die Nährstoffverfügbarkeit in der Aue hatte. Die aktive Aue wies eine höhere Verfügbarkeit von P<sub>sol</sub> auf, was mit höheren pH-Werten im Boden und höchstwahrscheinlich mit der aktiven Sedimentation von Flusspartikeln und dem Eintrag löslicher Nährstoffe aus dem Überschwemmungswasser zusammenhing. Ehemalige Auenböden sind stark versauert und wiesen eine geringere Nährstoffverfügbarkeit auf. Dies ist auf das Fehlen von Überschwemmungen zurückzuführen, die die Akkumulation und Zersetzung von organischem Material und eine weitere Bodenentwicklung ermöglichen.

In der zweiten Studie untersuche ich die Saftflussgeschwindigkeit von fünf Eichen (*Quercus robur*) und fünf Ulmen (*Ulmus laevis*) unter hohem Verdunstungsbedarf und unterschiedlicher Bodenwasserverfügbarkeit (hoch und niedrig) an zwei aktiven Auenwaldstandorten (sandig und lehmig). In dieser Studie wurden während der Vegetationsperiode 2020 kontinuierlich Bodenwasserparameter wie der volumetrische Wassergehalt und die Wasserspannung in definierten Tiefen (bis zu 1,6 m unter Geländeoberkante) sowie mikrometeorologische Parameter und die Saftflussgeschwindigkeit der Bäume gemonitort. Die Saftflussgeschwindigkeit der Bäume wurde mit selbstgebaute Heat-ratio Geräten an drei Positionen pro Baum gemessen. Diese Daten wurden für die fünf Bäume pro Art und Standort gemittelt. Auf der Grundlage der gemessenen Werte des atmosphärischen Wassersättigungsdefizits und der Globalstrahlung wurde der potenzielle Saftstrom unter nicht wasserlimitierten

Bedingungen mit Hilfe des Jarvis-Modells modelliert. Das Verhältnis zwischen modelliertem und gemessenem Saftfluss bei hoher und niedriger Wasserverfügbarkeit und für den sandigen und lehmigen Standort wurde anhand der gemessenen Bodenwasserspannung analysiert, um die Bedeutung des Bodenwassers für die Dynamik der Saftstromgeschwindigkeit zu bestimmen. Die Saftflussgeschwindigkeit von Ulmen war um bis zu 100 % höher als die der Eichen. Bei geringer Wasserverfügbarkeit, hohem Sättigungsdefizit und sandiger Textur verringerte *Ulmus laevis* die Saftflussgeschwindigkeit jedoch erheblich. *Quercus robur* wies geringere Saftflussgeschwindigkeiten sowie eine geringere Variabilität als *Ulmus laevis* auf und reagierte empfindlich auf das Bodensubstrat und die damit verbundene Wasserspeicherung im Boden. Die Saftflussgeschwindigkeit war bei sandiger Textur um 50 % niedriger als bei lehmiger Textur. Das Verhältnis zwischen gemessenem und modelliertem Saftfluss und dem Bodenwasserpotenzial zeigte, dass der gemessene Saftstrom auf dem sandigen Standort bei geringer Wasserverfügbarkeit vom potenziellen Saftfluss abweicht, was eine Verringerung der Saftflussgeschwindigkeit bei *Ulmus laevis* bedeutet. Mithilfe einer linearen Regression konnte ich zeigen, dass das Bodenwasserpotenzial einen Großteil der Variabilität der Saftflussgeschwindigkeit von *Ulmus laevis* erklären.

Beide Studien zeigen, wie wichtig es ist, die räumliche Komplexität der Bodeneigenschaften und -prozesse in Auen für Renaturierungsmaßnahmen zu berücksichtigen. Dies gilt insbesondere für die Wiederaufforstung mit Laubholzarten. Wir zeigen, dass die Nährstoffverteilung in den Auenböden von der Anbindung an die Flusshydrologie abhängt und dass die Standorte, die vom Fluss abgetrennt wurden, nicht den gleichen Nährstoffgehalt aufweisen wie diejenigen in der aktiven Aue. Die aktive Aue bietet in Bezug auf die Nährstoffverfügbarkeit ein höheres Potenzial für die

Wiederherstellung von Hartholzauwäldern. In der aktiven Aue erklärt das Bodenwasserpotenzial die Schwankungen des Safflusses in Trockenperioden und an sanddominierten Standorten. Was die Arten betrifft, so scheint *Quercus robur* toleranter gegenüber Trockenstress zu sein und sich besser an die Standortbedingungen anzupassen, indem die Safflussgeschwindigkeit in Zeiten von Wasserstress verringert wird. Daher ist diese Art möglicherweise besser gerüstet, um Probleme wie Kavitation bei der erwarteten Zunahme von Dürreereignissen zu vermeiden.



# Chapter 1

## Introduction, background and objectives

### 1.1 Introduction

Hardwood floodplain forests are ecosystems that are located along lowland rivers and experience seasonal flooding. These ecosystems are dominated by deciduous hardwood tree species, such as oaks (*Quercus robur*), elms (*Ulmus Laevis*) and ashes (*Fraxinus excelsior*) (Schnitzler, 1994). One of the main characteristics of these ecosystems is the landscape heterogeneity that results from hydrological exchanges (e.g. flooding, groundwater) between the river and the floodplain, which directly influence the amount and quality of water and nutrients available for vegetation growing in floodplain sediments (Hughes, 1997a). However, anthropogenic activities such as land-use and climate change, as well as flooding retention by diking have interfered with the natural processes, as for example periodic flood-pulses and sediment deposition, that occur between the river and its floodplain. As a result, the disconnection of the floodplain from the river hydrology has affected the soil physicochemical properties as well as the hydrological dynamics that hardwood floodplain forest need, to keep their extensive range of ecological functions and services (Krause et al., 2007).

In this context, my aim was to identify and evaluate soil properties and site-specific hydrological conditions and how they influence the predominant hardwood species *Quercus robur* and *Ulmus laevis* in the lower-middle section of the Elbe River in Germany. I evaluate this properties and conditions considering the floodplain hydromorphology, the anthropogenic influence of the dike and climate-induced stress.

## 1.2 Background

### *1.2.1 Floodplains and floodplain forests in Germany and in the Elbe Catchment.*

Floodplain forests are considered one of the most diverse and productive ecosystems in Europe. They are extremely valuable ecological systems given the variety of ecosystem services they provide (Tockner & Stanford, 2002). In Germany, some of the ecosystem services that floodplain forests provide are natural habitat to unique species of fauna and flora, they are seasonal migration corridors for migratory bird species (Hale, 2004). Floodplain forests, and floodplain forest soils have great potential for carbon storage, in biomass and as organic carbon in soils, respectively (Dybala et al., 2019; Heger et al., 2021a; Shupe et al., 2022). Furthermore, floodplain forest soils control nutrient and water availability and they provide runoff regulation (Hughes, 1997b). These ecosystems are not only endangered in Germany, but also throughout Europe, mainly due to anthropogenic pressure. Thus, their protection and restoration has increasingly become a topic of public interest (Koenzen et al., 2021).

Morphological floodplains are defined as the natural floodable areas of rivers (Koenzen et al., 2021). The morphological floodplains in Germany are divided in two main units due to diking activities; the active floodplain, which are areas that can still be flooded, and the former floodplain defined as areas cut off from the river's flooding regime (Koenzen et al., 2021). Two-thirds of the area of Germany's morphological floodplains are mainly former floodplains. Furthermore, over 80% of inundation areas in Germany, belonging mainly to the Rhine, Elbe, Oder and Danube rivers, have been lost, meaning they are not even flooded under a major flooding event (Koenzen et al., 2021). The remaining one-third of the floodplains are active floodplains, however, land-use change compromises near-natural floodplain biotopes consisting of a mosaic of wetland, grassland and floodplain forests. The actual ratio of land use in German floodplains

indicates the predominance of grasslands, arable lands and settlements over forests. Moreover, from the actual 16% of forests in floodplains, a vast portion do not exhibit characteristics of an alluvial forest any longer.

My study focuses on the floodplains of the lower middle Elbe river. A vast area of the Elbe catchment is located in the North German Plain. Approximately 50% of inundation areas in the lowland floodplains along the Middle Elbe are lost mainly due to dike protection measures (Koenzen et al., 2021) and the remaining floodplain areas, that are still actively connected to the Elbe, consist only of narrow bands. However, in comparison to other German rivers, the lower middle Elbe river floodplain are less severely altered. In fact, floodplain sections of the lower Middle Elbe floodplain still present large areas of coherent riparian mixed forests (Koenzen et al., 2021), which are of high interest for preservation and restoration.



Figure 1. Active floodplain forest site in Wittenberge, Brandenburg.

### *1.2.2 Floodplain geomorphology and soil properties, relevance for restoration.*

Floodplains are characterized by longitudinal, vertical and lateral heterogeneity due to the influence of the river hydrology. According to the flood pulse concept proposed by

Junk and Bayley (1989), the lateral exchange between the floodplain and the river results in nutrient recycling and dynamics, which have been acknowledge to play a significant role on biota, more than that of the longitudinal gradient.

In floodplains, the soils are nutrient-fed by the constant exchange with the river dynamic flood-pulses and through groundwater exchange. The lateral input that flood and groundwater provides to the soils is controlled as well by the changes in topography, creating geomorphic functional units (Noe et al., 2013). These functional units will impact the nutrient availability, microbial activity, lability of organic matter, which are all parameters that influence nutrient mineralization (Achat et al., 2016; Binkley & Hart, 1989; Noe et al., 2013).

In the lower middle Elbe, we focused on the functional geomorphic units displayed in the lateral gradient of the floodplain, which include the anthropogenic influence of the dike. As a result, of field observation during site selection, we defined four representative hydrogeomorphic units: Active floodplain Low (AL), Active floodplain High (AH), Former floodplain Seepage influenced (FS), and former floodplain disconnected from the Elbe hydrology (FD) (Vásconez Navas et al., 2023). These hydrogeomorphic units were expected to vary in soil physicochemical characteristics

based on the dynamics of sediment deposition, nutrient recycling, and hydrological processes connected to flooding and groundwater (Figure 2).

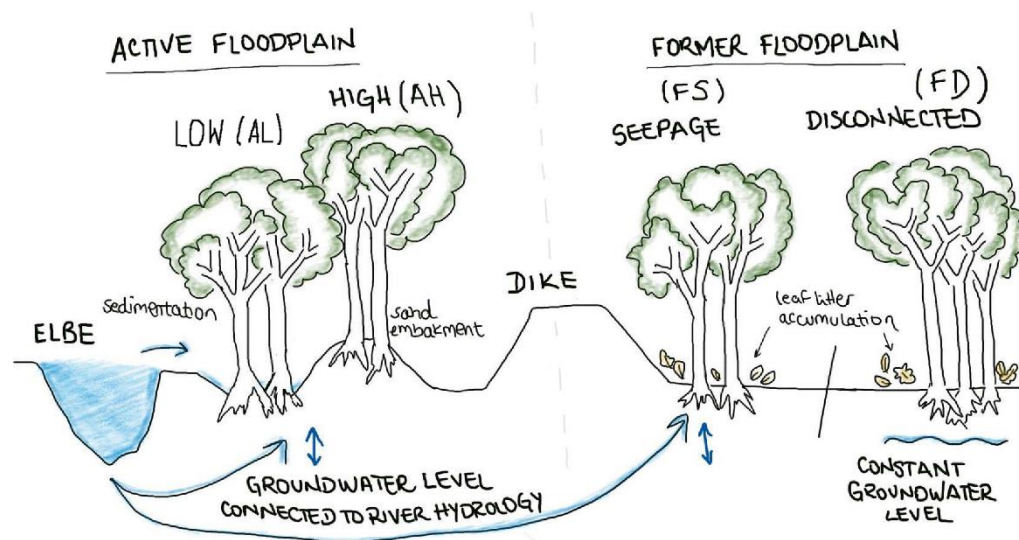


Figure 2. Scheme of the lateral gradient of the floodplain including four hydrogeomorphic units: Active floodplain low (AL), Active floodplain high (AH), Former floodplain seepage (FS) and, Former floodplain disconnected (FD).

### 1.2.3 Soil hydrology, drought and forest interactions

Tight interactions between ground and surface waters, as well as meteorological factors, as temperature, evaporative demand and precipitation, dictate the hydrological dynamics in the floodplain (Krause, Jacobs, et al., 2007). With the expected increase in frequency and intensity of droughts in Central Europe (Bednar-Friedl et al., 2022), streamflow drought, reduced precipitation, and soil drought will intensify, affecting the hydrological balance of the floodplain. Under conditions of water scarcity, the soil matrix plays a pivotal role by influencing rates of infiltration and deep percolation. Thus, strongly controlling rates of transpiration, carbon assimilation and biomass production (Porporato et al., 2002).

In addition, periods of low precipitation and high temperatures, are described as the leading factor of forest dieback (Allen et al., 2010; Stojanović et al., 2015). Other documented effects of global warming on forests are reduction of net primary productivity, shifts in community composition and lengthening of the vegetation period (Chmielewski, 2007; Porporato et al., 2004). As a result, the study of climate-induced physiological stress on trees, as well as phenological adaptations to water limitation, has come into focus of not only the scientific community, but also different stakeholders, politicians and society involved in the protection and restoration of forests.

In this context, an improved understanding and prediction of the ecological responses of hardwood floodplain forest species to climate change, in combination with the complexity of highly dynamic and heterogeneous nonlinear systems as floodplains and floodplain soils, is essential.

### 1.3 Objectives, research questions and study significance

The general objective of this dissertation is to determine the variability of soil physicochemical properties considering the lateral geomorphology of the floodplain including the influence of dikes; and to define how this variability and effects of climate change affect the typical hardwood floodplain forest species. In order to target this objectives the following research questions are addressed:

- Is the former floodplain able to provide similar conditions as the active floodplain, regarding soil physicochemical properties, with regards to forest restoration?
- Are the two main hardwood species, typical to this area, reacting similarly to periods of water stress? Under which conditions soil water availability exerts a stronger control than evaporative demand on the water transport of the studied tree species?

Both questions are targeted considering that floodplains are extremely productive ecosystems that offer a range of ecosystem services, which in the last few decades, have become a focal topic of research and preservation in the scientific community and by different stakeholders. As part of the interdisciplinary MediAN project, with this dissertation I hope to contribute to the understanding of processes between the soil physicochemical properties, soil water balance and typical floodplain forest species. Thus, backing-up efforts of protection and restoration of hardwood floodplain forests and their ecosystem services along the lower Middle Elbe River.

## Chapter 2

### Article 1: Are active and former floodplain soils of the lower middle Elbe similar? A study of soil characteristics and possible implications for forest restoration

#### 2.1 Abstract

The analyses of soil properties and processes under the consideration of the spatial complexity of floodplains is a key step in the preparation of floodplain restoration measures. In that context, we analyzed how hydrogeomorphology influences soil physicochemical properties and formation processes in hardwood floodplain forests at the local scale. Our analyses are based on, 44 mixed topsoil samples, 135 soil drillings (2.0 m depth) and 18 reference pits (1.6 m depth) distributed in 44 hardwood floodplain forests along 150 km of the middle Elbe River. We considered four hydrogeomorphic units (HGUs) along a lateral floodplain gradient. Two HGUs located in the active floodplain and defined by their morphology Active High (AH), and Active Low (AL), and two located in the former floodplain: seepage water influenced (FS), and disconnected from the river hydrology (FD). Our results indicate that the HGUs in the active floodplain benefit from a stronger connection to the river hydrology. Higher  $\text{pH}_{\text{CaCl}_2}$  values in the active HGUs as well as expected higher total P contents due to river deposition result in increased phosphorous availability. Physicochemical parameters as lower  $\text{pH}_{\text{CaCl}_2}$  and predominance of iron mottling found in the FD indicate increased P sorption, therefore lower  $\text{P}_{\text{sol}}$  availability. However, HGUs in the former floodplain, particularly those disconnected from the river hydrology, are characterized by higher total carbon and nitrogen content. These results improve our understanding of the soil physicochemical dynamics and their interactions in the different hydrogeomorphic units, and could allow the evaluation of floodplain restoration measures based on soil



nutrient distribution to increase the potential of restored forests to develop on the selected geographic setting.

## 2.2 Introduction

River-floodplain ecosystems in temperate regions have been heavily used and modified for industrial and agricultural purposes since the late 1800s (Bayley, 1995). Moreover, these ecosystems have undergone continuous hydrological disconnection from rivers due to dike construction and channelization measures for flood protection measures and increment of navigable watercourses (Damm, 2013). Consequently, the dominant physical and hydrological processes of floodplain ecosystems, for example infiltration potential, groundwater recharge capacity, sedimentation, and others, have been affected, and result in the absence of natural functions and reduction of primary productivity. This is particularly true for Germany, where only 10% of the morphological floodplains are in near natural state (Buijse et al., 2002; Jungwirth et al., 2002), only 8% of the active floodplain are defined as ecologically functional (which implies the ability to fulfil functions that benefit flora, fauna and society) (Koenzen et al., 2021), and where hardwood forests cover only 1% of the overall floodplain area (Scholz et al., 2012; Shupe et al., 2021).

The degradation of hardwood floodplain forests particularly threatens four ecosystem services: i) preservation of biodiversity (Buijse et al., 2002; Schnitzler, 1994; Steiger et al., 2005); ii) floodwater retention; iii) increase in carbon sequestration value (Dybala et al., 2019); and, iv) attenuation of nutrients and pollutants (Krause et al., 2007). Thus, there has been increased attention towards restoration of floodplain areas and afforestation with native hardwood species along many European rivers (Baker et al., 2001; Jungwirth et al., 2002; Rives et al., 2020; Schindler et al., 2021).

Hardwood floodplain forests are dominant natural floodplain ecosystems, commonly composed by a combination of oaks, elms and ashes (Schnitzler, 1994). They are one of the most productive and species-rich forest ecosystems in Europe and are likely to modify soil properties, at least with regards to long term carbon storage (Dybala et al., 2019; Heger et al., 2021b; Marks et al., 2020). All actions and strategies to maintain and improve ecosystem services of floodplains need to consider the hydrogeomorphology, which is characterized by the high variability in longitudinal and lateral direction within the floodplain (Hughes, 1997b; Noe et al., 2013).

In floodplains, the high input and availability of nutrients such as N and P, related to the flood pulse, play a particularly important role for primary productivity (Noe et al., 2013; Spink et al., 1998). Consequently, all hydrological exchanges between the river and the floodplain-soil matrix influence the amount and quality of water and nutrients available for vegetation growing in floodplain sediments (Poff et al., 1997a). Furthermore, among the main characteristics that define the physical habitat of a floodplain ecosystem are morphology of the channel that controls the duration and impact of flooding water (erosion, sedimentation) and the heterogeneity in sediment texture distribution, which is responsible for soil water and nutrient storage. Both characteristics are interlinked and result from the movement and deposition of sediments and other transportable materials created by former flow processes (Poff et al., 1997b).

Floodplain soils form an essential part of the ecosystem (Schoenholtz et al., 2000), thus the analyses of soil properties and processes under the consideration of the spatial complexity of the floodplain is a key step in the preparation of floodplain restoration measures. The sustainability of a forest ecosystem relies on soil physical, chemical and biological properties that differ across spatial scales (Schoenholtz et al., 2000). Thus, the definition of a set of soil characteristics and their dynamics in different

sections of a floodplain will certainly result in more effective restoration approaches of hardwood floodplain forests, especially if areas with soil quality indicators are targeted. Aiming to understand the variability of soil physicochemical properties in the lateral hydrogeomorphic gradient of the lower Middle Elbe, we selected 44 sites covered by hardwood forests of varying characteristics (age and density of forest) and located in representative hydrogeomorphic units (HGUs) distributed in the lateral gradient of the floodplain (active and former). Our analyses were guided by three objectives:

- 1) To identify the distribution of soil properties, soil types and soil forming processes in the HGUs.
- 2) To analyze the influence of the hydrological processes (e.g. flooding days, lateral distance to the river) on soil physicochemical properties.
- 3) To understand the interactions between soils physicochemical properties within defined hydrogeomorphic units.

Taking into account that the percentage of active and former floodplain area is 27% and 68%, respectively, in the Elbe catchment (Koenzen et al., 2021), we try to answer the following question: are soils in the former floodplain capable to provide similar conditions as soils in the active floodplain, in particular regarding soil nutrient distribution, for restoration of hardwood floodplain forest? Given increased interests in floodplain ecosystem recovery and hardwood forest restoration, this study focuses exclusively on hardwood forest sites, in contrast to already existing soil analyses along the Middle Elbe floodplains -which have focused on grasslands (Meyer & Miehlich, 1983; Schwartz et al., 2003a). Moreover, the assessment of soil properties with relation to forests has been centered on forest productivity in particular of plantation forests (Burger & Kelting, 1998; Watt et al., 2005), or on the influence of forest management practices on soil productivity (Grigal, 2000). However, the assessment of soil

physicochemical properties in the lateral gradient of a temperate floodplain, with the objective of defining areas for forest restoration and ecosystem protection, has not been approached before with such specificity.

## 2.3 Methodology

### 2.3.1 Research area and plot selection

The research area covers a 150 km section of the lower Middle Elbe River (lon.: 10.5 - 12.1, lat.: 52.85 - 53.38) (Figure 3). The area is part of the *UNESCO Biosphere Reserve River Landscape Elbe* and is located in the federal states of Brandenburg and Lower Saxony, Germany. A transition between maritime and continental climate characterizes this region (von Storch et al., 2018) with a mean annual temperature of 9.7 °C and a mean annual precipitation of 578 mm as recorded from annual regional data for 30 years (1990-2020) by the Climate Data Center of the German Weather Service (DWD, 2021). Regarding sedimentological and pedological processes, the area has been described as a Holocene alluvial plain in which the geologic substrate consists of Pleistocene and Holocene sands, overlain by Holocene alluvial sands, loams and clays (Gröngröft et al., 2005; Schwartz et al., 2003b).

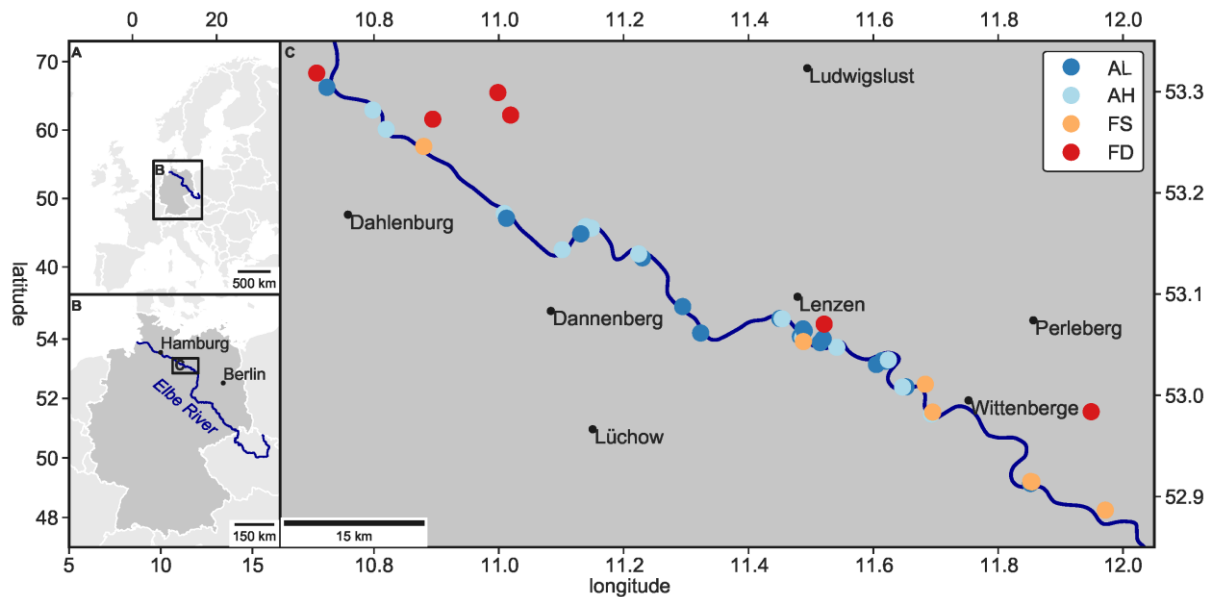


Figure 3. Study area and selected study plots. AL active floodplain, low; AH active floodplain, high; FS former floodplain, seepage influence; FD former floodplain, disconnected from the river hydrology. Longitude-Latitude coordinates of every plot can be found in *Appendix E*.

We selected 44 plots (each 2500 m<sup>2</sup>) in remaining patches of hardwood floodplain forests. Depending on the size and shape of the forest patch, the plots were 50 m x 50 m or 25 m x 100 m and were covered mainly by a combination of two hardwood species: *Quercus robur L.* and *Ulmus laevis Pall.* (*Querco-Ulmetum minoris*).

We defined four HGUs based on their position on the landscape and the hydrologic situation. Two HGUs were located in the active floodplain, directly connected to the river hydrology and flooding regime, and were divided into Active Low (AL) -which included forest patches with more flooding days, and Active High (AH) -which consisted of forest patches located in sand embankments and where less flooding was expected due to higher relative elevation. The other two HGUs were located in the former floodplain of the Elbe River. The former floodplain was once part of the Elbe floodplain but given the current anthropogenic influence of a dike, it is not directly flooded by the river. Within the former floodplain, we selected forest patches located in the seepage water zone (FS) -which are sites directly located behind the dike and influenced by

groundwater fluctuations connected to the Elbe hydrology, and forest plots far away from the dike (FD) with no connection to river hydrology and in which a more stable groundwater table is expected. The main characteristics of the HGUs are given in Table 1 and more detailed information in Appendix A.

Table 1. Characteristics of the hydrogeomorphic units (HGUs)

HGU	Number of plots	Mean lateral distance to the river [m] ( $\pm$ SD) <sup>1</sup>	Dominating soil reference groups <sup>2</sup>	Mean forest age [years] ( $\pm$ SD) <sup>3</sup>
AL – Active, Low	n=18	333 (224)	Fluvic Cambisol	97.7 (65.3)
AH – Active, High	n=13	185 (152)	Fluvic Arenosol	131.9 (27.5)
FS – Former, Seepage	n=7	313 (80)	Gleyic Fluvisol	125.9 (31.9)
FD – Former, Disconnected	n=6	5540 (3920)	Fluvic Gleysol	130.2 (30.7)

<sup>1</sup> Data provided by Timo Hartmann, UFZ Leipzig (unpublished)

<sup>2</sup> (IUSS Working Group WRB, 2015)

<sup>3</sup> Data provided by Heather Shupe, Institute of Plant Ecology, University of Hamburg (Shupe et al., 2022)

### 2.3.2 Lateral distance to the and river and flooding days per year

The lateral distance between the MediAN study plots and the Elbe River was measured with ArcMap Version 10.7 by using the NEAR-Tool that calculates the shortest distance between two features. For the Elbe River, a line feature was used given by the Geoportal called FLYS of the German Federal Institute of Hydrology (BfG). For the plots, a point feature with the geographic coordinates of the middle points per plot measured with a Garmin GPS.

Flooding duration was obtained from modelled flooding duration based on a 35 year period including the years 1990–2016. A one-dimensional model integrating data from various data sources (DEM1, digital elevation model with 1 m resolution) was used as

described by Weber and Hatz (2020) and Weber and Rosenzweig (2020). The resulting parameter was defined as Fdays indicating mean flooding days per year per plot.

### *2.3.3 Soil survey and sampling*

Every plot was divided into four quadrants (25 m \* 25 m). In the center of three of the quadrants, we drilled two meters below surface with an Edelman auger for soil classification purposes and to identify soil forming processes. In addition, three soil pits were opened in the fourth quadrant of six intensive study sites representing the HGUs, thus 18 soil pits of 1.6 m depth were sampled, three per HGU to study the soil in an undisturbed way and identify the heterogeneity of soil profiles over a small scale. We described topographic and surface characteristics. For each horizon, we determined the horizon label, Munsell soil color, soil texture and hydromorphic mottling. We classified the soils according to the International Soil Classification System (IUSS Working Group WRB, 2015).

We recorded the depth with the first appearance of hydromorphic mottling in every drilling and profile, i.e., starting depth where redoximorphic features covered an area of > 5% of the soil horizon according to Ad-hoc-AG Boden (2005) and calculated a mean starting depth of hydromorphic characteristics per study site, referred to as "HCD" in meters [m].

In every plot, we collected a mixed topsoil sample from the top 10 cm of the mineral soil layer along a transverse section of the plot. The samples were collected every 8 meters, resulting in 12 sampling points per plot. All the samples were transported to the laboratory (Institute of Soil Science, University of Hamburg, Germany) where they were prepared (mixed, air-dried, sieved < 2mm) for physicochemical analyses.

### *2.3.4 Soil laboratory analyses*

The grain size distribution was determined for topsoil samples. According to DIN ISO 11277, Grain size distribution of the topsoil samples was determined using sieving and sedimentation method (DIN ISO 11277). The sand fraction (63  $\mu\text{m}$ –2000  $\mu\text{m}$ ) was analyzed by a vibratory sieve shaker (Vibro, Retsch GmbH, Germany), and for the fine soil particles (<63  $\mu\text{m}$ ), a Sedimat 4-12 (Umwelt-Geräte-Technik GmbH, Germany) was used.

Soil pH was measured using multimeter probes in a suspension of soil in  $\text{H}_2\text{O}$  with a ratio of 1:2.5. Additionally,  $\text{pH}_{\text{CaCl}_2}$  was determined in a suspension of 0.01 M  $\text{CaCl}_2$ . Base saturation (BS) and effective cation exchange capacity (CEC) were determined following two consecutive steps: Initially,  $\text{Na}^+$ ,  $\text{K}^+$ ,  $\text{Ca}^{2+}$ , and  $\text{Mg}^{2+}$  were measured by extracting bounded cations using 25mL of extractant ( $\text{NH}_4\text{Cl}$ -solution 1M); afterwards, the extraction solution was filtrated and the exchange cations were analyzed on an atomic absorption spectrometer (AA280FS, Varian Inc., Palo Alto, USA). The sum of the measured cations was expressed in percentage of CEC as base saturation (BS) (DIN ISO 11260). The centrifuge residue was filled up with 5mL 0.01 M  $\text{NH}_4\text{Cl}$  solution and centrifuged at 3000 rpm, the solution was decanted. 25 mL of 1M  $\text{KCl}$  solution were added to the centrifuged solution to remove the  $\text{NH}_4^+$  from the clay surface. After filtration the  $\text{NH}_4^+$ - ions were determined in a photometer (DR 5000, Hach Lange GmbH, Berlin, Germany). The measured amount of  $\text{NH}_4^+$ - ions represent the CEC expressed in  $\text{mmol}_{\text{eq}}/\text{kg}$ .

Total nitrogen (TN) and total carbon (TC) were determined by high temperature combustion (900°C). Depending on the expected TC, each sample consisted of 300 and 1000 mg of fine-ground sample material that was introduced into the element analyzer (VarioMaxCube, Elementar, Hanau, Germany) (DIN ISO 15936). TC is assumed organic carbon because all pH values were less than 6.8.



The plant-available phosphorus ( $P_{\text{sol}}$ ) and potassium ( $K_{\text{sol}}$ ) were extracted from the solid soil samples using a calcium lactate solution ( $\text{C}_6\text{H}_{10}\text{CaO}_6$ , Lactic Acid). The phosphorus content of the soil samples was then determined by photometrical analysis at 580 nm (DR 5000 UV/VIS Photometer, Hach Lange GmbH, Berlin, Germany), and the potassium content was determined by atomic absorption spectrometry (AA280FS, Varian Inc., Palo Alto, USA).

### 2.3.5 Statistical analyses

All statistical analyses were performed with *R v4.0.3* (*R Core Team 2020*). We used analysis of variance (ANOVA) to identify significant differences for single variables between HGUs, and applied a post-hoc Tukey HSD to identify group differences ( $p\text{-level} \leq 0.05$ ). The normality of residuals, as well as variance homogeneity were checked to ensure the correct application of the statistical tests. If these pre-conditions were not met, we used Kruskal-Wallis test followed by Dunn's test.

To visualize the similarities among HGUs we used a Non-metric Multi-dimensional Scaling (NMDS) ordination plot with the function `metaMDS` from the package `vegan`; additionally, soil physicochemical and hydrological variables were fitted as vectors by using the function `envfit` from the same package. A spearman correlation matrix and a correlation network plot were used to numerically and visually identify significant correlations between variables ( $p \text{ level} \leq 0.05$ ).

We implemented simple linear regressions between physicochemical variables and to assess the influence of the HGU on these interactions we used Analysis of Covariance (ANCOVA). The outcome of interest was the interaction term between the covariate and the categorical variable with a significance level of  $p < 0.05$ .

## 2.4 Results

### 2.4.1 Soil classification and soil forming processes

We found a dominant soil reference group for each hydrogeomorphic unit; the Active High (AH) had Fluvic Lamellic Arenosol as the predominant soil reference group, while the Active Low (AL), Former Seepage (FS) and Former Disconnected (FD) had Fluvic Cambisol, Gleyic Fluvisols and Fluvic Gleysol as their predominant soil type, respectively (IUSS Working Group WRB, 2015) (Figure 4). All AH soil profiles displayed higher contents of sand, AL and FS soil profiles had a higher content of clay and silt, while FD soil profiles were dominated by these finer soil textures (Figure 4).

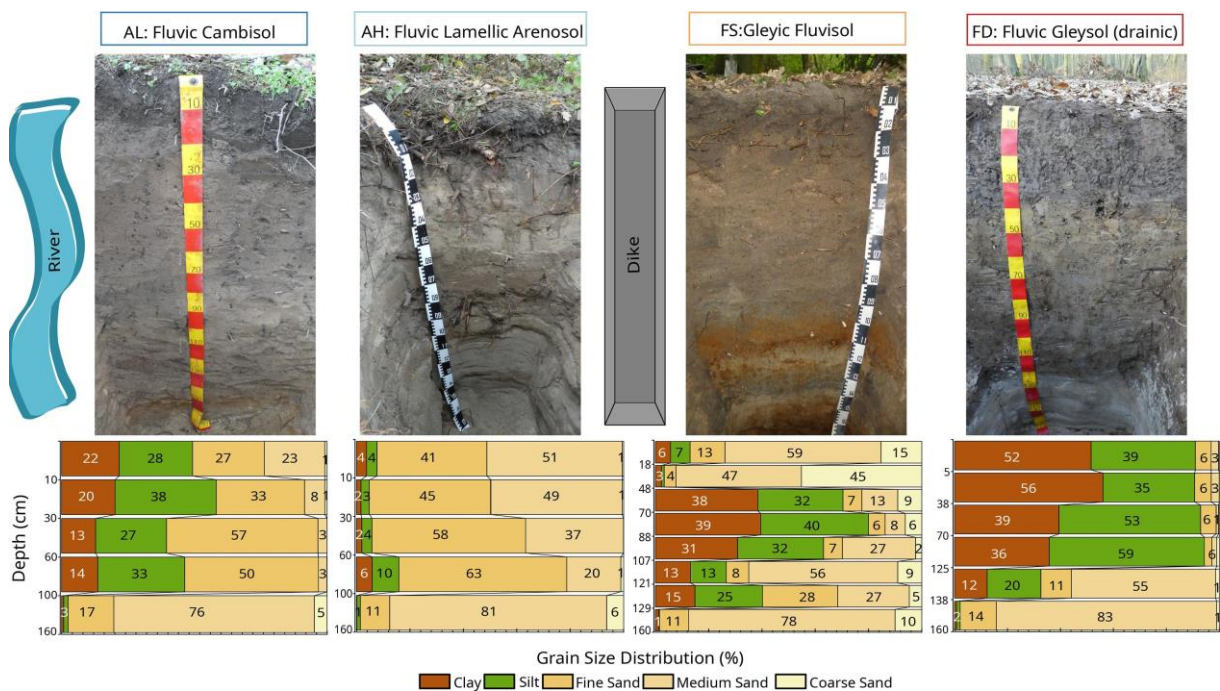


Figure 4. Dominating soil reference group per HGU and soil texture distribution per horizon. AL active floodplain, low; AH active floodplain, high; FS former floodplain, seepage influence; FD former floodplain, disconnected from the river hydrology.

Cambisols, in the AL are characterized by main textural properties that include a predominance of middle, but also finer soil textures with a good water holding capacity and high porosity (IUSS Working Group WRB, 2015). Arenosols in the AH displayed a dominance of total sand greater than 90% throughout the whole soil profile. In the

former floodplain with seepage influence, FS, the Fluvisols show normal characteristics of alluvial soil profiles, exhibiting signs of stratification in the upper part of the soil. Regarding the texture of these soils, the profiles were characterized by medium to coarse textures throughout the profile. In the disconnected section of the floodplain, FD, Gleysols showed a predominance of finer soil textures and slow rate of organic matter decomposition. These soils evidenced in their characteristics the presence of a higher and more constant groundwater table.

Iron mottling and other hydromorphic features occurred in all floodplain soils and were affected by the impact of flooding and groundwater level fluctuations. Thus, the depth of the upper part of the soil, that was unaffected by changing redox conditions and has no or almost none (< 5% of iron mottles), varied significantly between the studied soils within the HGUs. When the mean starting depth of appearance of hydromorphic mottling was considered per HGU, significant differences were identified (Figure 5). We found that in the active high unit (AH) mottling starts at a mean depth of 120 cm, which was deeper than the 47, 46 and 40 cm for AL, FS and FD, respectively. The variability of the starting depth of appearance of hydromorphic characteristics was lower in the FD than in other HGUs (Levene's test  $p < 0.05$ ).

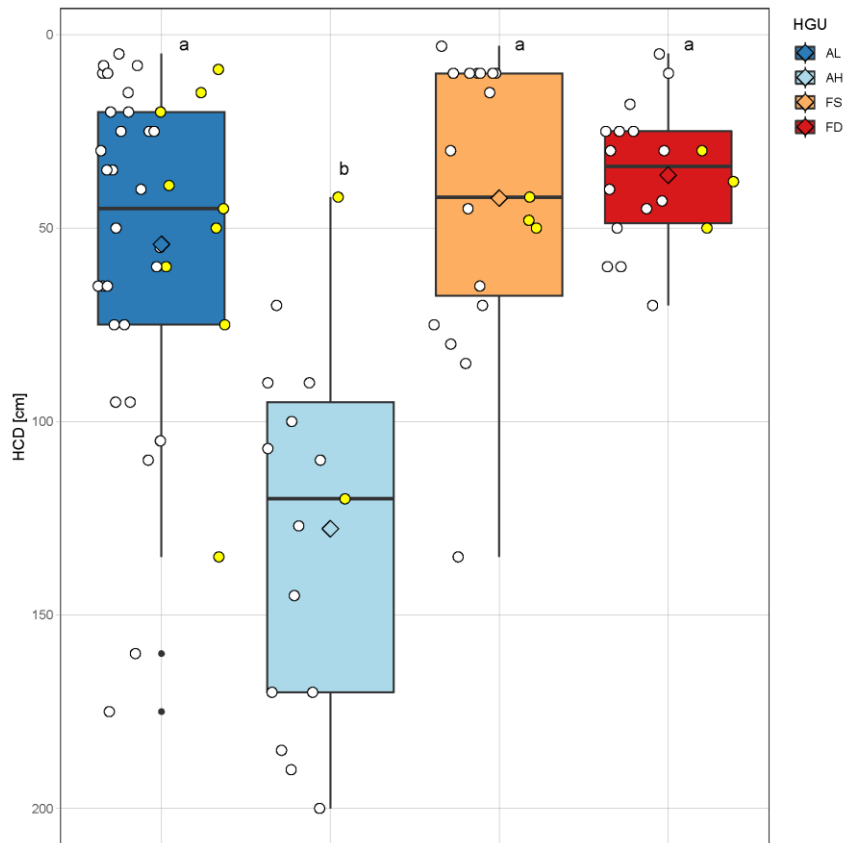


Figure 5. First depth of appearance of hydromorphic characteristics (HCD) in every hydrogeomorphic unit (HGU). Boxplots that do not share the same letter have significant different means ( $p < 0.05$ ). Active floodplain -Low (AL), Active floodplain-High (AH), Former floodplain- seepage influenced (FS), Former floodplain – disconnected from the river hydrology (FD). Boxes and whiskers represent the 1x and 1.5x interquartile range, black strips median, and rhombus the mean. Black dots denote potential extreme values. White and yellow dots denote single observations, soil drillings and soil pits, respectively.

#### 2.4.2 Variability of topsoil physicochemical properties among HGUs

The location of the polygons representing the HGUs, reflect the variability that exists among them, in relation to their position in the landscape (Figure 6). The Active Low and Active High HGU ordination space in the NMDS overlap. The large size of the AL polygon shows a strong variability within this HGU. Plots behind the dike but with seepage water influence (FS) had only small overlap to the active floodplain, indicating the connection to the river through seepage water. Plots protected from flooding and in distance to river influence (FD) had a distinct NMDS ordination and did not overlap in the ordination space at all with those plots in the active floodplain. Both former floodplain HGUs had higher C/N ratio, total carbon (TC), and total nitrogen TN as well

as lower pH values, which is evidence in the vector positioning. Base cations, base saturation (BS) and plant available P ( $P_{sol}$ ) were associated to higher pH values, which mainly occurred in the active floodplain, thus the vectors of these parameters point in the same direction.

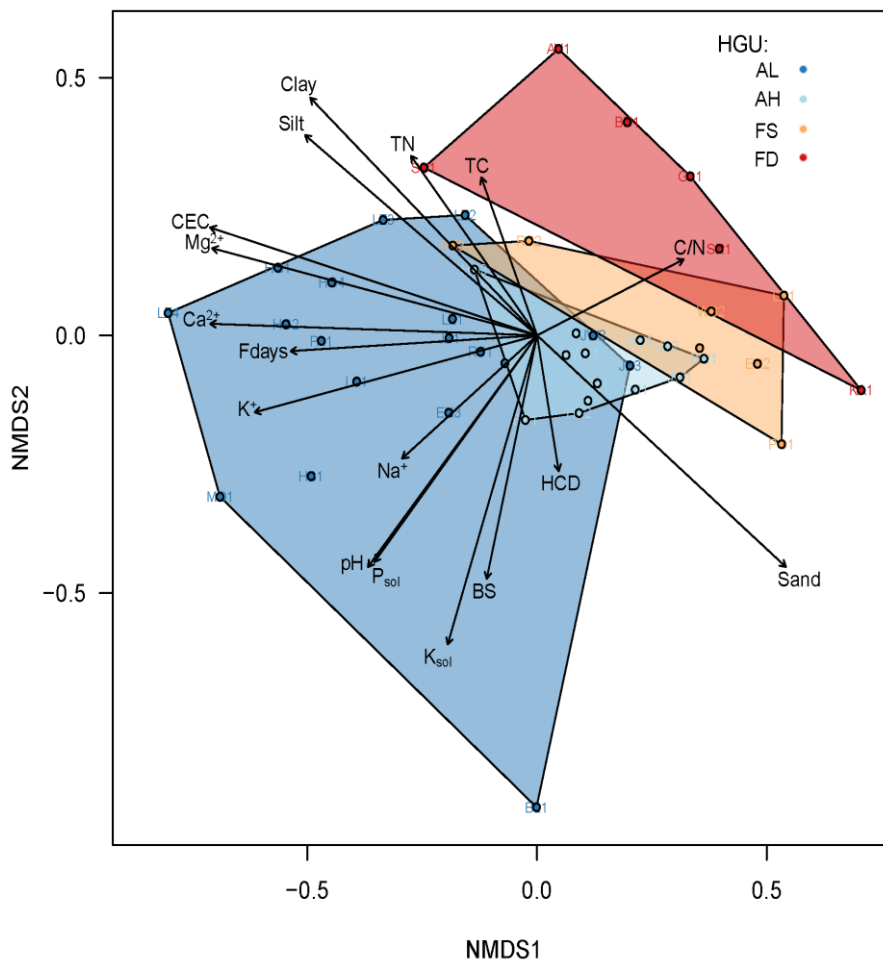


Figure 6. NMDS ordination plot including all studied parameters in the topsoil mineral layer. Points denote plots and the polygons the respective HGU. Vectors denote each physicochemical property and how it is tending to a HGU. Distance= Bray Curtis,  $k=2$ , stress = 0.062. HGU- hydrogeomorphic unit: Active floodplain -Low (AL), Active floodplain-High (AH), Former floodplain- seepage influenced (FS), Former floodplain – disconnected from the river hydrology (FD). TN (total Nitrogen), TC (total Carbon), CEC (cation exchange capacity), C/N (C/N ratio),  $Mg^{2+} - K^{+} - Ca^{2+} - Na^{+}$  (Magnesium, Potassium, Calcium and Sodium base cations, respectively),  $K_{sol}$  (soluble Potassium),  $P_{sol}$  (soluble Phosphorus), BS (Base saturation). LDR (lateral distance to the river), HCD (hydromorphic characteristics starting depth)

Soil pH<sub>CaCl2</sub>, P<sub>sol</sub>, CEC, TC, and TN differed significantly between HGUs (Figure 7). Mean pH<sub>CaCl2</sub> in the active floodplain ranged between 5.0 and 5.8, compared to sites in the former floodplain that were more acid, with pH<sub>CaCl2</sub> 3.5 - 4.2 (Figure 7 d). The variability of pH values and soluble phosphorous among units was similar. The active low HGU presented the highest content of P<sub>sol</sub>, as well as the highest pH values (Figure 7 (d, f)). The P<sub>sol</sub> ranged between 12.6 and 234.0 [mg/Kg] in the mineral topsoil layer of our plots. Total carbon and total nitrogen showed a similar distribution as clay content among the HGUs (Figure 7 (a, b, c)). The highest values of total carbon and total nitrogen were found in the AL and FD units. The effective CEC was not different between the AL, FS, and FD (Figure 7 (e)), which in general present higher clay content than the active high sites. FD, in particular, presents higher accumulation of organic matter. The potential CEC of these soils thus should be almost equal. However, the effective CEC in the disconnected former floodplain sites is less than those in the active low sites. This difference is explained by the substantial lower pH of former disconnected sites. A summary table of all measured parameters in the topsoil samples can be found in (Appendix A).

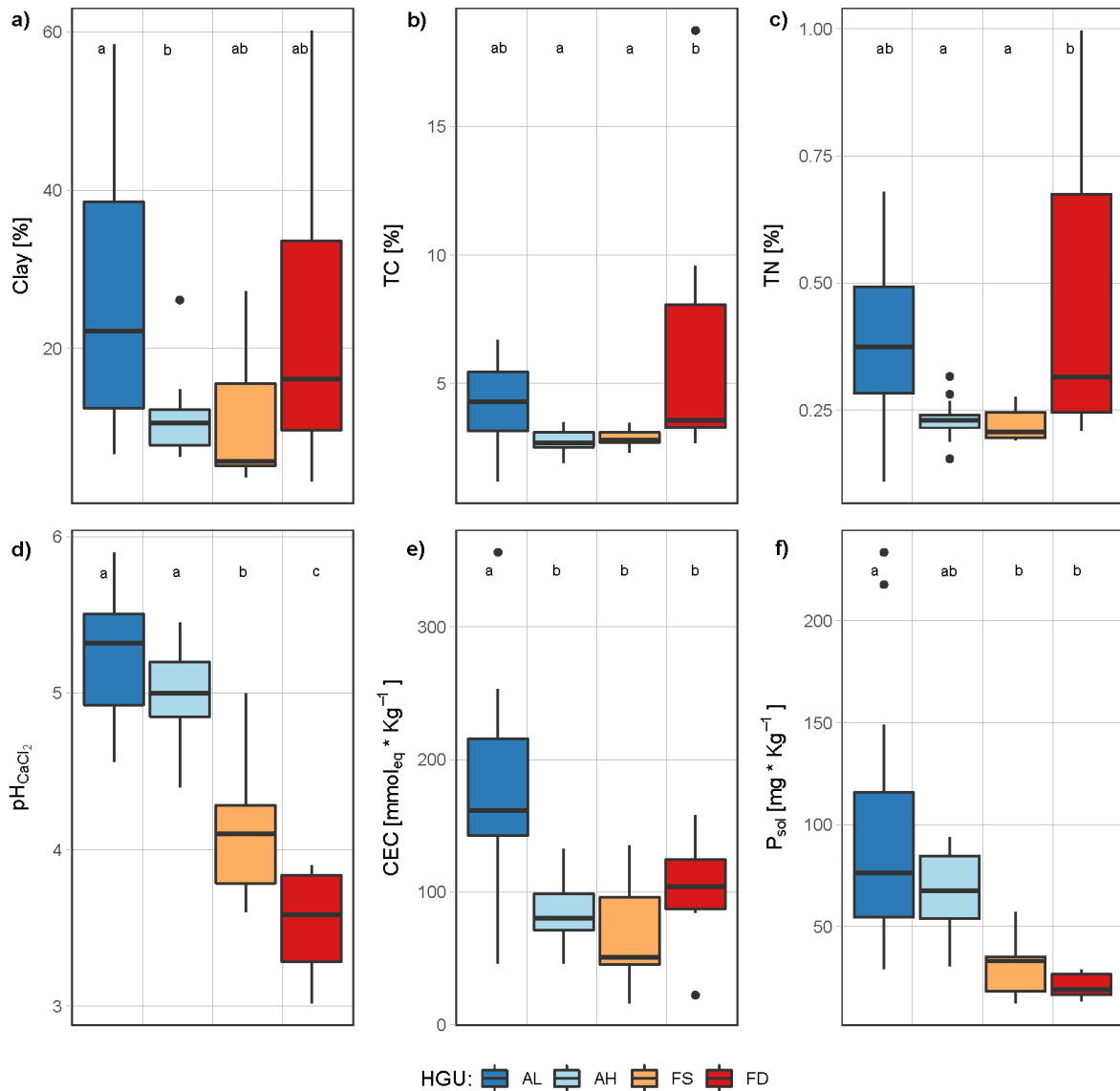


Figure 7. Variability of physicochemical parameters among hydrogeomorphic unit (HGUs): Active floodplain -Low (AL), Active floodplain-High (AH), Former floodplain- seepage influenced (FS), Former floodplain – disconnected from the river hydrology (FD). HGUs that do not share the same letter have significant different means ( $p \leq 0.05$ ). Boxes and whiskers represent the 1x and 1.5x interquartile range, black strips median, and dots potential extreme values.

### 2.4.3 Correlation analyses between physicochemical variables

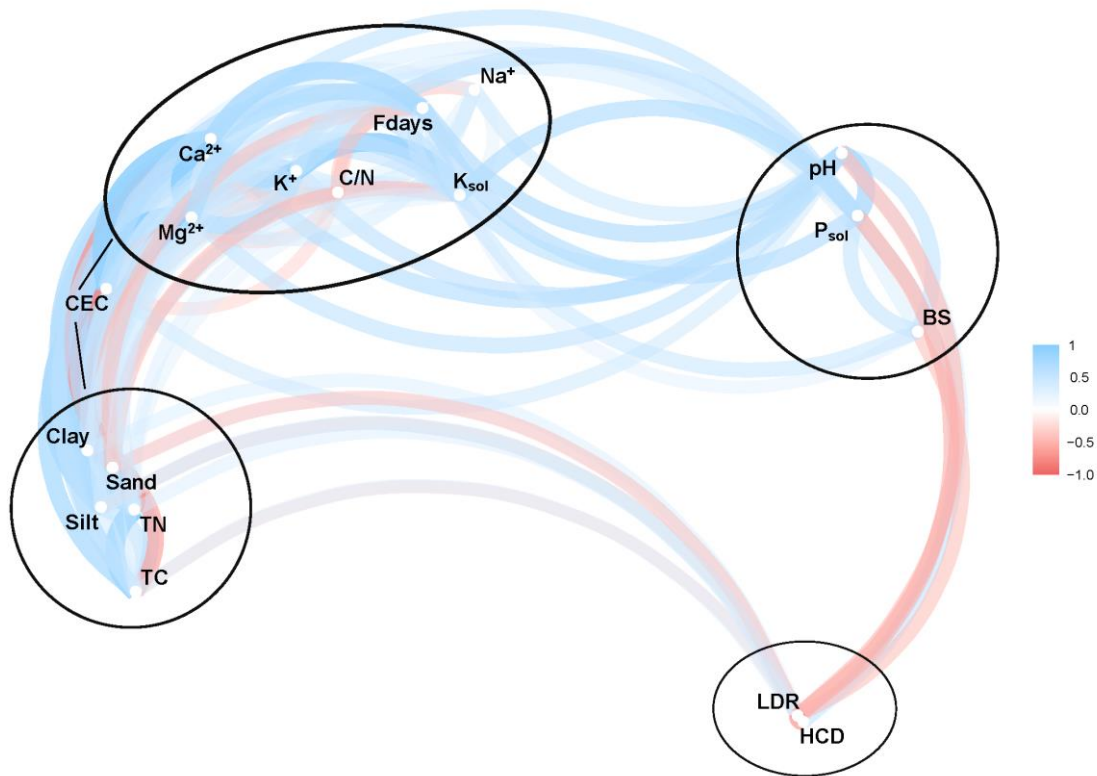


Figure 8. Correlation network plot (spearman correlation), minimum correlation = 0.3, p level  $\leq 0.05$  for all measured physicochemical and hydrological variables in the mineral topsoil (blue positive correlations; red negative correlations). TN (total Nitrogen), TC (total Carbon), CEC (cation exchange capacity), C/N (C/N ratio),  $Mg^{2+} - K^+ - Ca^{2+} - Na^+$  (Magnesium, Potassium, Calcium and Sodium base cations, respectively),  $K_{sol}$  (soluble Potassium),  $P_{sol}$  (soluble Phosphorus), BS (Base saturation). LDR (lateral distance to the river), HCD (hydromorphic characteristics starting depth)

With a correlation network plot, we identified four clusters of variables (Figure 8). The first cluster included flooding days, available base cations and  $K_{sol}$ , positively correlated to each other. In this cluster, we also found C/N ratio correlated negatively to Fdays. A second cluster included different soil textures types, total carbon and total nitrogen. Total carbon and total nitrogen showed a significant correlation with finer soil texture ( $r_s = 0.6$ ;  $0.7$  respectively) (Appendix B). These parameters, along with clay content, displayed a significant positive correlation to CEC. Therefore, CEC did not align in a cluster and acted as a connecting parameter between the first and second



cluster. The third cluster of variables included  $pH_{CaCl_2}$ ,  $P_{sol}$  and BS. In this cluster a significant strong correlation between  $P_{sol}$  and  $pH$  was found ( $r_s = 0.73$ ). The influence of hydrological variables as the lateral distance to the river and the starting depth of appearance of hydromorphic characteristics (HCD) constituted the fourth cluster; these variables were negatively correlated to all variables in the third cluster, which indicated that plots located far from the river are likely to present lower  $P_{sol}$  and BS.

2.4.4 Physicochemical interactions within the hydrological gradient

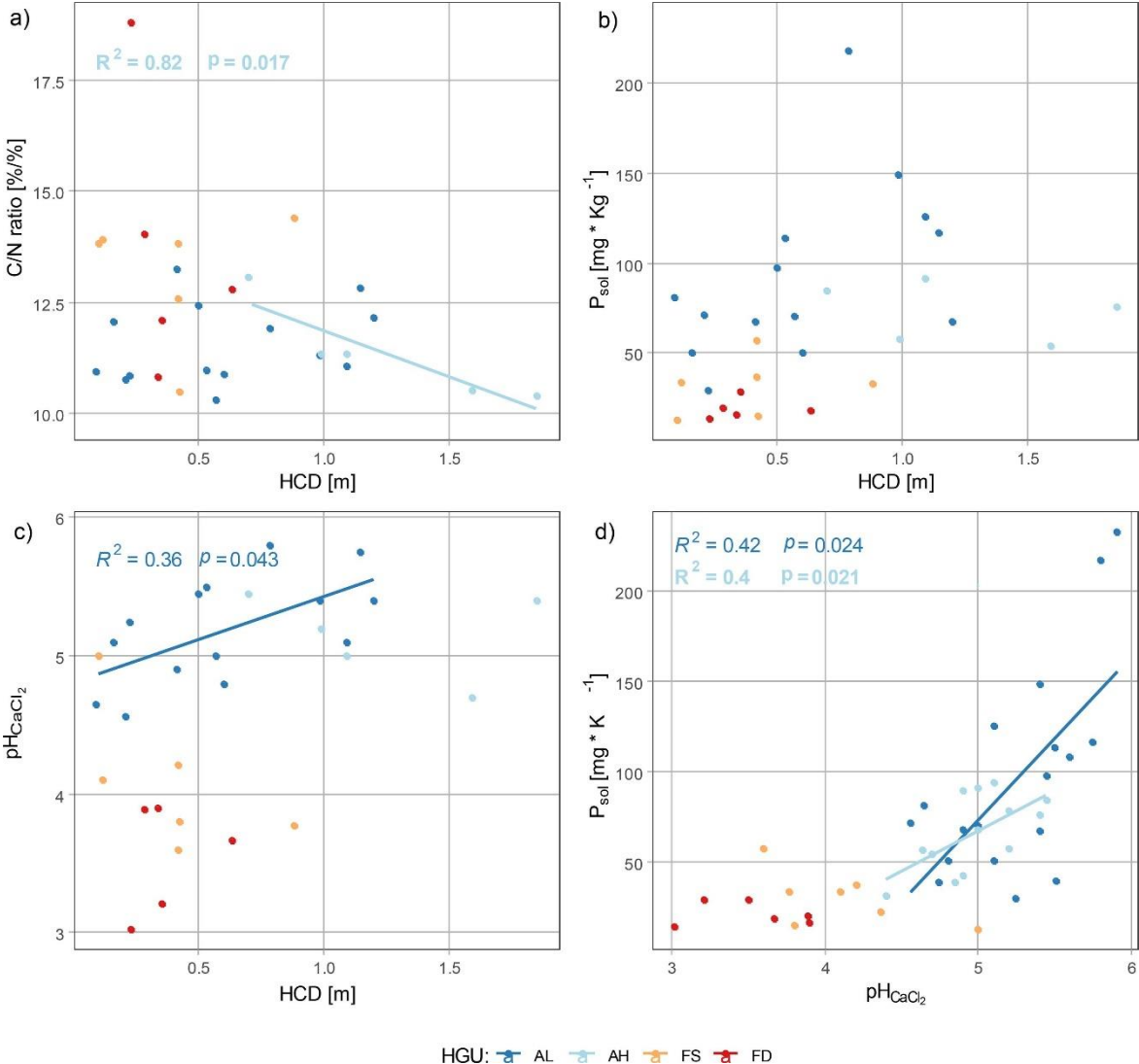


Figure 9. Regression analysis between the starting depth of appearance of hydromorphic characteristics (HCD) and (a) C/N ratio, (b)  $P_{sol}$ , (c)  $pH$  and the effect of  $pH$  on (d)  $P_{sol}$ . Linear regression line and  $R^2$  is only showed for significant regressions ( $p < 0.05$ ). HGU- Hydrogeomorphic Unit: Active floodplain-Low (AL), Active floodplain-High (AH), Former

floodplain- seepage influenced (FS), Former floodplain – disconnected from the river hydrology (FD).

Soil pH had a positive correlation to  $P_{\text{sol}}$  (Figure 9 d). In the AL, for example the increment of  $\text{pH}_{\text{CaCl}_2}$  from 4.5 to 5.9, depicted a linear increment in  $P_{\text{sol}}$  from around 30mg/kg up to 150 mg/kg. The same effect was found for AH, but the increment in  $P_{\text{sol}}$  ranged from around 50 mg/kg to 100 mg/kg. The effect of  $\text{pH}_{\text{CaCl}_2}$  on  $P_{\text{sol}}$  in the former floodplain HGUs was not significant. The results of the ANCOVA analyses proved that there is an influence of the HGU on the relation between  $P_{\text{sol}}$ - $\text{pH}_{\text{CaCl}_2}$  ( $\text{Pr} (>F)$  0.011). No influence of the HGU was observed in the relation between HCD and  $P_{\text{sol}}$  (Figure 9b); however an overall correlation between these two parameters was observed (Appendix B). We found a strong exponential fit between  $\text{pH}_{\text{CaCl}_2}$  and  $P_{\text{sol}}$  if the HGU categorization is neglected (Figure 10). A positive correlation was also identified between HCD and  $\text{pH}_{\text{CaCl}_2}$  for AL, the deeper the topsoil without hydromorphic mottling the higher the pH value (Figure 9c). In AH a negative effect of the hydromorphic mottling was identified for the C/N ratio, the deepest the first appearance of hydromorphic characteristics, the smallest the C/N values (Figure 9a).

The number of flooding days in the active floodplains (AL and AH) had a positive correlation in relation to topsoil clay content (Appendix C). In addition, with increasing number of flooding days the first depth of appearance of hydromorphic characteristics was found closer to the soil surface. There was no influence of the position in the active floodplain low or high (AL and AH) in the effect of flooding days on other physicochemical parameters (Appendix C).

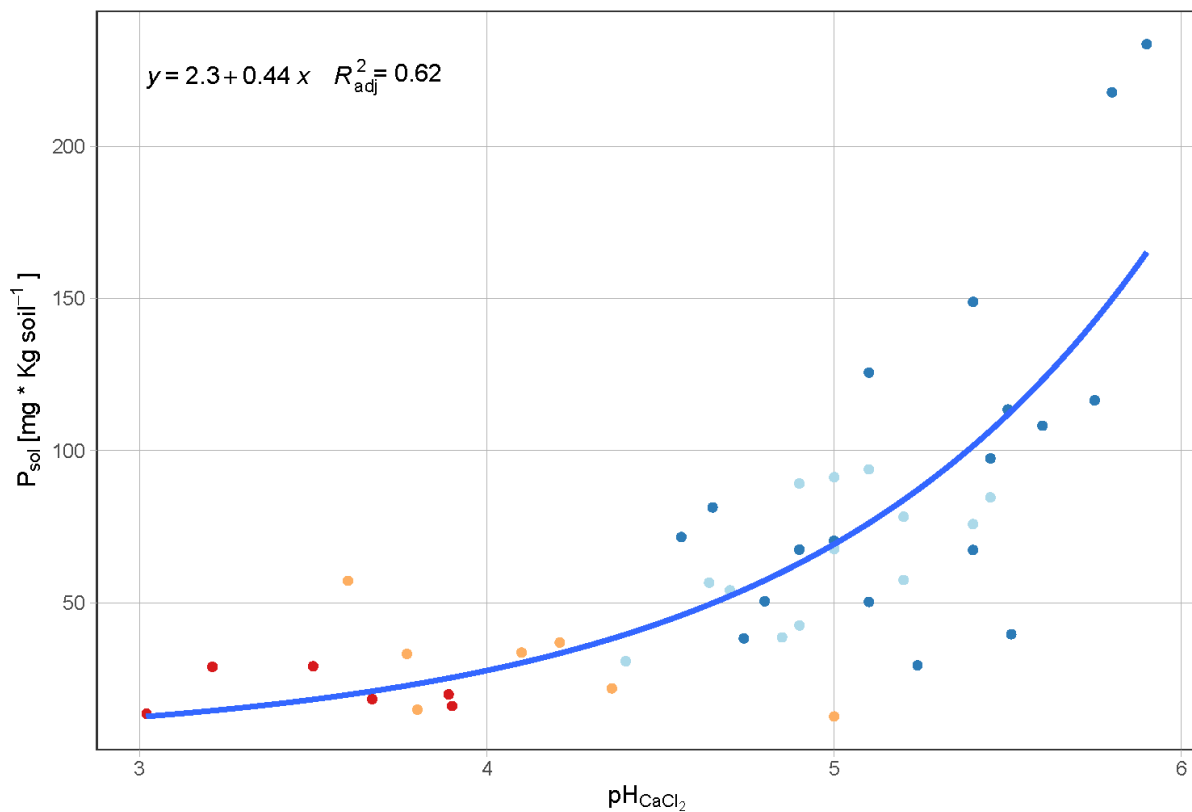


Figure 10. Exponential regression between pH<sub>CaCl<sub>2</sub></sub> and P<sub>sol</sub>. Dark blue dots: Active floodplain-Low (AL), Light blue dots: Active floodplain-High (AH), Orange dots: Former floodplain- seepage influenced (FS), Red dots: Former floodplain – disconnected from the river hydrology (FD).

## 2.5 Discussion

### 2.5.1 Distribution of soil types, formation processes and properties per HGU

Floodplain soils reflect the influence of flooding water, groundwater, static and seepage water on their formation processes (Rinklebe & Langer, 2008). Furthermore, the highly dynamic geomorphology of the floodplain plays a role on how the hydrological processes influences the soil matrix. Fluvic Cambisols dominated the active low floodplain (AL). Cambisols are particularly common in alluvial and eolian deposits. In wetlands they usually co-occur with Fluvisols and Gleysols (IUSS Working Group WRB, 2015). In the context of the Elbe floodplains, Fluvic Cambisols have been

identified in the stream banks of the active floodplain as Eutri-Fluvic Cambisols (Schwartz et al., 2003b) and mentioned as the dominant soil type by Schirmann, et al. (2016) in an agricultural study performed in young groundwater-influenced floodplain deposits of the Elbe river in Eastern Germany.

The soils in the active high floodplain (AH) are Fluvic Lamellic Arenosols. In these soils, the short distance to the river leads to low groundwater levels during most summer and autumn periods. Combined with water extraction by deep rooting trees, soils in the active high floodplain become rather dry with strong and deep soil aeration. Thus, topsoil is free of hydromorphic properties. Moreover, the high porosity and the rare flooding leads to a soil development, where hydromorphic properties are restricted to the deep subsoil and with the exception of humus accumulation, no evidence of pedogenic alteration is obvious.

The predominant soils in the former floodplain, seepage (FS) were classified as Gleyic Fluvisols. These soils are characteristic of periodically flooded areas with prominent redoximorphic features at least in the subsoil (IUSS Working Group WRB, 2015). Given the empoldered nature of the soils of this HGU, the sedimentation of particulate matter from the Elbe River is prevented; nevertheless, stratification and clear signs of reduction and oxidation were evident due to frequent influence of groundwater fluctuations (Figure 5). In the Elbe floodplain, Fluvisols have been identified by Schwartz, et al., (2003b) as Humic - Epigleyic Fluvisols in the relictic floodplain and in the recent floodplain as Humic - Endogleyic Fluvisols or as Eutric Fluvisols by (Rinklebe & Langer, 2008).

On the disconnected former floodplain (FD), the dominating soil reference group was Fluvic Gleysols. These plots had a higher and more constant groundwater table than

those plots connected to the river hydrology in FS, AH and AL. Gleysols are soils with high groundwater table and located in deeper sections of the landscape (Hourani & Broll, 2021). These soils are associated to higher carbon content (IUSS Working Group WRB, 2015; Rinklebe & Langer, 2008) increased base saturation, CEC as well as higher contents of P and K compared to highland soils (IUSS Working Group WRB, 2015). Gleysols in FD were characterized by higher contents of TC and TN, but presented the lowest values in BS, CEC and P content when compared to all the other HGUs. This may be related to a higher nutrient input in the active floodplain zones and recent sedimentation events in these units.

AH presented the deeper starting point of hydromorphic features in comparison to all other HGUs. This could be attributed to the high position of these plots in the floodplain landscape and the predominance of sand through the whole profile (Figure 4), which results in enhanced percolation. Sand dominated saturation may occur in deeper areas where they become in contact with the phreatic level (Veneman et al., 1998).

In the profiles with finer soil textures, hydromorphic features were found within the first 50 cm, directly below the Ah horizon - a strong indicator of long-term saturation and/or a high ability of accumulation of precipitation water (Kawalko et al., 2021). The soils located in FD with predominant finer textures, presented hydromorphic characteristics closest to the topsoil. Located in the former floodplain, but far away from the Elbe River, these sites are not directly influenced by the river water fluctuations. To control the hydrology, these areas are managed with nearby drainage ditches that remove excessive water. The actual moisture regime is thus controlled by an almost constant groundwater level in the sandy underground that is connected to the drainage system, and the low permeability of the upper layers of the fine-grained fluvial deposits. These

soil layers prevent a fast deep drainage and lead to long-lasting wetness even in the topsoil.

Within the near-dike seepage zone (FS), in case of high water in the river the soil water movement is directed upward. Especially in coarse textured soils, large amounts of water are flowing to the soil surface, inundate the woodland and may be transported off by a drainage system. Groundwater enriched in reduced iron and manganese meet the oxidized topsoil and the diffusing oxygen from the air, and thus leading to the precipitation of hydroxide, partly in concretions. In most cases, hydromorphic features started within the upper 50 cm, and iron concretions and mottling increased in deeper layers (Figure 4). The deep aeration of these soils in case of mean and below mean river water levels are a reason for the broad band of hydromorphic properties, which characterize the soils of this HGU. Similar characteristics have been observed in a coarse loamy catena in a coastal plain in North Carolina, where redoximorphic features ranged from 40 to 125 cm with increasing abundance in depth (Severson et al., 2008).

The identification of the depth of hydromorphic characteristics, in the different units in the lateral gradient of the floodplain, could serve as a proxy of oxygen availability for the hardwood species. However, a deeper analysis of soil water balance and soil hydraulic properties would be necessary to identify zones in which new seedlings would not be at risk of anoxic conditions. As in wetlands, the effects of inundation and saturation were intensely reflected in oxygen availability and redox potential at 30 cm below soil surface, which is considered a critical depth with respects to plant growth and survival in this ecosystem (Faulkner & Patrick, 1992).

### *2.5.2 Influence of the hydrological processes (e.g. flooding days, lateral distance to the river) on soil physicochemical properties.*

The influence of the lateral floodplain gradients (i.e. geomorphic functional units), and how they lead to strong variability of different soil parameters, has been acknowledged for different catchments around the world (Noe et al., 2013; Steiger et al., 2005). Pronounced differences were recognized between the four analyzed HGUs, especially regarding nutrient content (Figure 7 e, f ; Appendix D a). These differences were mainly explained by the lateral hydrological connectivity of the floodplain soils to the Elbe (Figure 6).

For instance, in the active floodplain (both, low and high) higher contents of  $P_{\text{sol}}$  and  $K_{\text{sol}}$  were identified (Figure 7 f), Appendix D a). The units in the former floodplain, seepage influenced and disconnected from the river, were related to higher TC and TN as well as lower pH values. Similar variability has been described for alluvial and non-alluvial soils of deciduous forest patches in Quebec-Canada (Saint-Laurent & Arsenault-Boucher, 2020). The authors attribute higher TC and TN content in non-alluvial soils, comparable to our FD plots, to a higher accumulation of litter, soil acidity and increased decomposition due to higher microbial activity, which is visible in soil characteristics as the dark color of the Ah horizons. These processes might have affected our FD study sites similarly, indicating the possibility of further soil development given little to no influence of flooding water and the absence of input of new sediments. Furthermore, FD plots, where the highest contents of TC, TN and C/N were observed (Figure 7), presented a higher content of clay when compared to AH and FS. Finer soil texture has been related to a higher presence of SOC in floodplains and hardwood floodplain forests (Graf-Rosenfellner et al., 2016; Heger et al., 2021; Steiger & Gurnell, 2003).

With  $\text{pH}_{\text{CaCl}_2}$  4.4 – 6.0, active sites were within the range of previously reported values in the Elbe floodplain (Rinklebe & Langer, 2008), while soils in the former floodplain were more acidic (Figure 7 d). Although the difference between the two units located in the active floodplain is not significant, higher pH values have been documented for low lying clay loams when compared to high positioned sandy loams in alluvial forested soils in the Raritan River in New Jersey (Frye & Quinn, 1979), the range of pH values was similar to those in our study sites.

Moreover, a mean pH value of 5.9, in actively flooded soils located in the Elbe floodplains was recently published Kaden et al., (2021) similar to our maximum value for the AL HGU (Appendix A). In general, soil pH in the Elbe floodplains is considered slightly to moderately acidic if compared to other bottomland floodplain soils of German rivers (e.g. Rhine, Weser, Danube) (Kaden et al., 2021). Nevertheless, the lowest topsoil pH values were found in FD, sites with practically no influence of flooding. The absence of flooding in the disconnected sections of the floodplain, favors the accumulation of litter layers over time, as there is neither burial by sediment deposition nor washing out of litter, thus increasing the production of organic acids during decomposition processes (Hong et al., 2019). In addition, the accumulation of soil organic matter could contribute to the release of  $\text{H}^+$  into the soil water solution, thus decreasing the pH values (Hong et al., 2019; Kirschbaum, 1995) . Moreover, Shupe et al. (2021), reported different species composition in these former floodplain forests with no connection to the Elbe hydrology, where tree species as *Alnus glutinosa* and *Carpinus betulus* were dominating species in addition to *Quercus robur* and *Ulmus laevis* - the main species in the other HGUs.

The difference in species compositions results in different litter quality and root exudates which could influence soil properties (e.g. pH) and soil microbial community



(Chandra et al., 2016; Devi, 2021; Haghverdi & Kooch, 2019). This also supports the fact that forest soils have lower pH when compared to grassland soils and thus influencing soil bacterial community and decomposition (Kaiser et al., 2016). The pH values reported for high and low grassland soils in the lower middle Elbe nearby our plots were slightly higher than forested plots (Heger et al., 2021). The difference of topsoil pH of the FD HGU to other parts of the floodplain may additionally be interpreted with the long-lasting and constant soil development: no supply of bases by flooding since dyke construction in the 12th century and no input of nutrients by forestry in contrast to the surrounding agricultural grasslands.

### *2.5.3 Interactions between soils physicochemical properties*

In floodplain soils phosphorus and nitrogen mineralization is expected to increase in places with a stronger hydrologic connection to the river, downstream and in lower geomorphic units (Binkley & Hart, 1989; Noe et al., 2013). Our results show that  $P_{\text{sol}}$  is higher in the active floodplain HGUs (AL, AH) when compared to the HGUs in the former floodplain (FS, FD) (Figure 7 f), and that the difference was significant. The topsoil accumulation of P is promoted by the sedimentation of particles from the Elbe River, which was characterized by strong nutrient enrichments in the past and still exhibits elevated levels of nutrients (Petersen & Callies, 2002). Lowest  $P_{\text{sol}}$  availability in the former floodplain HGUs, in particular in FD, could be the result of increased Al and Fe oxides, increasing reactive surfaces, which promote P sorption. Concurrently, the lower pH values as well as a stronger presence of Fe and Mn oxides mottling, evidenced in FD, could be contributing to increased P sorption and P trapped in nodules and concretions (Achat et al., 2016; Gasparatos et al., 2019), respectively.

#### *2.5.4 Implications for hardwood floodplain forest restoration and potential for replicability at the regional scale.*

Hardwood floodplain forests in the lower middle Elbe have been severely degraded and intensively used for hundreds of years. When an ecosystem undergoes such severe degradation, successful restoration processes require a sophisticated understanding of the physical, chemical and biological properties of soils (Heneghan et al., 2008). In the case of forest restoration, physical and chemical parameters of soils as for example soil texture, pH, cation exchange capacity and others, are indicators of water availability and nutrient cycling, respectively (Lozano-Baez et al., 2021; Schoenholtz et al., 2000). These variables, directly relate to forest restoration practice as they affect seed germination, seedling survival, biomass accumulation and forest productivity. An increase of plant available phosphorous, an essential mineral for primary productivity, connected to higher pH values in active compared to former floodplain sites, indicates that the active floodplain could be a favorable location for forest restoration with typical hardwood floodplain forests species. Nevertheless, available and total phosphorous are not necessarily coupled and this could have different implications for nutrient recycling. In the case of the former floodplain, the predominance of acidifying soils hints that reforestation efforts should consider species that are adapted to this type of condition, as for example, Birches (*Betula* spp.) which tolerate a wide spectrum of soil pH, in fact they prefer rather acidic soils and their optimal pH ranges between 4.0 and 5.0 (Jonczak et al., 2020), yet this should be tested under the specific conditions of our study sites located in this section of the floodplain.

Shupe, et al. (2021) did not find significant difference in aboveground C stocks of old forests when the hydrological condition of the floodplain (i.e. HGUs in our study) is considered. However, *Quercus robur* L., a typical species of this ecosystem presents the highest sequestration rates in the active Elbe floodplain, particularly under flooding

conditions, which was related to higher P availability (Shupe et al., (2022)). Our analyses showed that sites in the active floodplain – high and low – as well as those in the seepage water influenced sites benefit from the hydrological connection to the river in terms of nutrient availability for plant development. These relationships are likely transferable to other central European lower catchments, in cultural landscapes that experienced substantial anthropogenic modification through diking, such as Danube, Rhine, Elbe and Oder Rivers (Koenzen et al., 2021). However, river sediment loads and particulate nutrient contents (Beusen et al., 2005), as well as local floodplain ecology can vary substantially (Arias et al., 2018; Hughes, 1997), which highlights the need of further localized studies under varying environmental conditions.

## 2.6 Conclusions

This study provides insight into the distribution of soil types, formation processes, physicochemical characteristics, and their interactions, in four different hydrogeomorphic units, two in the active floodplain and two in the former floodplain, in remnant hardwood forests of the lower middle Elbe river floodplains. We found that diking had a strong influence on floodplain soil development and controls nutrient availability. In the active floodplain of the Elbe River, soil reference groups that indicate fresh sediment deposition as well as slow soil development were prevalent (Fluvisols and Fluvisols). Fluvisols (FS) and Gleysols (FD), both reflecting former alluvial or groundwater influence, characterized former floodplains.

Active HGUs were related to higher availability of important nutrients (e.g.  $P_{\text{sol}}$ ), which could be attributed to active sedimentation of riverine particulate matter as well as the input of soluble nutrients from the flooding water. In contrast, former floodplain soils acidified significantly and showed lower nutrient availability, already in the seepage

zone behind the dike. This occurs in the absence of flooding, which results in increased litter accumulation, decomposition and further soil development.

Direct relationships between phosphorous availability and pH were apparent, particularly in the active low and high zones of the floodplain, which does not occur in the HGUs in the former floodplain.

We conclude that the active floodplain could provide a higher potential for forest restoration projects regarding soil physicochemical parameters, particularly nutrient availability. Since possible areas for forests restoration in the former floodplain could be reactivated by means of dike relocation projects, forests behind the dike could develop in the direction of typical riverine floodplains. Soil quality evaluation in the light of restoration projects is pivotal for meeting the needs of the biotic component of the ecosystem, especially hardwood forests.

## Chapter 3

### Article 2: Sap flow velocity under drought and high evaporative demand: A comparison of two hardwood floodplain forest species under different soil conditions

#### 3.1 Abstract

Hardwood floodplain forest species like *Quercus robur* (*Q.robur*) and *Ulmus laevis* (*U. laevis*) are adapted to the hydrological fluctuations of floodplain soils connected to the river hydrology. The expected increase in soil drought, as well as lower groundwater levels in Central Europe pose challenges for these species, prompting various physiological adaptations to survive periods with water limitation. Thus, we aimed to assess the variability of sap flow velocity of both species under different situations of soil water availability, in sandy and loamy soils under high evaporative demand.

We conducted the study in the active floodplain of the lower middle Elbe. Two sites were selected representing contrasting soil texture (sand and loam). Sap flow was measured in five trees per species per site, using heat-ratio method devices. Three soil profiles per site were instrumented with sensors to measure volumetric water content and water tension up to a depth of 1.60 m. We selected two weeks during vegetation period representing high soil water availability and the other to represent low soil water availability, both periods experienced high vapor pressure deficit (VPD). A VPD driven model (Jarvis) estimating potential sap flow velocity was used to identify deviations due to soil water limitation and soil texture.

*Ulmus laevis* consistently had higher daytime sap flow velocity than *Q. robur* (e.g. in loamy soils: 12 cm/h and 7 cm/h, for *U. laevis* and *Q. robur*, respectively), but displayed greater variability within each period, decreasing sap flow velocity with increasing

drought. *Q. robur* maintained constant daytime sap flow velocity within each period, however showed a reduction in sap flow in the sandy site when compared to the loamy site. The Jarvis model predicted higher sap flow under non-limited conditions, indicating soil water potential's stronger role in regulating velocity than vapor pressure deficit particularly in sand dominated soils.

Our findings highlight the influence of site-specific conditions on *Q. robur* and *U. laevis* adaptation to water limitation.

## 3.2 Introduction

The impacts of climate change in Europe, and the associated damages to ecosystems have been acknowledged by the IPCC with very high confidence (Bednar-Friedl et al., 2022). Warming exerts particularly strong pressure on habitat conditions of terrestrial ecosystems, leading to anticipated changes in functions and shifts in species compositions (Dale et al., 2000). European forests, are experiencing the effects of drier and hotter summers, which have been documented to elicit species-specific responses of trees to water availability, heat waves and evaporative demand have been documented (Allen et al., 2010; Hacke & Sperry, 2001a; Martínez-Sancho et al., 2017; Weigel et al., 2023). Furthermore, in Central Europe, the projected increase of streamflow drought, soil moisture drought and lower groundwater levels (Bednar-Friedl et al., 2022) directly threatens the periodic flooding and water availability that floodplain forests depend on to maintain their ecological value (Havrdová et al., 2023).

Hardwood floodplain forests are one of the most productive and species-rich forest ecosystems in Europe, providing various essential ecosystem services at the regional and global scale, including biodiversity preservation (Havrdová et al., 2023), and long term carbon storage (Dybala et al., 2019; Heger et al., 2021b; Marks et al., 2020). Natural hardwood floodplain forests in Europe are commonly dominated by a combination of *oaks*, *elms* and *ashes* (Schnitzler, 1994). Among these, *Q. robur* and *U. laevis* exhibit the highest aboveground carbon storage in the floodplain forests of the lower middle Elbe (Shupe et al., 2021). Both species are adapted to the typical hydrological fluctuations of floodplain soils.

Considering the highly dynamic hydrological conditions of floodplain soils, physiological water management strategies of trees play a main role for vitality and survival. Trees coordinate hydraulic and stomatal regulation to manage water use

under periods of stress (Klein, 2014; Mcdowell et al., 2008). While xylem traits (e.g. vessel width) offer long time control, stomata regulation responds to environmental signals by adjusting leaf transpiration (Cochard et al., 1996; Tyree & Zimmermann, 2002). Different tree species use different water use management strategies to adapt to soil water availability, either isohydric or anisohydric strategy. The isohydric strategy as defined by Tardieu & Simonneau, (1998) consists in keeping leaf water potential constant over time, while the anisohydric strategy leaf water potential shifts with changes in evaporative demand. *U. laevis* is a riparian species characterized by its high water demand and tolerance to water logged environments (Venturas et al., 2014). Studies have shown that *U. laevis* has higher survival and increased growth rates in heavy clay soils with prolonged water logging compared to other elm species (Cicek et al., 2007; Venturas et al., 2014). Flood-tolerant species like *U. laevis*, possess anatomical and physiological traits such as large xylem vessels and high vessel frequency, enabling greater water transport capacity (Venturas et al., 2013). However, the presence of large xylem vessels also makes them more susceptible to drought-induced cavitation and less resistant to drought (Hacke & Sperry, 2001b; Tyree & Zimmermann, 2003; Venturas et al., 2013). *Q. robur*, commonly found in mesic areas within floodplains and valleys of major European rivers, possesses a significant capacity to adapt to drought periods, unlike *U. laevis* (Mikac et al., 2018; Schnitzler, 1994). *Quercus spp.* are considered drought tolerant due to their deep-rooting capability and substantial stomatal control, allowing them to avoid xylem dysfunction during drought periods (Bose et al., 2021; Cochard et al., 1996, 2000)

The main abiotic factors influencing tree water use are global radiation, vapor pressure deficit and soil water availability (Granier et al., 2000; Guillén et al., 2022a; Wilson et al., 2008). Tree response to atmospheric water demand has been widely documented



(López et al., 2021), the influence of edaphic water stress however is not clear, and in some cases it has been considered less relevant or just an additive effect for tree water management (Guillén et al., 2022b; Sancho-Knapik et al., 2022). Therefore, it is crucial to gain understanding of pedogenic controls on drought intensity and duration, as they play a vital role in determining species-specific strategies for performance and survival (Martínez-Sancho et al., 2017).

In floodplains, soils are extremely heterogeneous due to the geomorphological variability caused by flooding and sedimentation. Within the active floodplain of the Elbe, two distinct hydrogeomorphological units can be identified; elevated sites characterized by sand predominance, and depressions and plains with a higher loam content and greater influence of flooding water (Vásconez Navas et al., 2023). Within the rooting zone, the textural composition of the soil substrate, like alluvial loams and sands, determines the total pore volume and the pore size distribution and thus the amount of plant available water – defined as the water content between field capacity and permanent wilting point.

Given the expected increase in drought frequency and intensity (Bednar-Friedl et al., 2022), we aim to provide insights into the implications of drought on temperate hardwood floodplain forests. Therefore, we investigate the influence of high vapor pressure deficit and different soil hydrology regimes on sap flow velocity patterns in two major co-occurring hardwood floodplain forest species (*Q. robur* and *U. laevis*). We also identify their adaptation strategies in contrasting soil substrate composition. Our objectives are to determine and compare the changes in sap flow velocity of *Q. robur* and *U. laevis* in the lower middle Elbe floodplain, (i) during drought periods with high VPD but contrasting soil water availability and (ii) in two different active floodplain sites dominated by contrasting soil substrate (loam and sand).

### 3.3 Methodology

#### 3.3.1 Research area and forest selection

The research area is part of the *UNESCO Biosphere Reserve River Landscape Elbe* and is located in the federal states of Brandenburg and Lower Saxony, Germany (Figure 11). This region is characterized by a transition between maritime and continental climate (von Storch et al., 2018) with a mean annual temperature of 9.7 °C and a mean annual precipitation of 578 mm as recorded from annual regional data for 30 years (1990-2020) by the Climate Data Center of the German Weather Service (DWD, 2021). Regarding sedimentological and pedological processes, the area has been described as a Holocene alluvial plain in which the floodplain parent material has developed from the sedimentation of Pleistocene and Holocene sands, later superimposed by Holocene alluvial sands, loams and clays (Gröngröft et al., 2005; Schwartz et al., 2003b). Diking since the 13th century has cut off large areas of the floodplain from regular flooding thus dividing the plain in an active and former floodplain.

Within the research area, we selected two hardwood forests located in the active floodplain of the lower Middle Elbe River. Both forest sites comprised typical hardwood-floodplain-forest species (*Quercus-Ulmetum*), but differed in terms of landscape position and hydrological condition within the floodplain. One forest was situated on a levee, characterized by fewer flooding days and predominantly sandy soil texture in topsoil and subsoil. This site will be referred to as “sandy site”. The other forest was located in a depression, characterized by more flooding days and predominance of loamy texture throughout the profile. This site will be referred to as “loamy site”. Within each forest site, a study plot of 2500 m<sup>2</sup> (25 m x 100 m) was established.



Figure 11. Location of the sandy (Lat=53.1796°, Long=11.0087°, Elbe km 526) and loamy (Lat=53.0877°, Long=11.2945°, Elbe km 498) study sites in the active floodplain of the lower middle Elbe.

### 3.3.2 Soil sampling and instrumentation.

Three soil profiles per site were sampled to a depth of 1.6 m. At the sandy site, the soils were classified as Fluvic Arenosols and at the loamy site as Fluvic Cambisols (IUSS Working Group WRB, 2015).

A mixed soil sample (~ 500 g) per horizon was taken and prepared (air-dried and sieved <2 mm) for grain size distribution analyses according to the sedimentation method stated in DIN ISO 11277. The sand fraction (63 µm–2000 µm) was analyzed by dry sieving using a vibratory sieve shaker (Vibro, Retsch GmbH, Germany), soil particles <63 µm were analyzed by sedimentation in a Sedimat 4–12 (Umwelt-Geräte-Technik GmbH, Germany). Detailed information on soil profiles data and grain size distribution data are available in Appendix A.

To quantify soil water characteristics, the three soil profiles per site were instrumented at defined depths of 10, 30, 60, 100 and 160 cm. For the monitoring of soil volumetric

water content ( $\Theta$ ; vol%) and soil water tension ( $\Psi$ ; hPa), one soil water content reflectometer (CS650, Campbell Scientific, Inc., Logan, UT, USA) and a watermark sensor (200SS, Irrrometer, Riverside, CA, USA) were installed in each depth (in total 5 per profile). The  $\Theta$  data was recorded by a CR300 data logger (CR300, Campbell Scientific, Inc., Logan, UT, USA). The  $\Psi$  data of the watermark sensors was collected with an Irrrometer data logger (Watermark Monitor, Irrrometer, Riverside, USA). Both data loggers continuously recorded data in an hourly resolution. All data was corrected for temperature effects as suggested by the manufacturers. Additionally, a groundwater diver was installed in each forest site with a TD-Diver (TD-Diver, Van Essen Instruments, Delft, Netherlands) complemented with a Baro-Diver (Baro-Diver, Van Essen Instruments, Delft, Netherlands) at one of the sites to allow a barometric pressure correction.

### *3.3.3 Soil water data analyses*

Measurements of  $\Psi$  (hPa) and  $\Theta$  (vol%) across the three profiles were averaged per depth. We then calculated a mean value of  $\Psi$  for the 160 cm of soil by averaging the depth-weighted  $\Psi$  at all measured depths. Additionally, the amount of water stored in the upper 160 cm of the soil profile was calculated and expressed in millimeters as the soil water storage (SWS). To determine the SWS, five depth intervals were created over the entire 160 cm depth, and their values were summed up. The upper and lower boundaries of these depth intervals were defined as the midpoint between the sensors. The 160 cm sensor's lower boundary was defined as 160 cm, as no further soil depths were studied. The mean daily  $\Psi$ ,  $\Theta$  and SWS data per depth as well as the averaged values for the 160 cm of soil are shown in Appendix D for every site and period.

### 3.3.4 Meteorological data and study period selection

Outside of each forest we installed a meteorological station in an open place. At each station, relative humidity (RH) and air temperature (T) were measured with a CS215 sensor (CS215, Campbell Scientific, Inc., Logan, UT, USA), global radiation (R<sub>g</sub>; W/m<sup>2</sup>) was recorded with a pyranometer (CS300, Campbell Scientific, Inc., Logan, UT, USA), and the precipitation was measured by a rain gauge (Kalyx-RG, Campbell Scientific, Inc., Logan, UT, USA) in the loamy site and by a (MR2-01m, Meteoservis v.o.s., Vodňany, Czech Republic) in the sandy site. Meteorological data was recorded every 30 minutes using an automated logging system (CR1000, Campbell Scientific, Inc., Logan, UT, USA).

The vapor pressure deficit (VPD) was calculated using the values of relative humidity (RH, %) and air temperature (T, °C) applying Eq. 1:

$$\text{Equation 1} \quad VPD = 0.001 * \left(1 + \frac{RH}{100}\right) * 610.7 * 10^{\left(\frac{7.5T}{237.3+T}\right)}$$

Based on the recorded meteorological and soil water data, two study periods were selected during the vegetation season of 2020. The first period, named high water availability, was from June 21 until June 27 and represented high evaporative demand at high soil moisture availability. The second period, named low water availability, was from August 6 until August 12 and represented high evaporative demand at low soil moisture availability. For the statistical summary of micrometeorology and soil water data for the selected periods refer to Table 2.

### 3.3.5 Tree selection, tree xylem instrumentation and sap velocity calculation

At each study site, five *Q. robur* and five *U. laevis* were selected. Xylem sap flow was measured with self-constructed heat ratio method sensors based on (Burgess

et al., 2001). Every sensor unit consisted of two temperature probes and a heater unit that were introduced in the sapwood after removing the bark and reaching the cambium of every tree. The central heater sends a heat pulse and the sap flow moves the heat pulse by conduction and convection through the xylem. The temperature probes, equidistant above and below the heater, measure the absolute temperature rise, which is influenced by the sapwood thermal diffusivity, assumed to be  $2.5 \cdot 10^{-7} \text{ m}^2/\text{s}$  (Burgess et al., 2001), and the velocity of the sap flow. Thus, heat pulse velocity ( $V_h$ ; cm/h) is determined by the following equation:

$$\text{Equation 2} \quad V_h = \frac{k}{x} * \ln\left(\frac{t_1}{t_2}\right) * 3600$$

Where  $k$  is the sapwood thermal diffusivity,  $x$  is the distance between each probe and the heater ( $x=0.5 \text{ cm}$ ),  $t_1$  and  $t_2$  are the measured increases in temperature downstream and upstream at equidistant points of the heater, after the heat pulse was sent. Species-specific wood properties, like wood density and water content of the wood, should be considered to convert  $V_h$  to sap flow velocity, as they could affect the conduction. However, the use of  $V_h$  as a proper representation of sap flow dynamics is possible considering that no variables but only constants are used for the conversion, thus the relative proportions are expected to be similar (Burgess et al., 2001), we measured  $V_h$ , but the terminology used through the paper is sap flow velocity for simplification purposes. Further constants and equations used for corrections of possible misalignment were followed as describe by Burgess (2001).

The heat pulse was sent for 8 seconds, every 30 minutes, the heat dissipation was recorded for 80 seconds before and 100 after the pulse. The heater and temperature probes were connected via a self-built board to an Arduino (Arduino Mega 2560, Arduino, Arduino SA, Chiasso, Switzerland). The analog measurement data was converted into digital values using an analog-to-digital converter (ADS1115, Adafruit,

New York City, NY, USA). The measured data was stored onto an SD card and collected during field campaigns. The calculation of  $V_h$  (Equation 1) was performed with the collected temperature data using MATLAB (R2019b, The Mathworks, Inc., Natick, MA, USA).

We installed three sensors per tree at an approximate height of three meters to avoid possible damages caused by flooding or game. The three sensors were installed radially at congruent angles. The collected data for the inner and outer thermistors of every position was inspected, and after a first observation, we presume that the variability of sap velocity within the sapwood follows the following species-specific curves.

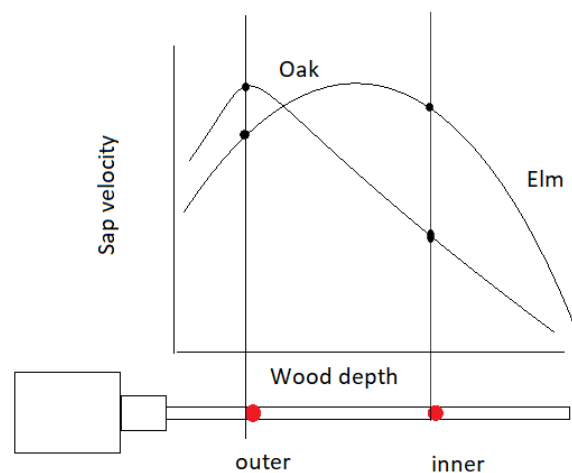


Figure 12. Proposed curves of sap velocity with increasing sapwood depth for *Q. robur* (Oak) and *U. laevis* (Elm).

The presented curve for *Q. robur* (Figure 12) is supported by literature where a peak for radial sap velocity closer to the cambium in the youngest ring has been described (Cermak et al., 1992; Granier et al., 1994) and also in studies done in *Quercus pubescens* (Cermak & Nadezhdina, 1998; Poyatos et al., 2007). For *U. laevis* no specific literature on radial sap flow patterns or curves was found, however high vessel frequency and high percentage of grouped vessels have been documented for this species in early and latewood (Venturas et al., 2013, 2015). Thus, the sap velocity

was averaged for the inner and outer position of every installed sensor per species to avoid under or overestimation of sap flow velocities. Mean daytime sap flow velocity was calculated by averaging the calculated  $V_h$  per tree during hours where global radiation ( $R_g$ ) was higher than zero.

### 3.3.6 Jarvis - Potential sap flow velocity model

Potential sap flow velocity ( $V_{h_{modeled}}$ , cm/h) was calculated using the Jarvis model (Dierick & Hölscher 2009; O'Brien et al. 2004) (Eq. 3), assuming that global radiation  $R_g$  ( $W/m^2$ ) and VPD (kPa) mainly control  $V_h$  under non-water-limited conditions. Thus,  $V_{h_{modeled}}$  is expected to equal  $V_h$  in periods with high water availability. A possible reaction of trees to soil drought is the reduction of sap flow velocity, in that case a deviation of  $V_h$  from  $V_{h_{modeled}}$  would be expected.

$$\text{Equation 3} \quad V_{h_{modeled}} = a \frac{R_g}{b+R_g} \times \frac{1}{1+\exp\left(\frac{c-VPD}{d}\right)}$$

The model parameters  $a$  (cm/h) represents the maximum modeled sap flow under optimal conditions, the model parameter  $b$  ( $W/m^2$ ) describes the measure of the light saturation level, parameters  $c$  and  $d$  represent the VPD response (kPa). Parameters  $a$ ,  $b$ ,  $c$ , and  $d$  in the response functions were estimated by minimizing the residual sum of squares using a Gauss-Newton algorithm. The model was calibrated by using our initial measurement period in June, as this time period was assumed to be non-water limited and hence we expected actual sap flow to follow potential sap flow. A ratio between modeled and measured sap velocity values ( $V_{h_{modeled}}/V_{h_{measured}}$ ) was calculated and plotted against the mean soil water potential ( $\Psi$ ) to depict if there is an influence of the soil drought on measured values of sap flow velocity when compared to potential modeled values. All calculations were performed by considering the daily



mean of daytime  $V_h$  and  $V_{h_{modeled}}$  values for both species, as well as the weighted daily means of  $\Psi$ .

### *3.3.7 Statistical analyses and data processing*

Statistical analyses were conducted using R 4.1.0 (R Core Team, 2021). We applied a linear mixed-effect model using the function 'lmer' from the package lme4 (Bates et al., 2015) to examine the influence of species, site conditions, water availability and their interaction on the mean daytime sap flow velocity (response variable). The starting model contained the three-way interaction of the factorial variables species, site and month; and measured positions as well as measured days were used as a random effect to account for repeated measurements. Normality and homoscedasticity assumptions were checked by visual inspection of the model residuals and significant differences were identified by a Tukey post-hoc test.

To test the influence of soil hydrology on sap flow velocity, we applied a multiple linear regression model (MLR). The MLR model was performed starting with all predictor variables ( $VPD$ ,  $R_g$ ,  $\Theta$ ,  $\Psi$ ) and the best fit was selected based on the Akaike Information Criterion (the smallest AIC was selected). Residuals were checked for normality using the Shapiro-Wilk test ( $p < 0.05$ ) and variance of inflation was used to check collinearity between the predictor variables.

## 3.4 Results

### 3.4.1 Meteorological data and soil hydrology data

Radiation, air temperature, air humidity and precipitation were in a similar range for both sites (Appendix C). Both studied periods and sites displayed high evaporative demand, VPD >1 (Table 2).

Table 2. Statistical summary of daytime micrometeorology and weighted means (160 cm – 3 soil profiles) of soil volumetric water content  $\Theta$  and water tension  $\Psi$  during 7 days in June (21.-27.) and 7 days in August (6.-12.), representing periods of high and low water availability respectively.

	High water availability		Low water availability	
	Loamy (n=7)	Sandy (n=7)	Loamy (n=7)	Sandy (n=7)
<b>VPD [kPa]</b>				
Mean (SD)	1.25 (0.134)	1.12 (0.182)	2.08 (0.203)	1.84 (0.241)
Median [Min, Max]	1.22 [1.13, 1.50]	1.08 [0.911, 1.47]	2.15 [1.71, 2.35]	1.86 [1.39, 2.15]
<b>Rg [W/m<sup>2</sup>]</b>				
Mean (SD)	341 (35.4)	348 (47.3)	347 (19.6)	337 (14.6)
Median [Min, Max]	334 [286, 397]	363[274, 403]	359 [318, 364]	339 [313, 353]
<b><math>\Theta</math> [%vol]</b>				
Mean (SD)	15.9 (0.364)	4.44 (0.272)	14.9 (0.061)	3.04(0.063)
Median [Min, Max]	15.9 [15.5, 16.5]	4.41 [4.10, 4.86]	14.9 [14.8, 15.0]	3.03 [2.96, 3.13]
<b><math>\Psi</math> [hPa]</b>				
Mean (SD)	- 1270 (59.3)	- 393 (59.7)	-1820 (32.5)	- 1010 (46.6)
Median [Min, Max]	- 1270 [-1360, -1200]	-379 [-488, -321]	- 1820 [-1850, -1770]	- 1010 [-1060, -933]

During both periods, the mean  $\Theta$  in the loamy site was up to three times higher than in the sandy site. Water tension at the loamy site was more negative than at the

sandy site (Table 2). Detailed information per site on the daily variations of  $\Theta$ ,  $\Psi$  and SWS at defined soil depths is given in Appendix D.

### 3.4.2 Differences of mean daytime sap flow velocity, the influence of site conditions, month and species

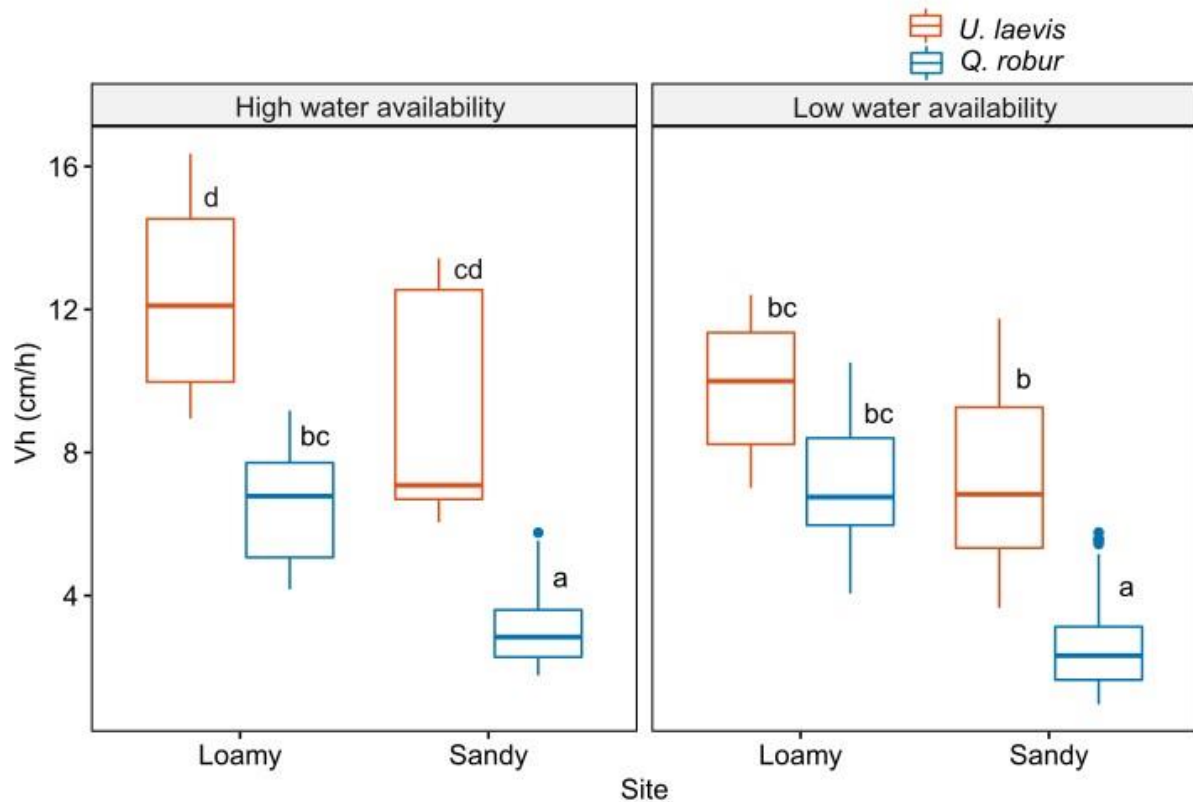


Figure 13. Differences between mean daytime sap flow velocities ( $V_h$ ) of *Q. robur* and *U. laevis* in loamy and sandy soils under periods of high and low water availability. Boxes and whiskers represent the 1x and 1.5x interquartile range, strips median. Letters represent significant differences between groups ( $p < 0.05$ ). The table result of the Imem is presented in Appendix E.

During both periods and at both sites, *U. laevis* showed about two times higher sap velocity than *Q. robur*. *Q. robur* displayed significantly higher values in the loamy site than in the sandy site under conditions of high and low water availability (Figure 13). Although no significant differences were registered for *U. laevis* between sites, a site related trend can also be seen for this species. Mean daytime  $V_h$  was the highest for the *U. laevis* under high water availability (June) in the loamy site reaching a mean value of 12 cm/h, while *Q. robur* presented a mean daytime  $V_h$  of 7 cm/h under similar

conditions. *Q. robur* in the sandy site presented the lowest Vh with a mean daytime value of 2.5 cm/h.

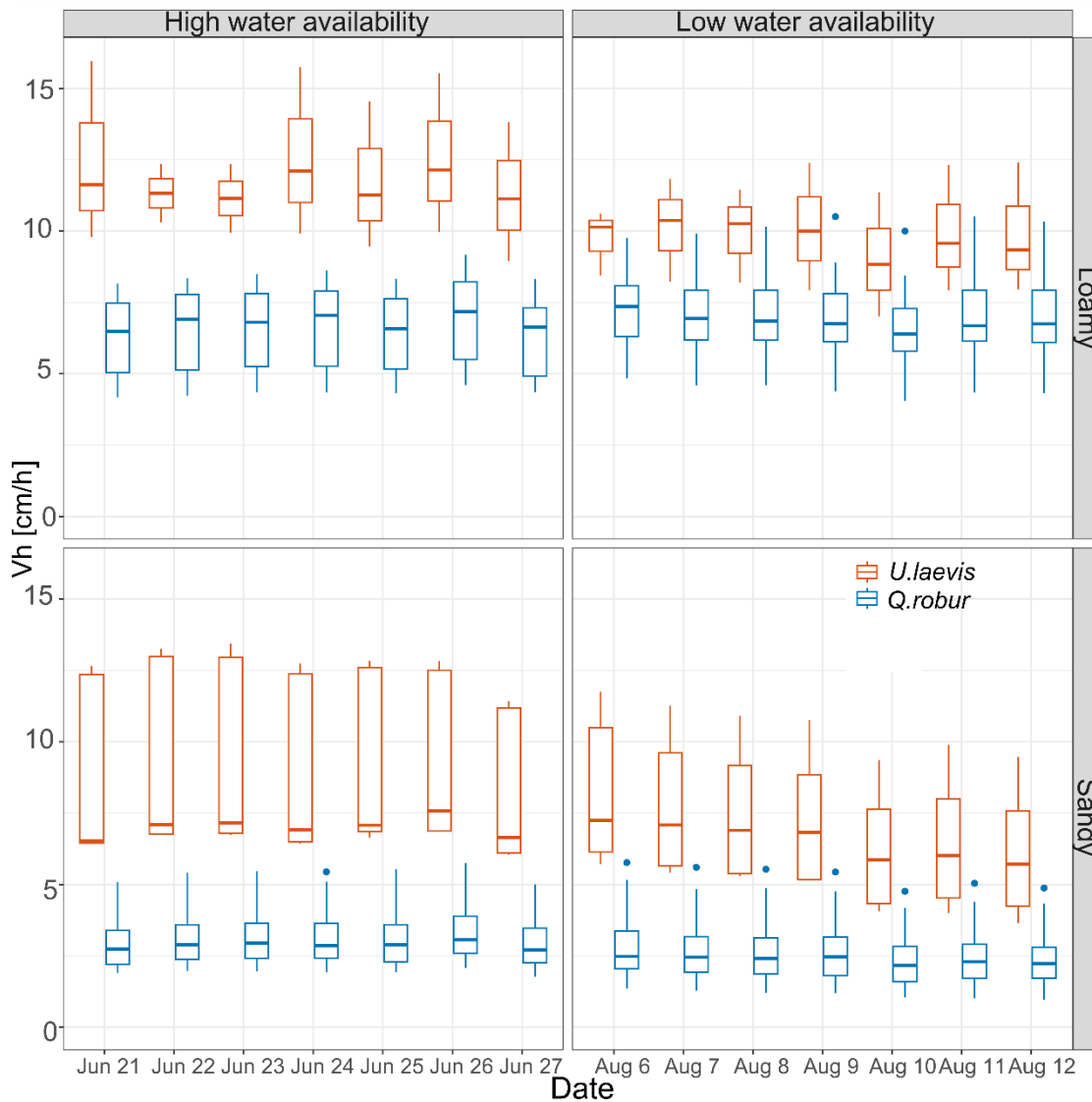


Figure 14 Daily mean of daytime sap flow velocity (Vh) of *Q. robur* and *U. laevis* under periods of high and low water availability in a loamy (upper row) and sandy (lower row) site. Boxes and whiskers represent the 1x and 1.5x interquartile range, black strips median. Every box ( $\approx 15$  working sensors per species in hourly intervals between 4 am and 9 pm)

Significant differences in sap flow velocity (Vh) were observed between both species on most days. *U. laevis* presents higher Vh than *Q. robur* throughout all measured days

(Figure 14). *U. laevis* reduced sap flow velocity by approximately 40% between the period with high water availability in June and low water availability in August (Figure 14).

### 3.4.3 Modeled hourly sap flow velocity

In the loamy site, during the period of high water availability, the potential sap flow velocity ( $V_{h_{\text{modeled}}}$ ) effectively captured the observed dynamics of the measured sap flow velocity ( $V_h$ ) for both species (Figure 15). However, under low water availability in the loamy soils,  $V_{h_{\text{modeled}}}$  aligned with the  $V_{h_{\text{measured}}}$  only for *Q. robur*. For *U. laevis* the modeled  $V_h$  exceeded the measured  $V_h$  (Figure 15), indicating the relevance of soil water availability limitation.

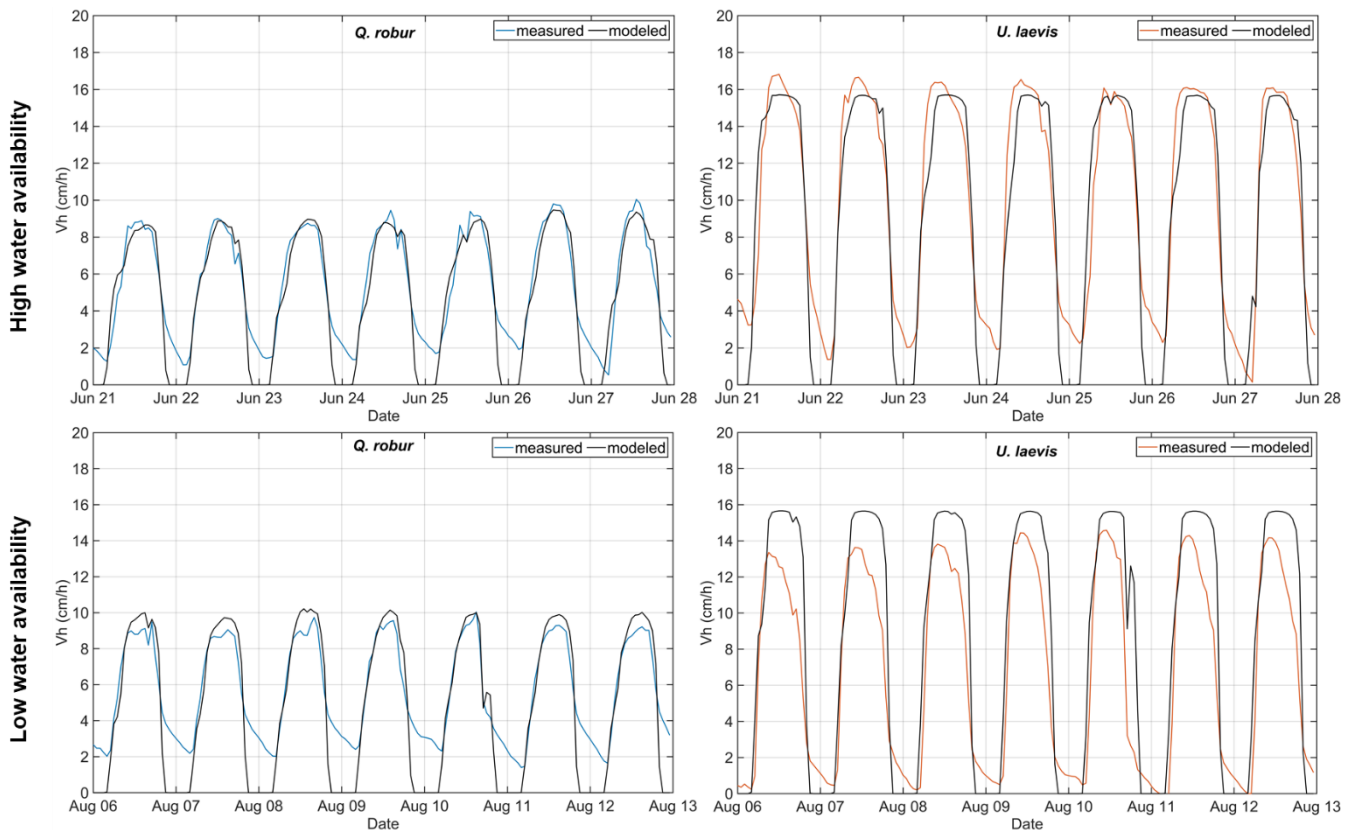


Figure 15. Modeled  $V_h$  (cm/h) in the loamy site (black lines), measured  $V_h$  for *Q. robur* (blue lines, left column) and *U. laevis* (orange lines, right column) under periods of high water availability (above row) and low water availability (below row).

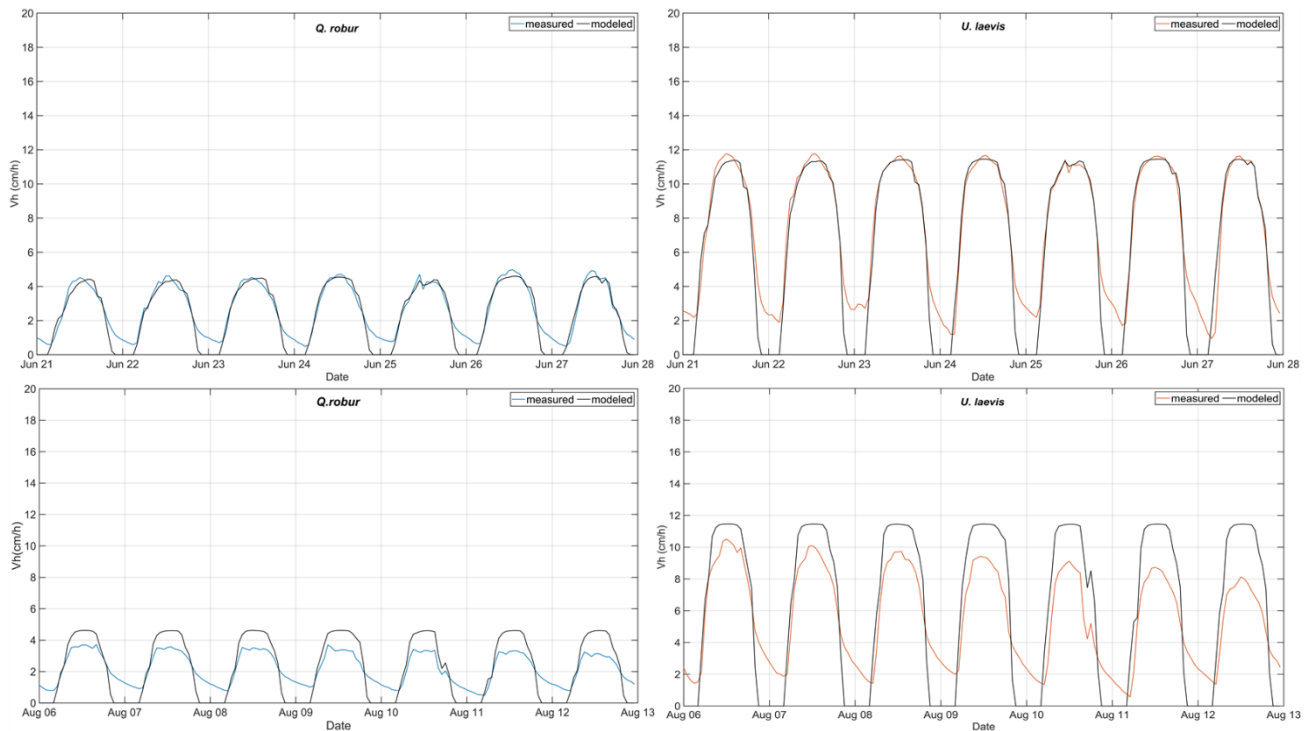


Figure 16. Modeled Vh (black lines) and measured Vh for *Q. robur* (blue lines, left column) and *U. laevis* (orange lines, right column) in the sandy site under periods of high water availability (above row) and low water availability (below row).

In the sandy site, the measured Vh for both species was well represented by  $Vh_{\text{modeled}}$ , during periods of high potential evapotranspiration and high water availability (Figure 16). However, during periods of low water availability and high potential evapotranspiration, a deviation of the measured Vh from the potential  $Vh_{\text{modeled}}$  was observed for both species. The measured Vh was lower than the  $Vh_{\text{modeled}}$ , with *U. laevis* showing a more pronounced deviation towards the end of the period with low water availability (Figure 16). Specifically, for *U. laevis* under low water availability in the sandy site, a continuous decrease in measured Vh was observed, which  $Vh_{\text{modeled}}$  was unable to accurately capture. The mean daytime measured Vh per day exhibited an overall decrease of 2.5 cm/h between the 6<sup>th</sup> and the 12<sup>th</sup> of August (Figure 16).

### 3.4.4 Ratio between measured and modeled $V_h$ and the relation to $\Psi$ .

To test the response of  $V_h$  to soil water tension  $\Psi$ , we calculated the ratio between potential sap flow velocity ( $V_{h_{\text{modeled}}}$ ) and the measured  $V_h$ , and plotted it against  $\Psi$  (Figure 17). Under high water availability, we found no significant effects on daytime  $V_{h_{\text{measured}}}/V_{h_{\text{modeled}}}$  for both tree species and in both sites (Figure 17 a, b). The calculated ratios under this condition were all between 0.9 and 1.1.

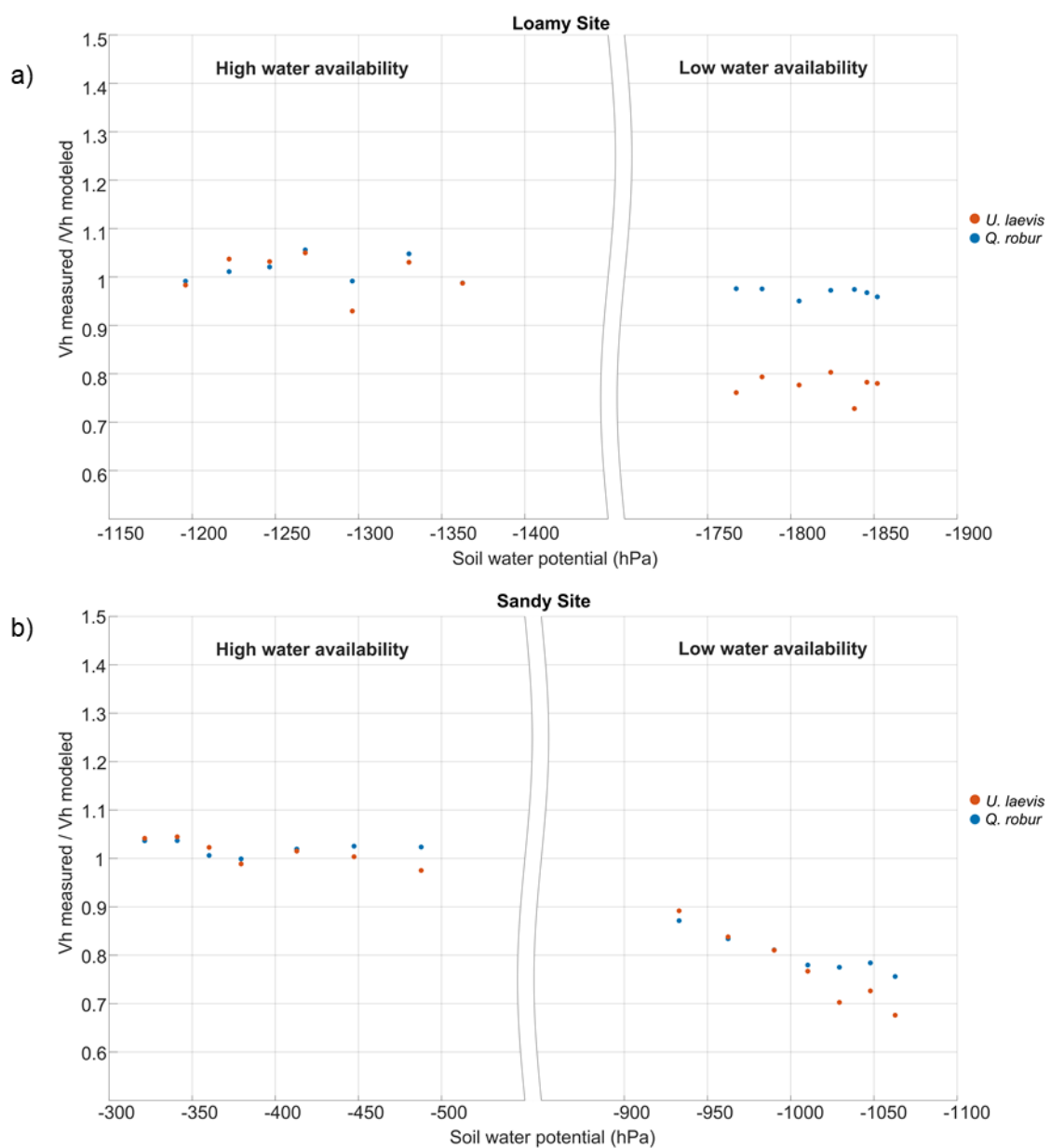


Figure 17. Relationship between the daily means of measured and modeled daytime sap flow velocities ( $V_{h_{\text{measured}}}/V_{h_{\text{modeled}}}$ ) of *Q. robur* and *U. laevis* and the daily weighted mean soil water

potentials under periods of high and low water availability in the a) loamy site and b) sandy site.

In the loamy site during low water availability, the  $V_{h_{\text{measured}}}/V_{h_{\text{modeled}}}$  ratio for *Q. robur* were slightly lower compared to those under high water availability. However, these differences were still within the defined deviation of 0.1 thus, not significant. For *U. laevis*, the ratio decreased significantly under low water availability in the loamy soil ( $V_{h_{\text{measured}}}/V_{h_{\text{modeled}}} \approx 0.8$ ), resulting in a relative reduction of almost 20% in  $V_h$  for this species. In the sandy site and under low water availability, both species exhibited a continuous decrease in  $V_{h_{\text{measured}}}/V_{h_{\text{modeled}}}$  ratios (from 0.9 to 0.7), following the decrease in soil water potential. This reduction in ratios led to a significant reduction of sap flow velocities under low water availability for the sandy site.

We conducted a multiple linear regression model to define the most important factors influencing daytime sap flow velocity and to understand the role of soil variables under high VPD. The model was applied separately for both species in order to avoid clusters in the data, and we report the results for *U. laevis* as the calculated ratio showed pronounced effects. The best performing model for the *U. laevis* included VPD (kPa), soil water tension  $\Psi$  (hPa) and volumetric water content  $\Theta$  (%) as predictors (Equation 4) and it explained 93% (adjusted  $R^2=0.9342$ ,  $p \leq 0.001$ ) of the variance of the sap flow velocity in *U. laevis*. The significance of the predictor variables are shown in Table 3. Soil water tension  $\Psi$  and volumetric water content  $\Theta$  were the most significant predictor variables.

Equation 4 
$$F_{elms} = 7.457 + 1.002(VPD) + 0.532(\Theta) + 0.004(\Psi)$$



Table 3. Multiple linear regression model, summary results for the best-fit model explaining sap flow velocity of *U. laevis*.

Predictor	Estimate	Std.error	t value	p <sup>a</sup>
Intercept	7.4574216	0.5372596	13.880	5.80e-13 ***
VPD	1.0017087	0.5250375	1.908	0.0684 .
Θ	0.5325492	0.0432101	12.325	7.18e-12 ***
Ψ	0.0040546	0.0006707	6.046	3.05e-06 ***
<sup>a</sup> Signif. codes: 0 '***' 0.001 '**' 0.01 '*' 0.05 '.' 0.1 ' ' 1				

### 3.5 Discussion

#### 3.5.1 Differences of daytime sap flow velocity between species daytime sap velocity of *U. laevis* higher than *Q. robur*.

The sap flow velocity of *U. laevis* and *Q. robur* was analyzed under periods of high VPD and different soil water availability (high and low) in two sites of the active floodplain, a sandy site and a loamy site, of the lower middle Elbe.

Tree species is a main factor controlling sap flow velocity patterns (Appendix E). A similar result was reported by Hassler et al. (2018), who found that tree- and site-specific factors controls sap velocity patterns in the landscape, particularly tree species, diameter and geology. Mean daytime sap velocity was overall higher for *U. laevis* than for *Q. robur* (Figure 14). We have not found previous studies comparing these two co-occurring hardwood floodplain tree species in terms of sap flow velocity. However, similar trends in which *Q. robur* species presented slower sap flow velocity than concurrent hardwood species have been reported for temperate forests in West Virginia (Guillén et al., 2022a), for the Atert catchment in Luxembourg (Hassler et al., 2018), and also in suburban and urban sites in Germany (Thomsen et al., 2020).

*U. laevis* and *Q. robur* are both ring porous species, a trait that facilitates rapid sap movement (Venturas et al., 2014). However, the higher sap flow velocity observed in

*U. laevis* compared to *Q. robur* can be attributed to the species' efficient water transport, which has evolved in adaptation to waterlogged environments (Venturas et al., 2014). *U. laevis* is characterized by large xylem vessels, high vessel frequency and a significant presence of grouped vessels in both early and latewood, all of which contribute to enhanced water transport capacity (Venturas et al., 2013, 2015). On the other hand, *Q. robur* exhibits higher water use efficiency, especially in its large-diameter early wood vessels when water is not limited (Abrams, 1990). During periods of drought, *Q. robur* is capable of sustaining slower but consistent water movement through narrower latewood vessels (Abrams, 1990). This might explain the low but constant sap velocity observed for *Q. robur* in our study (Figure 15).

Another explanation for the low sap flow velocity of *Q. robur* is the stronger stomatal control amidst drought stress (Breda et al., 1993). Recent research has further supported the notion of *Q. robur* possessing important physiological flexibility in response to drought, which grants the species an efficient survival mechanism (Mikac et al., 2018). In contrast, *U. laevis* has been reported to show no difference in minimal stomatal conductance between well-watered plants and those under drought condition (Eller et al., 2016). This indicates a possible lack of stomatal control for this species under water-limited conditions. However, our findings showed a significant decrease of sap flow velocity with increased drought for *U. laevis* (Figure 17) under low water availability in loamy and sandy soils. This indicates either clear stomatal control in this species, or it could be interpreted as a result of increased fine root mortality, which has been reported for this species under drought (Leonova et al., 2022). Additionally, the deep rooting traits of *Q. robur* may also play a role in maintaining constant sap flow velocity. *Q.robur* has shown preference for deep rooting and has been attributed the capacity of performing hydraulic lifting, allowing it to access deeper water sources

(Leonova et al., 2022). This could explain the constant sap flow velocities we recorded for this species, which did not change with increasing soil water potential (Figure 17). Moreover, the increase in sap flow velocity for *Q. robur* in periods of low water availability in the loamy site, despite lower  $\Theta$ ,  $\Psi$ , suggests constant connection to deep water sources (Figure 14).

#### 4.2 Effect of site conditions (soil substrate) and soil water potential

Previous research on forests and tree species around the world has consistently indicated that VPD and  $R_g$  are primary drivers of sap flow, while little to no effect of soil hydrology was reported, even under water limitation (Guillén et al., 2022a; O'Brien et al., 2004; Oogathoo et al., 2020). However, our findings suggest that soil parameters, particularly soil water potential, play a significant role in controlling sap flow velocity of *Q. robur* and *U. laevis*, under low water availability in floodplain soils. (Figure 17, Appendix F, Table 3). Soil hydraulic properties and plant water availability is tightly controlled by soil texture (Hultine et al., 2006; McDowell et al., 2008; Sperry et al., 2002). In sandy soils, the predominance of large pores results in higher water conductivity under saturated conditions than loamy soils. However, this also leads to higher water loss and lower unsaturated conductivity in sandy soil (Hultine et al., 2006). Thus, a fast depletion of water supply would be expected in trees growing in sandy substrates compared to those in fine texture soils, despite presenting less negative water potentials (Hultine et al., 2006). In the loamy site, the ratio between measured and modeled sap flow velocities ( $V_{h_{\text{measured}}}/V_{h_{\text{modeled}}}$ ) for *Q. robur* ratio is about 1, indicating its ability to extract water at high and low water availabilities, even with increased water tension (Figure 17, a). In contrast, *U. laevis* in the loamy site under low water availability, exhibited a ratio reduction from 1 to 0.8, which indicates their lack of extraction ability compared to *Q. robur* (Figure 17, a). Furthermore, *Q. robur* displayed lower sap flow velocities at higher soil water potentials, but showed less

sensitivity to changes in soil water tension particularly in the loamy site (Figure 15 and Figure 16). Sap flow velocity was reduced for *Q. robur* in the sandy site under low water availability (Figure 17 b) probably due to the lower unsaturated conductivity in the sandy soil.

This suggests that *Q. robur* is able to access water, despite strong water tension in the soil (e.g. -1800 hPa in loamy soils); however is limited by water replenishment. In contrast, there are no significant differences in the sap flow velocity of *U. laevis* between sites (Figure 13), indicating a lack of adaptation to site conditions. *U. laevis* maintained high relative sap flow velocities despite the reduction in soil moisture under all conditions (Figure 14, 17). This may have resulted in a faster and earlier depletion of water in the rooting space below *U. laevis* compared to *Q. robur*, causing even worsening conditions for *U. laevis*. Consequently, the reduction in sap flow velocity for *U. laevis* in the sandy site during low water availability, could also lead to an increase in loss of conductive xylem area due to cavitation, which has been identified as a tradeoff for water transport efficiency (Venturas et al., 2013).

### 3.6 Conclusions

The two analyzed tree species, *Q. robur* and *U. laevis*, displayed significant differences in sap flow velocity and sap flow velocity regulation under high VPD, different soil substrates, and periods of water availability. These differences can primarily be attributed to physiological traits. On the one hand, *U. laevis* had higher sap flow velocity than *Q. robur*, however displayed a reduction in sap flow velocity due to low water availability, particularly in the sandy site. This response was evident because of high water demands and limited water delivery caused by low water content and low unsaturated water conductivity of sandy soils. *Q. robur* on the other hand, seem to regulate water transport and significantly decreased sap flow velocity in the sandy site compared to the loamy site, indicating adaptive features to specific site conditions.

While *Q. robur* displayed lower sap flow velocities than *U. laevis* at higher soil water potentials, they showed less sensitivity to changes in soil water tension within each study period.

The Jarvis model was able to reflect sap flow velocity under high potential evapotranspiration. In the period of high water availability the ratio of modeled to measured values did not show an influence of soil water potential on sap flow velocity for both species and in both sites, sandy and loamy. In the period of low water availability, in the loamy site, *Q. robur* was able to keep sap flow velocity despite high soil water potentials while *U. laevis* reduced sap flow by almost 20% compared to the period with high soil water availability. In the sandy site under low water availability, the ratio of measured and modeled sap flow velocity for *U. laevis* and *Q. robur* reduced significantly, depicting almost a 40% reduction in sap flow velocity for both species within this period indicating a strong influence of water conductivity on the regulation of sap flow.

Our findings emphasize the importance of considering physiological traits and soil properties in assessing the vulnerability and adaptive capacity of tree species to changing water availability. This knowledge can contribute to informed decision-making and the development of effective strategies for mitigating the impacts of drought on hardwood floodplain forests in a changing climate.

## Chapter 4.

### Synthesis, conclusions and outlook.

#### 4.1 Synthesis and summary of results

Floodplains sustain highly diverse and productive ecosystems, like hardwood floodplain forests. Under natural or near-natural conditions, hardwood floodplain forests present increased potential for carbon storage in the soils, in the trees, and in the root biomass (Heger et al., 2021b; Leonova et al., 2022; Shupe et al., 2021) . They act as natural water retention zones given their rough characteristics in topography and geomorphology, which simultaneously promotes a range of different habitats for conservation of several species of fauna and flora. Furthermore, the active hydrological connection of the predominant sand and loam soils to the river results in nutrient enrichment in soils that contribute to high primary productivity (Vásconez Navas et al., 2023). All these ecosystem characteristics and services provide multiple benefits to society.

Given the benefits provided by floodplains to humans, settlements were common in the nearby areas of rivers, which resulted in the need for flood protection measures. Thus, the degradation of floodplain forests, and in general of the floodplain ecosystems in their natural state, started almost a millennium ago in Europe with the construction of the first dikes, as well as the intensive use of the forest for timber (Koenzen et al., 2021). It intensified with industrialization that brought activities like river channelization for commercial purposes and the increment of land-use activities as agricultural and pasture lands, which are still ongoing. These almost thousand years of use and degradation have resulted in a highly fragmented and debilitated floodplain forest ecosystem (ESSFORES, 2016; Koenzen et al., 2021) that is also affected by the effects of global warming experienced in the last decades.

With increasing attention into the effects of climate change, in addition to increased knowledge on the benefits attributed to the preservation of natural ecosystems to buffer/diminish this effects, the first steps to the restoration of floodplain forests start at the end of the 20<sup>th</sup> century in Europe. Since then, different projects of conservation and restoration of floodplain ecosystems have taken place in different catchments of big rivers in Europe (Schneider, 2010)

In 2017, the MediAN project started with the aim of understanding the underlying processes and quantifying the spatio-temporal variability of the ecosystem services provided by hardwood floodplain forests in the lower middle Elbe, one of the last floodplains in Germany that still presents a relatively large area of coherent floodplain forests. A multidisciplinary collaboration between scientist and implementation partners was organized to work on this aim covering along 150 river km of the lower middle Elbe. As the soil science subproject, within the MediAN project, we focused on i) the process-based characterization of the soil carbon balance in the forest floor, and ii) the interactions between the edaphic properties and the hardwood forest, accounting for effects of the hydrologic gradient and the landscape geomorphology. In this dissertation, I focused on the latter by considering the following aspects: the influence of the floodplain hydrogeomorphology on the distribution of soil physicochemical properties and soil processes; the interaction between soil substrate, water availability and hardwood trees; finally the implications of these aspects for forest restoration.

### ***Influence of the floodplain hydrogeomorphology***

On chapter two of this dissertation, I show that based on hydrologic and topographic gradients and the dike influence on the floodplain, hydrogeomorphic units control soil properties distribution and soil development. The identified units along the lower middle

Elbe are high and low active floodplain and seepage-influence and disconnected former floodplain. Main differences were found between the active floodplain and the former floodplain overall, highlighting the influence of the dike. On the one hand, **the active floodplain, displays higher availability of nutrients, in particular plant available phosphorus ( $P_{\text{sol}}$ )** compared to the former floodplain, with values reaching up to 234 mg/Kg (Figure 7) in the active low floodplain sites. **Soil pH plays an important role on the availability of phosphorus** in the active floodplain, an exponential increase in availability is related to the more basic pH values found in the active floodplain compared to the former floodplain (Figure 10).

On the other hand, **the former floodplain displays acidification that occurs amidst disconnection from the river** promoting higher rates of litter accumulation. The mean pH ranged between 3.6 and 4.2 in the hydrogeomorphic units of the former floodplain, with the lowest values in the former disconnected (FD). The  $P_{\text{sol}}$  availability in the former floodplain was as low as 12.4 mg/Kg. The acidification of the former floodplain can include effects related increased Al, Fe and Mn oxides, increasing reactive surfaces, which promote P sorption (Noe et al., 2013; Saint-laurent et al., 2019). The acidification may also be interpreted with the constant soil development, as there has been no supply of bases by flooding and sedimentation since the dyke construction.

The **hydrogeomorphology influence on soil properties** as pH, soil texture and nutrient content **affected also the soil organic carbon storage and carbon storage in the biomass**. The highest soil organic carbon stocks (149 t/ha) and tree biomass carbon stocks (180.4 Mg/ha) were also found in the active floodplain (Heger et al., 2021b; Shupe et al., 2021)



### ***Interaction between soil substrate, water availability and hardwood trees***

On chapter 3, I show that the sap flow velocities of *Quercus robur* and *Ulmus laevis* differed due to physiological adaptations, and that these adaptations in combination to soil hydraulic properties, as soil water tension and soil water storage, result in different dynamics of water transport under periods of high evaporative demand and different soil water availability. *Ulmus laevis* presented overall higher sap flow velocities than *Quercus robur* (Figure 13).

The combination of **low water availability, high evaporative demand, and sand dominated soil substrate resulted in an evident reduction of sap flow velocity for the *Ulmus laevis*** (Figure 16). The high water demand nature of the *Ulmus laevis* in combination to the low water content and conductivity in the sandy site explains this reaction. ***Quercus robur* displayed lower sap flow velocities at higher soil water potentials, but showed less sensitivity to changes in the soil water tension span within each study site.**

Fine root dynamics and rooting depth for *Quercus robur* and *Ulmus laevis* could explain our observed trends for these species. ***Quercus robur* is deep-rooting and hydraulic lift as well as lower fine root mortality were reported for *Quercus robur*** under drought compared to *Ulmus laevis* (Leonova et al., 2022).

Finally, I showed that the reduction of the ratio of modeled to measured sap flow under low water availability in sand dominated sites (Figure 17) evidenced the restriction of sap by soil water tension.

### ***Implications for forest restoration***

Hydrogeomorphic and climatic features rank high in the considerations for floodplain forest restoration (ESSFORES, 2016). Considering the highly dynamic nature of the

floodplain ecosystem in combination with processes of severe degradation, a sophisticated understanding of the physical, chemical and biological properties of soils (Heneghan et al., 2008) is essential for effective restoration. The restoration of floodplain forests need to consider physical and chemical parameters of soils as for example soil texture, pH, cation exchange capacity as they control processes of water availability and nutrient cycling (Lozano-Baez et al., 2021; Schoenholtz et al., 2000) and affect seed germination, seedling survival, biomass accumulation and forest productivity.

With the results in Chapter 2 of this dissertation, I show that **the active floodplain presents a high restoration potential promoting higher primary productivity as well as higher carbon sequestration** (Heger et al., 2021b; Shupe et al., 2021) due to the active connection to the river hydrology. Thus, reforestation with hardwood floodplain forest species should consider these sections of the floodplain. The indication of acidification found for the former floodplain could guide reforestation with tree species selection that show adaptation to these characteristics.

With the results of Chapter 3, I show that the two predominant hardwood floodplain forest species, *Quercus robur* and *Ulmus laevis*, present different adaptations to low and high water availability and to the different sites of the active floodplain. With the expected increase in intensity and frequency of soil droughts in the region, sites with finer soil texture and located in lower sites of the floodplain with a higher frequency of flooding than higher sites could imply better conditions for floodplain forest species regarding water availability. Moreover, species like *Quercus robur* should be considered as a more tolerant species to drought stress.

## 4.2 Conclusions and Outlook

In this thesis, I point to the beneficial conditions that the active floodplain present for hardwood forests concerning nutrient availability, carbon storage and soil water availability. A clear description of the differences between active and former floodplain with regards to soil physicochemical parameters is presented, and I linked this to the possible implication for forest restoration. Proposing for example to consider, typical hardwood floodplain species for reforestation in the active floodplain and, acid-tolerant species if reforestation is targeted in the former floodplain.

I show that the dominant hardwood floodplain forest species, *Quercus robur* and *Ulmus laevis*, display different water transport dynamics under periods of high and low water availability, and that they perform differently to variability in site conditions of the active floodplain (sandy and loamy). I conclude that *Quercus robur* reacts to site conditions by lowering sap flow velocity in the sandy site, which could imply an adaptation to control water extraction under lower soil water storage and low water conductivity. *Ulmus laevis* is anatomically adapted to conditions of high soil water availability, and thus uses high amounts of water which contributes to faster soil drying.

With the results presented in this dissertation, I show that soil characteristics evaluation in the light of restoration projects is pivotal for meeting the needs of the biotic component in floodplain ecosystems, especially for the hardwood forests. Considering this, a couple of ideas have come to my mind, regarding next steps to go even further in supporting the restoration efforts of our application partners in the floodplains forests of the lower middle Elbe. For example, a set up which allows to study seedlings of Oaks and Elms (considering ages and provenances used at the moment for restoration) under prepared soil conditions that simulate floodplain soils and their hydrology, while monitoring leaf water potentials, stomatal conductance, etc.

Here considerations of most dominant soil substrates behind the dike could be considered as well. This research could also include the adaptations of seedling to more frequent and prolonged drought. Another idea, could be to monitor in the field in more detail the reaction between soil hydrology dynamics and tree responses, by including less individuals but more parameters. One soil profile per tree could allow us to define species specific reactions and feedbacks to the soil matrix.

## References

- Abrams, M. D. (1990). Adaptations and responses to drought in *Quercus* species of North America. *Tree Physiology*, 7(1-2-3-4), 227–238.  
<https://doi.org/10.1093/TREEPHYS/7.1-2-3-4.227>
- Achat, D. L., Pousse, N., Nicolas, M., Brédoire, F., & Augusto, L. (2016). Soil properties controlling inorganic phosphorus availability : general results from a national forest network and a global compilation of the literature. *Biogeochemistry*, 127, 255–272. <https://doi.org/10.1007/s10533-015-0178-0>
- Ad-hoc-AG Boden. (2005). Bodenkundliche Kartieranleitung. In *Bundesanstalt für Geowissenschaften und Rohstoffe und den Geologischen Landesämtern in der Bundesrepublik Deutschland Hannover: Vol. 5*.
- Allen, C. D., Macalady, A. K., Chenchouni, H., Bachelet, D., McDowell, N., Vennetier, M., Kitzberger, T., Rigling, A., Breshears, D. D., Hogg, E. H. (Ted), Gonzalez, P., Fensham, R., Zhang, Z., Castro, J., Demidova, N., Lim, J. H., Allard, G., Running, S. W., Semerci, A., & Cobb, N. (2010). A global overview of drought and heat-induced tree mortality reveals emerging climate change risks for forests. *Forest Ecology and Management*, 259(4), 660–684.  
<https://doi.org/10.1016/j.foreco.2009.09.001>
- Baker, T. T., Lockaby, B. G., Conner, W. H., Meier, C. E., Stanturf, J. A., & Burke, M. K. (2001). Leaf Litter Decomposition and Nutrient Dynamics in Four Southern Forested Floodplain Communities. *Soil Science Society of America Journal*, 65(4), 1334–1347. <https://doi.org/10.2136/sssaj2001.6541334x>
- Bates, D., Mächler, M., Bolker, B. M., & Walker, S. C. (2015). Fitting linear mixed-effects models using lme4. *Journal of Statistical Software*, 67(1).  
<https://doi.org/10.18637/jss.v067.i01>
- Bayley, P. B. (1995). Understanding large river-floodplain ecosystems - Significant economic advantages and increased biodiversity and stability would result from restoration of impaired systems. *BioScience*, 45(3), 153–158.  
<https://doi.org/10.2307/1312554>
- Bednar-Friedl, B., Biesbroek, R., Schmidt, D. N., Alexander, P., Børsheim, K. Y., Carnicer, J., Georgopoulou, E., Haasnoot, M., Cozannet, G. Le, Lionello, P., Lipka, O., Möllmann, C., Muccione, V., Mustonen, T., Piepenburg, D., & Whitmarsh, L. (2022). Europe. In: *Climate Change 2022: Impacts, Adaptation and Vulnerability. Contribution of Working Group II to the Sixth Assessment Report of the Intergovernmental Panel on Climate Change* (M. T. H.-O. Pörtner, D.C. Roberts & B. R. E.S. Poloczanska, K. Mintenbeck, A. Alegría, M. Craig, S. Langsdorf, S. Löschke, V. Möller, A. Okem, Eds.). Cambridge University Press.  
<https://doi.org/10.1017/9781009325844.015>
- Binkley, D., & Hart, S. C. (1989). *The Components of Nitrogen Availability Assessments in Forest Soils* (pp. 57–112). Springer, New York, NY.  
[https://doi.org/10.1007/978-1-4613-8847-0\\_2](https://doi.org/10.1007/978-1-4613-8847-0_2)

- Bose, A. K., Scherrer, D., Camarero, J. J., Ziche, D., Babst, F., Bigler, C., Bolte, A., Dorado-Liñán, I., Etzold, S., Fonti, P., Forrester, D. I., Gavinet, J., Gazol, A., de Andrés, E. G., Karger, D. N., Lebourgeois, F., Lévesque, M., Martínez-Sancho, E., Menzel, A., ... Rigling, A. (2021). Climate sensitivity and drought seasonality determine post-drought growth recovery of *Quercus petraea* and *Quercus robur* in Europe. *Science of The Total Environment*, 784, 147222. <https://doi.org/10.1016/J.SCITOTENV.2021.147222>
- Breda, N., Cochard, H., Dreyer, E., & Granier, a. (1993). Field Comparison of Transpiration, Stomatal Conductance and Vulnerability To Cavitation of *Quercus-petraea* and *Quercus-robur* Under Water-stress. *Annales Des Sciences Forestieres*, 50(6), 571–582. <https://doi.org/10.1051/forest:19930606>
- Buijse, A. D., Coops, H., Staras, M., Jans, L. H., van Geest, G. J., Griff, R. E., Ibelings, B. W., Oosterberg, W., & Roozen, F. C. J. M. (2002). Restoration strategies for river floodplains along large lowland rivers in Europe. *Freshwater Biology*, 47(4), 889–907. <https://doi.org/10.1046/j.1365-2427.2002.00915.x>
- Burger, J. A., & Kelting, D. L. (1998). Soil quality monitoring for assessing sustainable forest management. In *The Contribution of Soil Science to the Development of and Implementation of Criteria and Indicators of Sustainable Forest Management* (Vol. 53, Issue 53, pp. 17–52). <https://doi.org/10.2136/sssaspecpub53.c2>
- Burgess, S. S. O., Adams, M. A., Turner, N. C., Beverly, C. R., Ong, C. K., Khan, A. A. H., & Bleby, T. M. (2001). An improved heat pulse method to measure low and reverse rates of sap flow in woody plants. *Tree Physiology*, 21(9), 589–598. <https://doi.org/10.1093/TREEPHYS/21.9.589>
- Cermak, J., Cienciala, E., Kucera, J., & Hallgren, J.-E. (1992). Radial velocity profiles of water flow in trunks of Norway spruce and oak and the response of spruce to severing. *Tree Physiology*, 10(4), 367–380. <https://doi.org/10.1093/treephys/10.4.367>
- Cermak, J., & Nadezhdina, N. (1998). Sapwood as the scaling parameter- defining according to xylem water content or radial pattern of sap flow? *Annals of Forest Science*, 55, 509–521. <https://doi.org/10.1051/forest:19980501>
- Chmielewski, F. (2007). Folgen des Klimawandels für die Land- und Forstwirtschaft. In *Der Klimawandel – Einblicke, Rückblicke und Ausblicke* (pp. 75–85). Endlicher W, Gerstengarbe FW (Hrsg.).
- Cicek, E., Tilki, F., Kulac, S., Yilmaz, M., & Yilmaz, F. (2007). Survival and Growth of Three Hardwood Species (*Fraxinus angustifolia*, *Ulmus laevis* and *U. minor*) on a BottomlandSite with Heavy Clay Soil. *Journal of Plant Sciences*, 2, 233–237. <https://doi.org/10.3923/jps.2007.233.237>
- Cochard, H., Bréda, N., & Granier, A. (1996). Whole tree hydraulic conductance and water loss regulation in *Quercus* during drought: evidence for stomatal control of embolism? *Annales Des Sciences Forestières*, 53(2–3), 197–206. <https://doi.org/10.1051/forest:19960203>

- Cochard, H., Martin, R., Gross, P., & Bogeat-Triboulot, M. B. (2000). Temperature effects on hydraulic conductance and water relations of *Quercus robur* L. *Journal of Experimental Botany*, *51*(348), 1255–1259. <https://doi.org/10.1093/jxb/51.348.1255>
- Dale, V. H., Joyce, L. A., McNulty, S., & Neilson, R. P. (2000). The interplay between climate change, forests, and disturbances. *The Science of the Total Environment*, *262*, 201–204. [https://doi.org/https://doi.org/10.1016/S0048-9697\(00\)00522-2](https://doi.org/https://doi.org/10.1016/S0048-9697(00)00522-2)
- Damm, C. (2013). Ecological restoration and dike relocation on the river Elbe, Germany. *Scientific Annals of the Danube Delta Institute*, *19*, 79–86.
- DWD. (2021). *Climate data center CDC—Annual regional averages of air temperature (annual mean) in °C (2 m above ground) version v19.3, last accessed: <25.1.2021>*. Version V19.3. [www.dwd.de](http://www.dwd.de)
- Dybala, K. E., Matzek, V., Gardali, T., & Seavy, N. E. (2019). Carbon sequestration in riparian forests: A global synthesis and meta-analysis. *Global Change Biology*, *25*(1), 57–67. <https://doi.org/10.1111/gcb.14475>
- Eller, F., Jensen, K., & Reisdorff, C. (2016). Nighttime stomatal conductance differs with nutrient availability in two temperate floodplain tree species. *Tree Physiology*, *37*(4), 428–440. <https://doi.org/10.1093/treephys/tpw113>
- ESSFORES. (2016). *Final Report Summary - ESSFORES (Evaluating the succes of floodplain forest restoration)*.
- Granier, A., Anfodillo, T., Sabatti, M., Cochard, H., Dreyer, E., Tomasi, M., Valentini, R., & Breda, N. (1994). Axial and radial water flow in the trunks of oak trees: A quantitative and qualitative analysis. *Tree Physiology*, *14*(12), 1383–1396. <https://doi.org/10.1093/treephys/14.12.1383>
- Granier, A., Loustau, D., & Bréda, N. (2000). A generic model of forest canopy conductance dependent on climate, soil water availability and leaf area index. *Annals of Forest Science*, *57*(8), 755–765. <https://doi.org/10.1051/forest:2000158>
- Grigal, D. F. (2000). Effects of extensive forest management on soil productivity. *Forest Ecology and Management*, *138*(1–3), 167–185. [https://doi.org/10.1016/S0378-1127\(00\)00395-9](https://doi.org/10.1016/S0378-1127(00)00395-9)
- Gröngroft, A., Krüger, F., Grunewald, K., & Meißner, R. (2005). *Plant and Soil Contamination with Trace Metals in the Elbe Floodplains : A Case Study after the Flood in August 2002*. 466–474. <https://doi.org/10.1002/aheh.200400596>
- Guillén, L. A., Brzostek, E., McNeil, B., Raczka, N., Casey, B., & Zegre, N. (2022a). Sap flow velocities of *Acer saccharum* and *Quercus velutina* during drought: Insights and implications from a throughfall exclusion experiment in West Virginia, USA. *Science of the Total Environment*, *850*(August). <https://doi.org/10.1016/j.scitotenv.2022.158029>

- Guillén, L. A., Brzostek, E., McNeil, B., Raczka, N., Casey, B., & Zegre, N. (2022b). Sap flow velocities of *Acer saccharum* and *Quercus velutina* during drought: Insights and implications from a throughfall exclusion experiment in West Virginia, USA. *Science of The Total Environment*, 850, 158029. <https://doi.org/10.1016/J.SCITOTENV.2022.158029>
- Hacke, U. G., & Sperry, J. S. (2001a). Functional and ecological xylem anatomy. In *Perspectives in Plant Ecology, Evolution and Systematics* (Vol. 4, Issue 2). <https://doi.org/10.1007/978-3-319-15783-2>
- Hacke, U. G., & Sperry, J. S. (2001b). Functional and ecological xylem anatomy. In *Perspectives in Plant Ecology, Evolution and Systematics* (Vol. 4, Issue 2). <https://doi.org/10.1007/978-3-319-15783-2>
- Hale, B. W. (2004). *Conservation in temperate river-floodplain forests: A comparative analysis of the lower Wisconsin State riverway and the middle Elbe Biosphere Reserve*. University of Wisconsin-Madison.
- Hassler, S. K., Weiler, M., & Blume, T. (2018). Tree-, stand- and site-specific controls on landscape-scale patterns of transpiration. *Hydrology and Earth System Sciences*, 22, 13–30. <https://doi.org/https://doi.org/10.5194/hess-22-13-2018>, 2018
- Havrdová, A., Douda, J., & Doudová, J. (2023). Threats, biodiversity drivers and restoration in temperate floodplain forests related to spatial scales. *Science of the Total Environment*, 854(August 2022), 158743. <https://doi.org/10.1016/j.scitotenv.2022.158743>
- Heger, A., Becker, J. N., Vásconez Navas, L. K., & Eschenbach, A. (2021a). Factors controlling soil organic carbon stocks in hardwood floodplain forests of the lower middle Elbe River. *Geoderma*, 404(April). <https://doi.org/10.1016/j.geoderma.2021.115389>
- Heger, A., Becker, J. N., Vásconez Navas, L. K., & Eschenbach, A. (2021b). Factors controlling soil organic carbon stocks in hardwood floodplain forests of the lower middle Elbe River. *Geoderma*, 404(April). <https://doi.org/10.1016/j.geoderma.2021.115389>
- Hughes, F. M. R. (1997a). Floodplain biogeomorphology. *Progress in Physical Geography*, 21(4), 501–529. <https://doi.org/10.1177/030913339702100402>
- Hughes, F. M. R. (1997b). Floodplain biogeomorphology. *Progress in Physical Geography*, 21(4), 501–529. <https://doi.org/10.1177/030913339702100402>
- Hultine, K. R., Koepke, D. F., Pockman, W. T., Fravolini, A., Sperry, J. S., & Williams, D. G. (2006). Influence of soil texture on hydraulic properties and water relations of a dominant warm-desert phreatophyte. *Tree Physiology*, 26(3), 313–323. <https://doi.org/10.1093/treephys/26.3.313>
- IUSS Working Group WRB. (2015). World Reference Base for Soil Resources 2014, update 2015: International soil classification system for naming soils and creating legends for soil maps. In *World Soil Resources Reports No. 106*. FAO.



- Jungwirth, M., Muhar, S., & Schmutz, S. (2002). Re-establishing and assessing ecological integrity in riverine landscapes. *Freshwater Biology*, 47, 867–887. <https://doi.org/10.1046/j.1365-2427.2002.00914.x>
- Junk, W., P.B. Bayley, and R. E. S. (1989). Junk, W., P.B. Bayley, and R.E. Sparks . 1989. The flood pulse concept in river-floodplain systems. Pages 110-127. *Canadian Special Publication of Fisheries and Aquatic Sciences*, 106, 110–127.
- Klein, T. (2014). The variability of stomatal sensitivity to leaf water potential across tree species indicates a continuum between isohydric and anisohydric behaviours. *Functional Ecology*, 28(6), 1313–1320. <https://doi.org/10.1111/1365-2435.12289>
- Koenzen, U., Kurth, A., & Detlef, G.-D. (2021). *Status Report on Floodplains 2021 - Floodplains in Germany*. <https://doi.org/10.19217/brs211en>
- Krause, S., Bronstert, A., & Zehe, E. (2007). Groundwater-surface water interactions in a North German lowland floodplain - Implications for the river discharge dynamics and riparian water balance. *Journal of Hydrology*, 347(3–4), 404–417. <https://doi.org/10.1016/j.jhydrol.2007.09.028>
- Krause, S., Jacobs, J., & Bronstert, A. (2007). Modelling the impacts of land-use and drainage density on the water balance of a lowland-floodplain landscape in northeast Germany. *Ecological Modelling*, 200(3–4), 475–492. <https://doi.org/10.1016/j.ecolmodel.2006.08.015>
- Leonova, A., Heger, A., Váscónez, L. K., Kai, N., & Christoph, J. (2022). Fine root mortality under severe drought reflects different root distribution of *Quercus robur* and *Ulmus laevis* trees in hardwood floodplain forests. *Trees*, 0123456789. <https://doi.org/10.1007/s00468-022-02275-3>
- López, J., Way, D. A., & Sadok, W. (2021). Systemic effects of rising atmospheric vapor pressure deficit on plant physiology and productivity. *Global Change Biology*, 27(9), 1704–1720. <https://doi.org/10.1111/GCB.15548>
- Marks, C. O., Yellen, B. C., Wood, S. A., Martin, E. H., & Nislow, K. H. (2020). Variation in Tree Growth along Soil Formation and Microtopographic Gradients in Riparian Forests. *Wetlands, PHYSICAL AND BIOTIC DRIVERS OF CHANGE IN RIPARIAN ECOSYSTEMS*. <https://doi.org/https://doi.org/10.1007/s13157-020-01363-9>
- Martínez-Sancho, E., Váscónez-Navas, L. K., Seidel, H., Dorado-Liñán, I., & Menzel, A. (2017). Responses of contrasting tree functional types to air warming and drought. *Forests*. <https://doi.org/10.3390/f8110450>
- McDowell, N., Pockman, W. T., Allen, C. D., Breshears, D. D., Cobb, N., Kolb, T., Plaut, J., Sperry, J., West, A., Williams, D. G., & Yezpe, E. A. (2008). Mechanisms of plant survival and mortality during drought: why do some plants survive while others succumb to drought? *New Phytologist*, 178(4), 719–739. <https://doi.org/10.1111/j.1469-8137.2008.02436.x>

- Mcdowell, N., Pockman, W. T., Allen, C. D., Breshears, D. D., Cobb, N., Kolb, T., Plaut, J., Sperry, J., West, A., Williams, D. G., Yepez, E. A., Mcdowell, N., Pockman, W. T., Allen, C. D., David, D., Mcdowell, N., Cobb, N., Kolb, T., Plaut, J., & Sperry, J. (2008). *Mechanisms of Plant Survival and Mortality during Drought: Why Do Some Plants Survive while Others Succumb to Drought?* Published by: Wiley on behalf of the New Phytologist Trust Stable URL : <http://www.jstor.org/stable/30149305> REFERENCES Linked refere. 178(4), 719–739.
- Meyer, H., & Miehlich, G. (1983). Einfluß periodischer Hochwässer auf Genese, Verbreitung und Standortseigenschaften der Böden in der Pevestorfer Elbaue (Kreis Lüchow-Dannenberg). In *Abh. Naturwiss. Ver. Hamburg (NF)* (Vol. 25).
- Mikac, S., Žmegač, A., Trlin, D., Paulić, V., Oršanić, M., & Anić, I. (2018). Drought-induced shift in tree response to climate in floodplain forests of Southeastern Europe. *Scientific Reports*, 8(1), 16495. <https://doi.org/10.1038/s41598-018-34875-w>
- Noe, G. B., Hupp, C. R., & Rybicki, N. B. (2013). Hydrogeomorphology Influences Soil Nitrogen and Phosphorus Mineralization in Floodplain Wetlands. *Ecosystems*, 16(1), 75–94. <https://doi.org/10.1007/s10021-012-9597-0>
- O'Brien, J. J., Oberbauer, S. F., & Clark, D. B. (2004). Whole tree xylem sap flow responses to multiple environmental variables in a wet tropical forest. *Plant, Cell and Environment*, 27(5), 551–567. <https://doi.org/10.1111/j.1365-3040.2003.01160.x>
- Oogathoo, S., Houle, D., Duchesne, L., & Kneeshaw, D. (2020). Vapour pressure deficit and solar radiation are the major drivers of transpiration of balsam fir and black spruce tree species in humid boreal regions, even during a short-term drought. *Agricultural and Forest Meteorology*, 291(May), 108063. <https://doi.org/10.1016/j.agrformet.2020.108063>
- Poff, N. L., Allan, J. D., Bain, M. B., Karr, J. R., Prestegard, K. L., Richter, B. D., Sparks, R. E., & Stromberg, J. C. (1997a). The natural flow regime: A paradigm for river conservation and restoration. *BioScience*, 47(11), 769–784. <https://doi.org/10.2307/1313099>
- Poff, N. L., Allan, J. D., Bain, M. B., Karr, J. R., Prestegard, K. L., Richter, B. D., Sparks, R. E., & Stromberg, J. C. (1997b). The natural flow regime: A paradigm for river conservation and restoration. *BioScience*, 47(11), 769–784. <https://doi.org/10.2307/1313099>
- Porporato, A., Daly, E., Rodriguez-Iturbe, I., & Rodriguez-Iturbe, I. (2004). Soil Water Balance and Ecosystem Response to Climate Change. *The American Naturalist*, 164(5), 625–632.
- Poyatos, R., Čermák, J., & Llorens, P. (2007). Variation in the radial patterns of sap flux density in pubescent oak (*Quercus pubescens*) and its implications for tree and stand transpiration measurements. *Tree Physiology*, 27(4), 537–548. <https://doi.org/10.1093/treephys/27.4.537>

- Rives, R. G., Knapp, B. O., Olson, M. G., Weegman, M. D., & Muzika, R. M. (2020). Regenerating mixed bottomland hardwood forests in north Missouri: Effects of harvest treatment on structure, composition, and growth through 15 years. *Forest Ecology and Management*, 475(May), 118371. <https://doi.org/10.1016/j.foreco.2020.118371>
- Saint-laurent, D., Arsenault-boucher, L., & Berthelot, J. (2019). Contrasting Effects of Flood Disturbance on Alluvial Soils and Riparian Tree Structure and Species Composition in Mixed Temperate Forests. *Air, Soil and Water Research*, 12, 1–15. <https://doi.org/10.1177/1178622119872773>
- Sancho-Knapik, D., Mendoza-Herrer, Ó., Alonso-Forn, D., Saz, M. Á., Martín-Sánchez, R., dos Santos Silva, J. V., Ogee, J., Peguero-Pina, J. J., Gil-Peigrín, E., & Ferrio, J. P. (2022). Vapor pressure deficit constrains transpiration and photosynthesis in holm oak: A comparison of three methods during summer drought. *Agricultural and Forest Meteorology*, 327, 109218. <https://doi.org/10.1016/J.AGRFORMET.2022.109218>
- Schindler, M., Donath, T. W., Terwei, A., & Ludewig, K. (2021). Effects of flooding duration on the occurrence of three hardwood floodplain forest species inside and outside a dike relocation area at the Elbe River. *International Review of Hydrobiology*, 0–1. <https://doi.org/10.1002/iroh.202002078>
- Schneider, E. (2010). Floodplain Restoration of Large European Rivers, with Examples from the Rhine and the Danube. In *Eiseltová, M. (eds) Restoration of Lakes, Streams, Floodplains, and Bogs in Europe. Wetlands: Ecology, Conservation and Management* (Vol. 3, Issue December, p. 9265). Springer, Dordrecht. [https://doi.org/https://doi.org/10.1007/978-90-481-9265-6\\_11](https://doi.org/https://doi.org/10.1007/978-90-481-9265-6_11)
- Schnitzler, A. (1994). European Alluvial Hardwood Forests of Large Floodplains. *Journal of Biogeography*, 21(6), 605–623.
- Schoenholtz, S. H., Miegroet, H. Van, & Burger, J. A. (2000). A review of chemical and physical properties as indicators of forest soil quality: Challenges and opportunities. *Forest Ecology and Management*. [https://doi.org/10.1016/S0378-1127\(00\)00423-0](https://doi.org/10.1016/S0378-1127(00)00423-0)
- Scholz, M., Mehl, D., Schulz-zunkel, C., Born, W., & Henle, K. (2012). Ökosystemfunktionen von Flussauen – Analyse und Bewertung von Hochwasserretention, Nährstoffrückhalt, Kohlenstoffvorrat, Treibhausgasemissionen und Habitatfunktion. *Naturschutz Und Biologische Vielfalt*, 124, 258.
- Schwartz, R., Gröngröft, A., & Miehlich, G. (2003a). Auenregeneration durch Deichrückverlegung? Bodenkundliche Aspekte am Beispiel der Mittel-elbe. *Wasser Und Boden*, 55(7-8), 36–39.
- Schwartz, R., Gröngröft, A., & Miehlich, G. (2003b). Pore Water Composition as Device for the Detection of Origin and Flow Direction of Soil Water in Alluvial Soils of the Middle Elbe River. *Acta Hydrochimica et Hydrobiologica*, 31(45), 423–435. <https://doi.org/10.1002/aheh.200300498>

- Shupe, H. A., Hartmann, T., Scholz, M., Jensen, K., & Ludewig, K. (2021). Carbon stocks of hardwood floodplain forests along the middle Elbe : the influence of forest age , structure , species , and hydro- logical conditions. *Water*, 1–18.
- Shupe, H. A., Jensen, K., Oldeland, J., & Ludewig, K. (2022). Droughts decrease and floods increase carbon sequestration rates of *Quercus robur* in hardwood floodplain forests. *Trees, Forests and People*, 9(June), 100294. <https://doi.org/10.1016/j.tfp.2022.100294>
- Sperry, J. S., Hacke, U. G., Oren, R., & Comstock, J. P. (2002). Water deficits and hydraulic limits to leaf water supply. *Environment*, 251–263. <https://doi.org/10.1046/j.0016-8025.2001.00799.x>
- Spink, A. J., Sparks, R. E., Oorschot, M. Van, & Verhoeven, J. T. A. (1998). Nutrient dynamics of large river floodplains. *Regulated Rivers: Research & Management*, 14, 203–219. [https://doi.org/10.1002/\(SICI\)1099-1646\(199803/04\)14](https://doi.org/10.1002/(SICI)1099-1646(199803/04)14)
- Steiger, J., Tabacchi, E., Dufour, S., Corenblit, D., & Peiry, J.-L. (2005). Hydrogeomorphic processes affecting riparian habitat within alluvial channel-floodplain river systems: a review for the temperate zone. *River Research and Applications*, 21(7), 719–737. <https://doi.org/10.1002/rra.879>
- Stojanović, D. B., Levanič, T., Matović, B., & Orlović, S. (2015). Growth decrease and mortality of oak floodplain forests as a response to change of water regime and climate. *European Journal of Forest Research*, 134(3), 555–567. <https://doi.org/10.1007/s10342-015-0871-5>
- Tardieu, F., & Simonneau, T. (1998). Variability among species of stomatal control under fluctuating soil water status and evaporative demand: modelling isohydric and anisohydric behaviours. *Source: Journal of Experimental Botany*, 49, 419–432.
- Thomsen, S., Reisdorff, C., Gröngröft, A., Jensen, K., & Eschenbach, A. (2020). “Responsiveness of mature oak trees (*Quercus robur* L.) to soil water dynamics and meteorological constraints in urban environments.” *Urban Ecosystems*, 23(1), 173–186. <https://doi.org/10.1007/s11252-019-00908-z>
- Tockner, K., & Stanford, J. (2002). Riverine flood plains: present state and future trends | Enhanced Reader. *Environmental Conservation*, 29(3), 308–330.
- Tyree, M. T., & Zimmermann, M. H. (2002). *Xylem Structure and the Ascent of Sap* (T. E. Timmel, Ed.; Second). Springer Series in Wood Science.
- Tyree, M. T., & Zimmermann, M. H. (2003). *Xylem structure and and the ascent of sap* (Second). Springer-Verlag. <https://doi.org/10.1007/978-3-662-08986-6>
- Vásconez Navas, L. K., Becker, J. N., Heger, A., Gröngröft, A., & Eschenbach, A. (2023). Are active and former floodplain soils of the lower middle Elbe similar? A study of soil characteristics and possible implications for forest restoration. *Catena*, 222. <https://doi.org/10.1016/j.catena.2022.106814>
- Venturas, M., Fuentes-Utrilla, P., López, R., Perea, R., Fernández, V., Gascó, A., Guzmán, P., Li, M., Rodríguez-Calcerrada, J., Miranda, E., Domínguez, J.,

- González-Gordaliza, G., Zafra, E., Fajardo-Alcántara, M., Martín, J. A., Ennos, R., Nanos, N., Lucena, J. J., Iglesias, S., ... Gil, L. (2014). *Ulmus laevis* in the Iberian peninsula: A review of its ecology and conservation. *IForest*, 8, 135–142. <https://doi.org/10.3832/ifor1201-008>
- Venturas, M., Fuentes-Utrilla, P., López, R., Perea, R., Fernández, V., Gascó, A., Guzmán, P., Li, M., Rodríguez-Calcerrada, J., Miranda, E., Domínguez, J., González-Gordaliza, G., Zafra, E., Fajardo-Alcántara, M., Martín, J. A., Ennos, R., Nanos, N., Lucena, J. J., Iglesias, S., ... Gil, L. (2015). *Ulmus laevis* in the Iberian Peninsula: a review of its ecology and conservation. *IForest - Biogeosciences and Forestry*, 8(2), 135. <https://doi.org/10.3832/IFOR1201-008>
- Venturas, M., López, R., Gascó, A., & Gil, L. (2013). Hydraulic properties of European elms: Xylem safety-efficiency tradeoff and species distribution in the Iberian Peninsula. *Trees - Structure and Function*, 27(6), 1691–1701. <https://doi.org/10.1007/s00468-013-0916-7>
- von Storch, H., Meinke, I., & Claußen, M. (2018). Hamburger Klimabericht Wissen über Klima, Klimawandel und Auswirkungen in Hamburg und Norddeutschland. In *Hamburger Klimabericht – Wissen über Klima, Klimawandel und Auswirkungen in Hamburg und Norddeutschland*. [https://doi.org/10.1007/978-3-662-55379-4\\_4](https://doi.org/10.1007/978-3-662-55379-4_4)
- Watt, M. S., Coker, G., Clinton, P. W., Davis, M. R., Parfitt, R., Simcock, R., Garrett, L., Payn, T., Richardson, B., & Dunningham, A. (2005). Defining sustainability of plantation forests through identification of site quality indicators influencing productivity - A national view for New Zealand. *Forest Ecology and Management*, 216(1–3), 51–63. <https://doi.org/10.1016/j.foreco.2005.05.064>
- Weber, A., & Hatz, M. (2020). Hyd1d – Algorithms to compute 1D water levels along German federal waterways Elbe and Rhine. *Journal of Ecohydraulics*.
- Weber, A., & Rosenzweig, S. (2020). HydFlood - algorithms to compute flood extent and duration along German federal waterways Elbe and Rhine. *Journal of Ecohydraulics*.
- Weigel, R., Bat-Enerel, B., Dulamsuren, C., Muffler, L., Weithmann, G., & Leuschner, C. (2023). Summer drought exposure, stand structure, and soil properties jointly control the growth of European beech along a steep precipitation gradient in northern Germany. *Global Change Biology*, 29(3), 763–779. <https://doi.org/10.1111/gcb.16506>
- Wilson, K. B., Wilson, K. B., Hanson, P. J., Hanson, P. J., Mulholland, P. J., Mulholland, P. J., Baldocchi, D. D., Baldocchi, D. D., Wullschleger, S. D., & Wullschleger, S. D. (2008). A comparison of methods for determining forest evapotranspiration and its components: sap- ow, soil water budget, eddy covariance and catchment water balance. *Agricultural and Forest Meteorology*, 106(2001), 153–168.

# Appendix

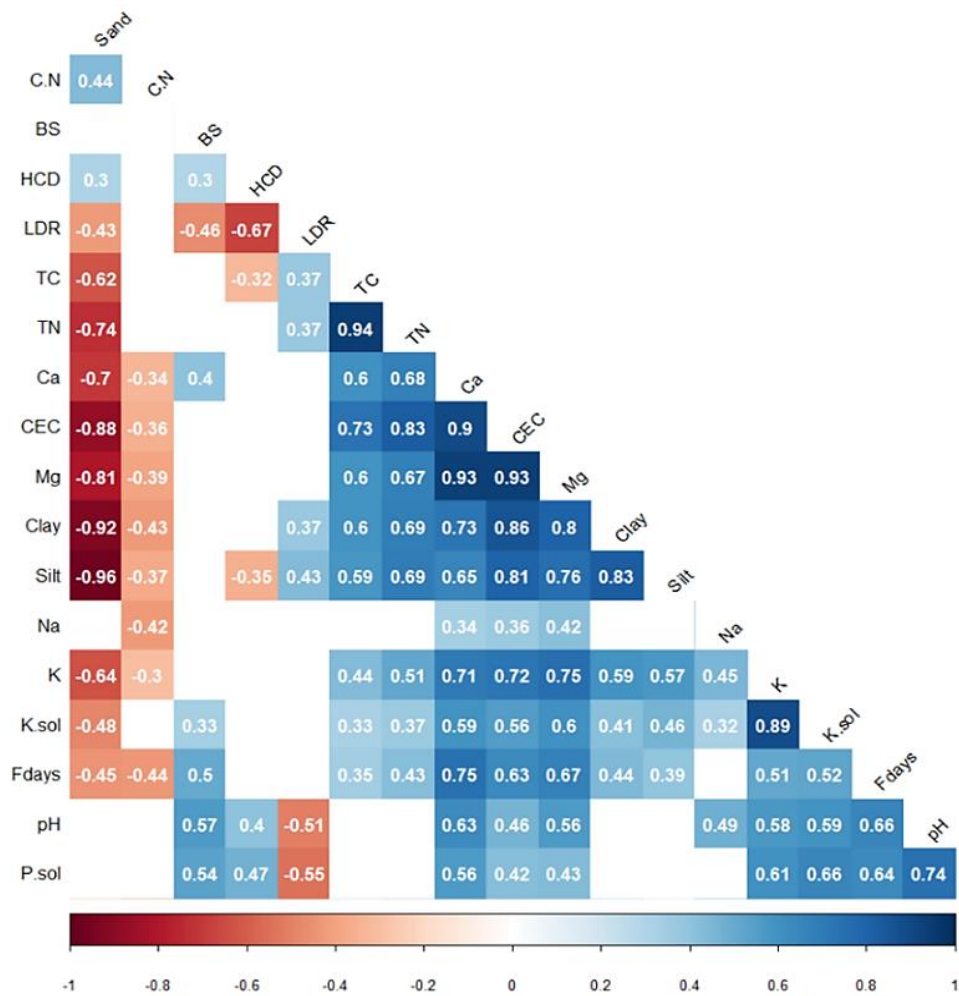
## 5.1 Appendix Article I

### Appendix A. – Statistical summary table of physicochemical parameters

	<b>Active Low (N=18)</b>	<b>Active High (N=13)</b>	<b>Former Seepage (N=7)</b>	<b>Former Disconnected (N=6)</b>	<b>Overall (N=44)</b>
<b>Clay [%]</b>					
Mean (SD)	26.5 (15.9)	11.4 (5.22)	11.2 (9.50)	23.8 (21.6)	19.2 (15.1)
Median [Min, Max]	22.2 [6.72, 58.4]	10.6 [6.38, 26.1]	5.73 [3.73, 27.2]	16.1 [3.24, 60.2]	12.6 [3.24, 60.2]
<b>Sand [%]</b>					
Mean (SD)	45.2 (29.4)	76.8 (14.4)	71.0 (27.5)	53.5 (30.6)	59.8 (28.6)
Median [Min, Max]	57.2 [2.98, 80.3]	82.6 [31.4, 86.1]	83.2 [21.2, 94.7]	53.4 [12.8, 94.0]	73.3 [2.98, 94.7]
<b>pH [CaCl<sub>2</sub>]</b>					
Mean (SD)	5.24 (0.409)	4.98 (0.299)	4.12 (0.472)	3.53 (0.360)	4.75 (0.726)
Median [Min, Max]	5.32 [4.56, 5.90]	5.00 [4.40, 5.45]	4.10 [3.60, 5.00]	3.59 [3.02, 3.90]	4.90 [3.02, 5.90]
<b>Total Carbon [%]</b>					
Mean (SD)	4.26 (1.57)	2.73 (0.477)	2.88 (0.398)	6.88 (6.35)	3.95 (2.76)
Median [Min, Max]	4.30 [1.20, 6.70]	2.68 [1.90, 3.50]	2.80 [2.31, 3.47]	3.57 [2.67, 18.7]	3.16 [1.20, 18.7]
<b>Total Nitrogen [%]</b>					
Mean (SD)	0.376 (0.147)	0.231 (0.0410)	0.222 (0.0363)	0.475 (0.334)	0.322 (0.175)
Median [Min, Max]	0.375 [0.110, 0.680]	0.230 [0.154, 0.316]	0.207 [0.191, 0.276]	0.315 [0.209, 0.997]	0.269 [0.110, 0.997]
<b>Carbon/nitrogen ratio</b>					
Mean (SD)	11.4 (0.960)	11.9 (1.13)	13.0 (1.37)	13.4 (2.85)	12.1 (1.59)
Median [Min, Max]	11.2 [9.84, 13.3]	11.7 [10.4, 14.4]	13.8 [10.5, 14.4]	12.5 [10.8, 18.8]	11.9 [9.84, 18.8]
<b>Cation exchange capacity [mmoleq/Kg]</b>					
Mean (SD)	173 (71.6)	84.2 (21.9)	69.4 (42.8)	100 (46.0)	120 (68.4)
Median [Min, Max]	162 [46.3, 356]	80.5 [46.2, 133]	50.9 [16.4, 135]	104 [22.4, 158]	102 [16.4, 356]
<b>Base saturation [%]</b>					
Mean (SD)	100 (0)	100 (0)	97.1 (7.79)	65.4 (23.2)	94.8 (14.5)
Median [Min, Max]	100 [100, 100]	100 [100, 100]	100 [79.4, 100]	62.7 [33.2, 100]	100 [33.2, 100]
<b>Soluble Potassium (K<sub>sol</sub>) [mg/Kg]</b>					
Mean (SD)	164 (165)	87.0 (33.4)	59.2 (22.8)	54.1 (24.9)	109 (116)
Median [Min, Max]	114 [43.5, 742]	80.2 [34.2, 168]	47.7 [36.7, 98.5]	46.4 [26.3, 95.9]	81.1 [26.3, 742]
<b>Soluble Phosphorous (P<sub>sol</sub>) [mg/Kg]</b>					
Mean (SD)	96.0 (57.7)	66.2 (21.2)	30.0 (15.3)	20.9 (6.59)	66.4 (48.4)

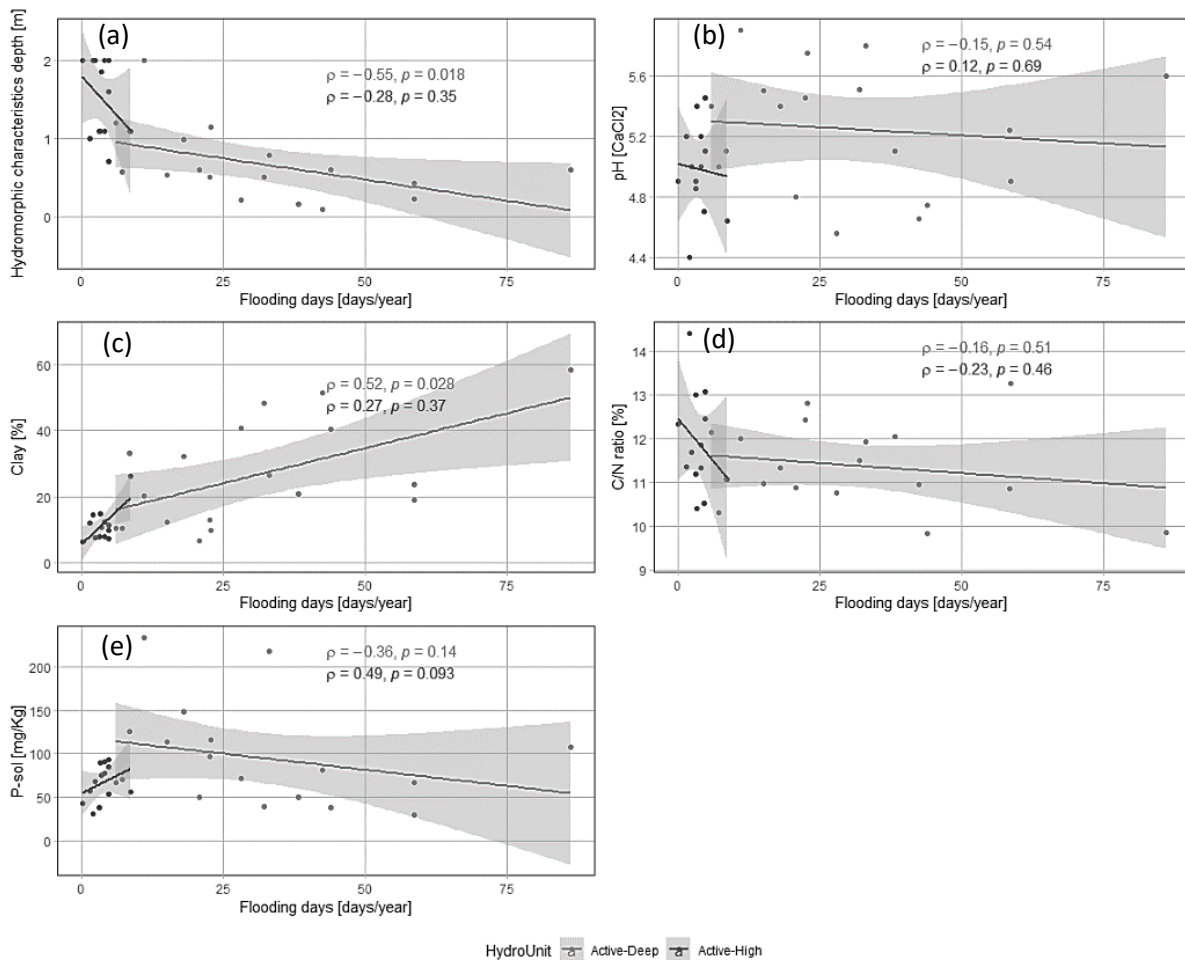
Median [Min, Max]	76.4 [29.4, 234]	67.7 [30.7, 93.8]	33.2 [12.6, 57.2]	19.1 [13.5, 29.1]	56.9 [12.6, 234]
<b>Hydromorphic characteristics</b>					
<b>depth [m]</b>					
Mean (SD)	0.608 (0.379)	1.24 (0.467)	0.393 (0.284)	0.368 (0.156)	0.631 (0.448)
Median [Min, Max]	0.553 [0.0930, 1.20]	1.09 [0.700, 1.85]	0.418 [0.100, 0.881]	0.338 [0.233, 0.633]	0.517 [0.0930, 1.85]
Missing	4 (22.2%)	8 (61.5%)	1 (14.3%)	1 (16.7%)	14 (31.8%)
<b>Lateral distance to the Elbe [m]</b>					
Mean (SD)	333 (224)	185 (152)	313 (79.5)	5540 (3920)	780 (1900)
Median [Min, Max]	308 [53.1, 854]	141 [20.1, 606]	282 [220, 421]	5730 [1340, 9360]	276 [20.1, 9360]
Missing	0 (0%)	0 (0%)	0 (0%)	2 (33.3%)	2 (4.5%)
<b>Flooding days [days/year]</b>					
Mean (SD)	30.7 (21.2)	3.64 (2.07)	0.390 (1.03)	0 (0)	13.7 (19.7)
Median [Min, Max]	25.4 [6.02, 86.1]	3.43 [0.142, 8.73]	0 [0, 2.73]	0 [0, 0]	4.42 [0, 86.1]

Appendix B. - Spearman correlation matrix for all mineral topsoil samples (0-10 cm). Only significant correlations are shown ( $p > 0.05$ )

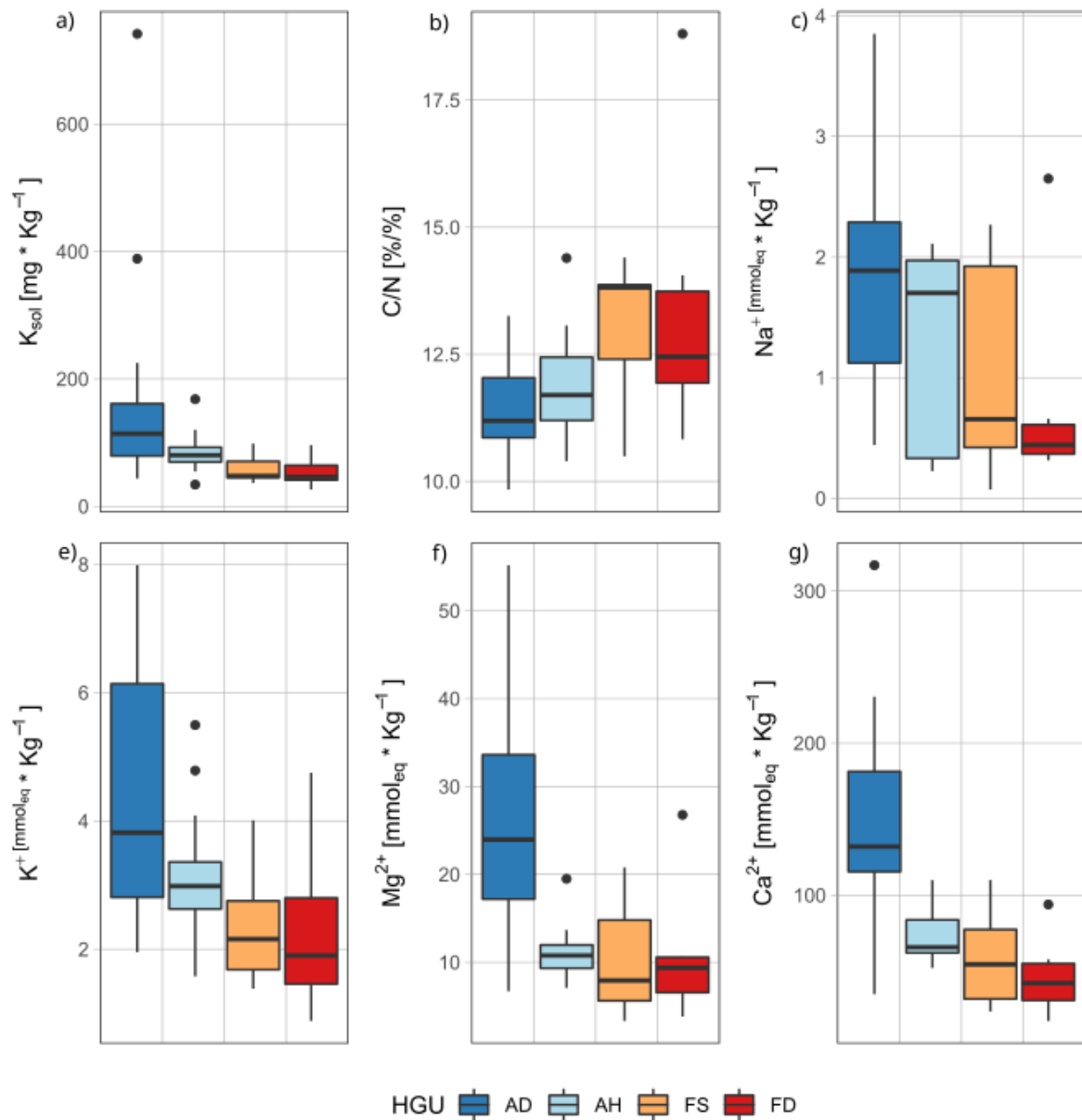




Appendix C Effect of flooding days on (a) depth of hydromorphic characteristics, (b)  $pH$ , (c) clay content, (d)  $C/N$  ratio and (e)  $P_{sol}$ . Spearman correlation coefficient ( $\rho$ ), significance level ( $p$ ), and confidence interval (grey) for simple linear regression are shown.



Appendix D Variability of other physicochemical parameters ( $K_{sol}$ , C/N,  $Na^+$ ,  $K^+$ ,  $Mg^{2+}$  and  $Ca^{2+}$ ) among HGUs. Boxes represent 25–75% of values, black strips medians, whiskers 1.5 interquartile ranges, and black dots outliers. HGU – Hydrogeomorphic Unit: Active floodplain -Low (AL), Active floodplain-High (AH), Former floodplain-seepage influenced (FS), Former floodplain – disconnected from the river hydrology (FD).



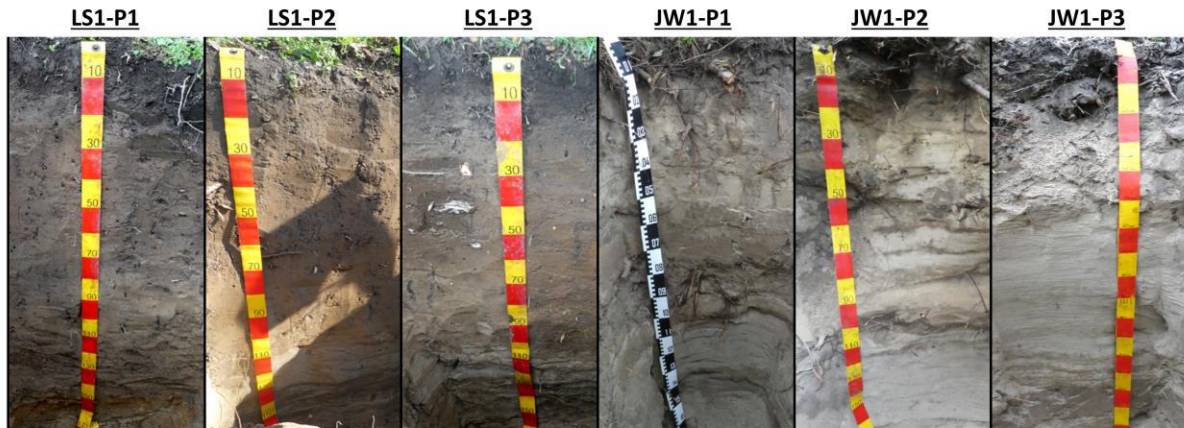
Appendix E. Long/Lat coordinates of the midpoints of every study plot from NW to SE.

	Site Name	Latitude	Longitude
1	AV1	53.3183	10.7082
2	BL1	53.3042	10.7245
3	BW1	53.2818	10.7981
4	NG1	53.2629	10.8196
5	PO1	53.2459	10.8796
6	SU1	53.2728	10.8942
7	JW1	53.1796	11.0087
8	JW2	53.1749	11.0123
9	ST1	53.1439	11.1016
10	SR1	53.2768	11.0189
11	BD1	53.2990	11.6616
12	JB3	53.1595	11.1313
13	JB2	53.1667	11.1394
14	JB1	53.1647	11.1426
15	JB4	53.1651	11.1484
16	WU1	53.1397	11.2241
17	WU2	53.1358	11.23
18	LS1	53.0877	11.2945
19	PA1	53.0615	11.3233
20	HB1	53.0759	11.4503
21	HB2	53.0756	11.4539
22	EH3	53.0582	11.483
23	EH1	53.0569	11.4867
24	LZ1	53.0656	11.4873
25	EH2	53.0531	11.4879
26	LZ2	53.0637	11.4893
27	LZ3	53.0521	11.5148
28	LZ4	53.0558	11.5197
29	GLN	53.0703	11.5212
30	BO1	53.0466	11.5341
31	HG1	53.0304	11.6049
32	HG2	53.0343	11.6143
33	HG4	53.0338	11.6202
34	HG3	53.035	11.6241

35	MD2	53.0081	11.6468
36	MD1	53.0084	11.6522
37	CL1	53.0109	11.6832
38	WB1	52.9816	11.693
39	WB2	52.9834	11.695
40	RS1	52.9129	11.8519
41	RS2	52.9149	11.8521
42	RS3	52.9145	11.8542
43	KA1	52.9838	11.949
44	LE1	52.8866	11.9716

## 5.2 Appendix Article II

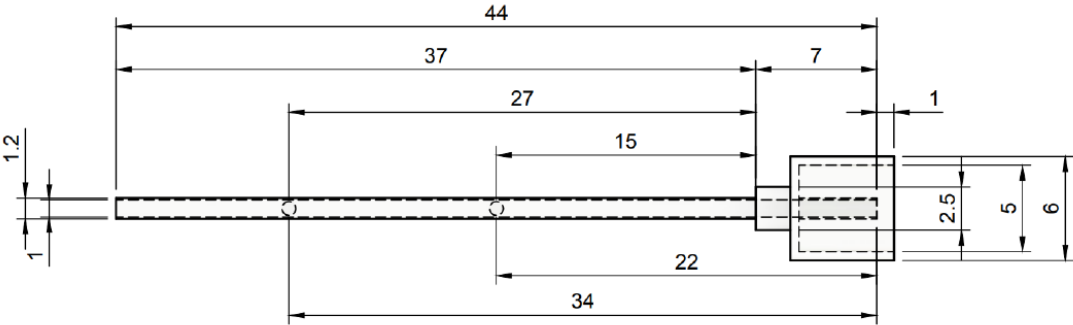
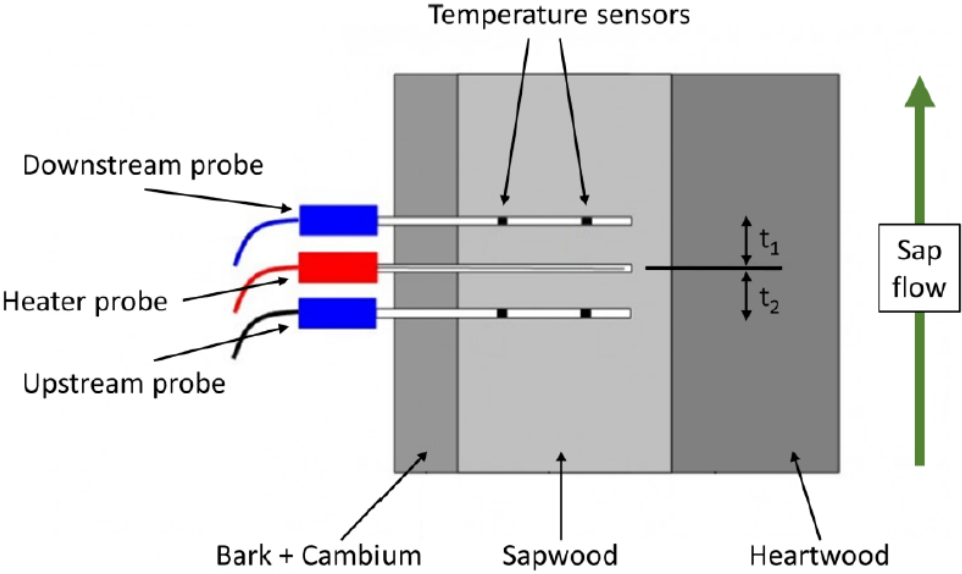
### Appendix A. Soil profiles and grain size distribution LS1 (loamy site), JW1 (Sandy site)J



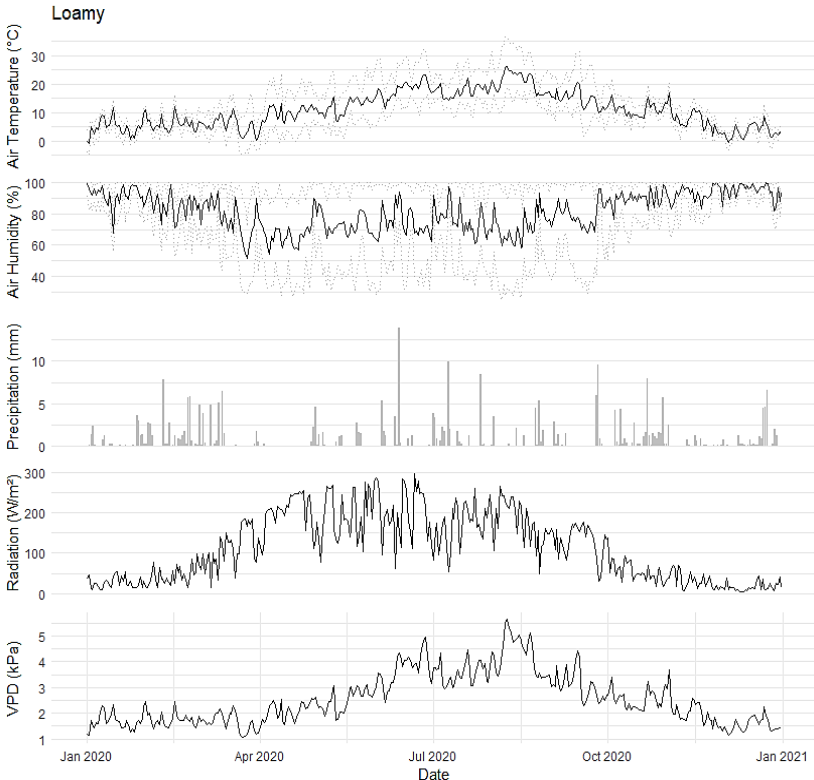
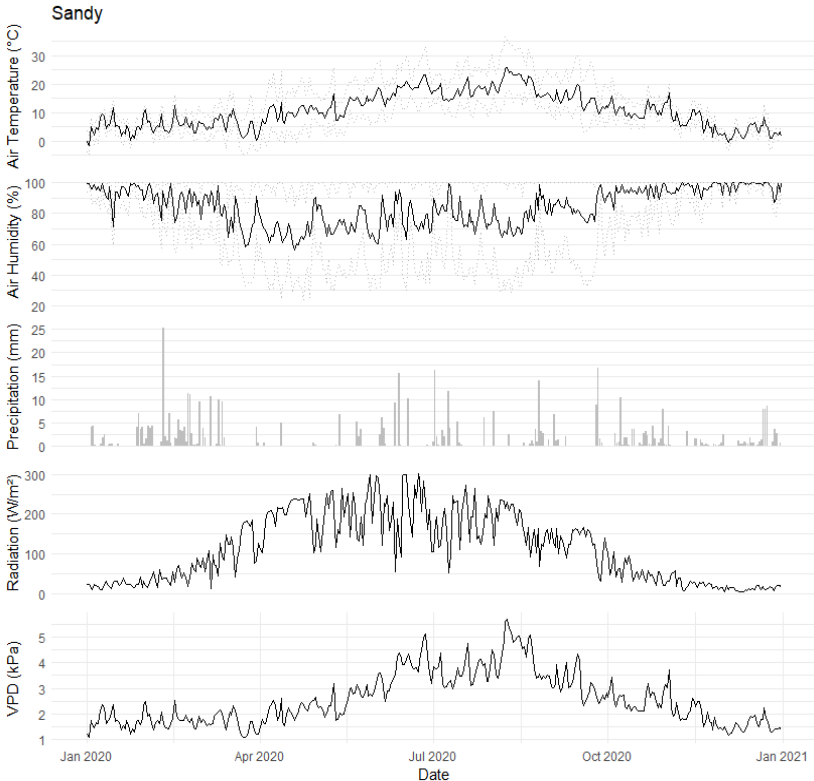
Lenzerwische 1					
Site - Soil profile	Depth (cm)	Soil texture (%)			Soil textural class
		Clay	Silt	Sand	
LS1 - P1	0-18	21.73	27.62	50.65	sandy clay loam
	18-75	20.16	38.09	41.75	loam
	75-108	12.83	26.75	60.42	sandy loam
	108-148	13.66	32.76	53.58	sandy loam
	148-160	0.83	1.61	97.56	sand
	0-160	15.75±6.18	30.50±10.50	53.75±16.03	sandy loam
LS1 - P2	0-15	21.62	18.89	59.48	sandy clay loam
	15-60	16.39	30.32	53.29	sandy loam
	60-108	7.53	11.37	81.09	loamy sand
	108-135	1.92	0.84	97.24	sand
	135-160	9.13	16.46	74.41	sandy loam
	0-160	10.65±6.77	16.43±11.38	72.93±17.52	sandy loam
LS1 - P3	0-15	27.95	31.47	40.58	clay loam
	15-50	19.06	33.75	47.20	loam
	50-75	9.26	18.15	72.60	sandy loam
	75-108	7.64	18.86	73.50	sandy loam
	108-130	5.72	15.11	79.17	loamy sand
	130-160	17.28	49.62	33.10	loam
		0-160	13.84±7.52	28.44±13.46	57.72±19.43

Junkerwerder 1					
Site - Soil profile	Depth (cm)	Soil texture (%)			Soil textural class
		Clay	Silt	Sand	
JW1 - P1	0-10	3.79	3.91	92.30	sand
	10-30	1.70	3.22	95.08	sand
	30-60	2.00	3.77	94.23	sand
	60-100	5.87	9.98	84.15	loamy sand
	100-160	0.12	1.33	98.55	sand
	0-160	2.34±2.54	4.35±3.81	93.32±6.31	sand
JW1 - P2	0-10	3.66	4.25	92.09	sand
	10-30	2.38	2.05	95.58	sand
	30-60	0.72	1.04	98.24	sand
	60-100	0.67	2.18	97.15	sand
	100-160	0.42	0.42	99.15	sand
	0-160	0.99±1.03	1.42±1.17	97.59±2.07	sand
JW1 - P3	0-10	6.09	5.72	88.20	sand
	10-30	3.32	4.82	91.87	sand
	30-60	1.49	1.73	96.78	sand
	60-100	0.52	0.93	98.55	sand
	100-160	2.76	4.73	92.51	sand
	0-160	2.24±1.59	3.29±2.03	94.47±3.52	sand

Appendix B. Installation of sensor set and dimensions of a temperature probe



Appendix C. Daily time series of micrometeorological variables for the a) Sandy site and the b) Loamy site for the year 2020





Appendix D. Daily averaged soil hydrology variables for the Loamy site (Lenzerwische) and the Sandy site (Junkewerder) during the periods of June (high water) and August (low water) at defined soil depths.

Lenzerwische 1 - June 2020									
	Depth (cm)	21. June	22. June	23. June	24. June	25. June	26. June	27. June	Change over the week
$\Psi$ (hPa)	10	-1895.0 ±78.0	-1945.4 ±43.4	-1984.8 ±14.0	-2009.1 ±26.8	-2051.2 ±20.9	-2097.3 ±19.7	-2127.7 ±24.8	-232.7
	30	-1943.3 ±10.5	-1949.6 ±11.6	-1952.8 ±13.4	-1954.6 ±16.0	-1972.0 ±16.1	-1997.1 ±12.0	-2022.9 ±13.3	-79.7
	60	-1423.8 ±457.3	-1450.8 ±431.2	-1479.5 ±406.1	-1505.1 ±382.3	-1534.7 ±356.7	-1571.4 ±331.1	-1613.2 ±305.1	-189.4
	100	-920.6 ±439.5	-946.0 ±429.3	-972.4 ±418.5	-1000.4 ±406.8	-1030.0 ±394.2	-1059.1 ±382.1	-1088.6 ±370.7	-168.0
	160	-301.0 ±201.5	-325.0 ±224.8	-350.0 ±248.8	-371.5 ±269.4	-394.3 ±290.9	-429.8 ±311.6	-465.1 ±328.1	-164.1
Lenzerwische 1 - August 2020									
	Depth (cm)	06. August	07. August	08. August	09. August	10. August	11. August	12. August	Change over the week
$\Psi$ (hPa)	10	-2081.7 ±27.7	-2134.9 ±29.1	-2201.0 ±29.8	-2226.7 ±43.9	-2215.8 ±72.0	-2187.4 ±87.1	-2167.2 ±96.5	-85.6
	30	-2017.2 ±17.7	-2046.5 ±18.3	-2087.0 ±16.5	-2125.9 ±14.4	-2155.1 ±12.7	-2163.3 ±13.4	-2166.0 ±13.3	-148.9
	60	-1966.6 ±12.5	-1975.7 ±12.4	-1992.5 ±12.0	-2014.9 ±10.8	-2037.9 ±9.5	-2056.5 ±8.5	-2067.7 ±8.0	-101.2
	100	-1913.0 ±7.0	-1914.5 ±6.8	-1919.3 ±6.8	-1927.2 ±6.2	-1938.7 ±6.1	-1951.0 ±5.4	-1962.8 ±5.0	-49.9
	160	-876.6 ±498.3	-886.4 ±495.6	-897.2 ±492.3	-909.2 ±488.6	-921.9 ±485.0	-934.1 ±482.5	-946.4 ±480.4	-69.8

Lenzerwische 1 - June 2020									
	Depth (cm)	21. June	22. June	23. June	24. June	25. June	26. June	27. June	Total change over time
Θ (vol.-%)	10	16.83 ±3.12	16.64 ±3.01	16.40 ±2.90	16.20 ±2.79	16.12 ±2.73	16.07 ±2.69	16.01 ±2.65	-0.83
	30	18.02 ±2.45	17.87 ±2.41	17.74 ±2.36	17.58 ±2.31	17.50 ±2.26	17.44 ±2.23	17.42 ±2.22	-0.60
	60	16.25 ±0.50	16.02 ±0.43	15.81 ±0.39	15.62 ±0.38	15.46 ±0.36	15.31 ±0.35	15.19 ±0.33	-1.05
	100	18.82 ±5.05	18.62 ±5.02	18.39 ±4.97	18.17 ±4.92	17.96 ±4.89	17.76 ±4.86	17.55 ±4.81	-1.27
	160	11.34 ±5.13	11.18 ±5.01	11.03 ±4.91	10.88 ±4.78	10.72 ±4.66	10.56 ±4.52	10.37 ±4.37	-0.98
SWS (mm)	0-160	263.71 ±43.26	260.68 ±42.56	257.56 ±41.88	254.52 ±41.19	252.06 ±40.61	249.78 ±39.98	247.60 ±39.34	-16.11
Ψ (hPa)	0-160	-1196.1 ±246.2	-1221.7 ±239.2	-1246.4 ±231.5	-1268.1 ±225.8	-1296.1 ±222.8	-1329.5 ±219.9	-1362.3 ±215.2	-166.2
Lenzerwische 1 - August 2020									
	Depth (cm)	06. August	07. August	08. August	09. August	10. August	11. August	12. August	Total change over time
Θ (vol.-%)	10	18.31 ±3.67	18.26 ±3.66	18.23 ±3.67	18.17 ±3.67	18.06 ±3.67	17.90 ±3.64	17.74 ±3.61	-0.57
	30	19.15 ±2.99	19.16 ±2.98	19.25 ±3.00	19.26 ±2.98	19.28 ±2.94	19.24 ±2.93	19.17 ±2.90	+0.02
	60	14.96 ±0.34	14.91 ±0.32	14.89 ±0.31	14.90 ±0.30	14.90 ±0.29	14.90 ±0.29	14.89 ±0.28	-0.07
	100	15.40 ±4.53	15.35 ±4.52	15.32 ±4.51	15.30 ±4.51	15.28 ±4.53	15.27 ±4.54	15.27 ±4.54	-0.13
	160	8.86 ±3.65	8.78 ±3.60	8.73 ±3.57	8.67 ±3.56	8.62 ±3.52	8.58 ±3.51	8.55 ±3.49	-0.31
SWS (mm)	0-160	240.40 ±34.76	239.71 ±34.80	239.49 ±34.86	239.15 ±34.95	238.73 ±35.01	238.17 ±35.21	237.50 ±35.21	-2.90
Ψ (hPa)	0-160	-1767.7 ±84.2	-1783.3 ±83.4	-1805.1 ±82.8	-1824.0 ±80.8	-1838.2 ±77.0	-1846.1 ±74.9	-1852.5 ±73.5	-84.8

Junkerwerder 1 - June 2020									
	Depth (cm)	21. June	22. June	23. June	24. June	25. June	26. June	27. June	Total change over time
$\Theta$ (vol.-%)	10	7.47 $\pm 0.97$	6.45 $\pm 0.63$	5.57 $\pm 0.53$	4.90 $\pm 0.57$	4.38 $\pm 0.63$	3.94 $\pm 0.66$	3.60 $\pm 0.66$	-3.87
	30	2.50 $\pm 0.46$	2.48 $\pm 0.43$	2.47 $\pm 0.43$	2.45 $\pm 0.41$	2.43 $\pm 0.39$	2.40 $\pm 0.39$	2.37 $\pm 0.38$	-0.13
	60	2.51 $\pm 0.42$	2.50 $\pm 0.42$	2.50 $\pm 0.42$	2.47 $\pm 0.42$	2.44 $\pm 0.44$	2.42 $\pm 0.43$	2.37 $\pm 0.43$	-0.15
	100	8.27 $\pm 5.67$	8.18 $\pm 5.60$	8.05 $\pm 5.53$	7.94 $\pm 5.44$	7.84 $\pm 5.33$	7.72 $\pm 5.23$	7.59 $\pm 5.14$	-0.69
	160	2.17 $\pm 0.82$	2.13 $\pm 0.83$	2.12 $\pm 0.84$	2.11 $\pm 0.85$	2.10 $\pm 0.85$	2.10 $\pm 0.85$	2.10 $\pm 0.85$	-0.07
SWS (mm)	0-160	77.84 $\pm 30.48$	75.13 $\pm 29.34$	72.69 $\pm 28.47$	70.58 $\pm 27.82$	68.86 $\pm 27.07$	67.25 $\pm 26.43$	65.62 $\pm 25.89$	-12.22
$\Psi$ (hPa)	0-160	-321.8 $\pm 33.0$	-340.6 $\pm 31.1$	-359.9 $\pm 25.8$	-379.4 $\pm 21.5$	-411.7 $\pm 15.2$	-447.3 $\pm 12.0$	-487.2 $\pm 12.3$	-165.4
Junkerwerder 1 - August 2020									
	Depth (cm)	06. August	07. August	08. August	09. August	10. August	11. August	12. August	Total change over time
$\Theta$ (vol.-%)	10	2.24 $\pm 0.44$	2.11 $\pm 0.39$	2.04 $\pm 0.34$	1.98 $\pm 0.30$	1.93 $\pm 0.27$	1.86 $\pm 0.25$	1.80 $\pm 0.25$	-0.44
	30	1.87 $\pm 0.24$	1.85 $\pm 0.24$	1.83 $\pm 0.23$	1.79 $\pm 0.24$	1.77 $\pm 0.24$	1.76 $\pm 0.23$	1.74 $\pm 0.23$	-0.12
	60	1.83 $\pm 0.52$	1.83 $\pm 0.52$	1.82 $\pm 0.51$	1.79 $\pm 0.50$	1.77 $\pm 0.52$	1.77 $\pm 0.52$	1.75 $\pm 0.52$	-0.08
	100	5.75 $\pm 3.56$	5.70 $\pm 3.50$	5.65 $\pm 3.46$	5.62 $\pm 3.43$	5.58 $\pm 3.39$	5.56 $\pm 3.36$	5.52 $\pm 3.33$	-0.23
	160	1.93 $\pm 0.83$	1.93 $\pm 0.83$	1.93 $\pm 0.83$	1.92 $\pm 0.84$	1.88 $\pm 0.86$	1.88 $\pm 0.86$	1.87 $\pm 0.87$	-0.07
SWS (mm)	0-160	50.11 $\pm 19.06$	49.55 $\pm 18.65$	49.09 $\pm 18.41$	48.56 $\pm 18.14$	48.04 $\pm 17.85$	47.70 $\pm 17.70$	47.32 $\pm 17.56$	-2.79
$\Psi$ (hPa)	0-160	-932.8 $\pm 196.1$	-961.3 $\pm 207.2$	-989.5 $\pm 217.0$	-1009.8 $\pm 222.3$	-1029.1 $\pm 223.8$	-1047.9 $\pm 226.9$	-1062.5 $\pm 233.1$	-129.7

Junkerwerder 1 - June 2020									
	Depth (cm)	21. June	22. June	23. June	24. June	25. June	26. June	27. June	Change over the week
Ψ (hPa)	10	-101.4 ±23.3	-170.8 ±49.9	-235.0 ±66.7	-292.7 ±91.1	-390.8 ±98.6	-497.7 ±121.3	-640.7 ±168.4	-539.3
	30	-811.6 ±588.8	-813.9 ±587.0	-815.8 ±583.8	-818.8 ±580.9	-828.5 ±584.6	-840.9 ±591.5	-854.5 ±598.8	-42.9
	60	-142.7 ±36.8	-143.3 ±36.7	-145.9 ±38.4	-147.4 ±39.0	-165.5 ±40.7	-185.0 ±42.1	-190.9 ±44.3	-48.2
	100	-411.5 ±185.9	-435.4 ±199.6	-465.9 ±218.1	-499.4 ±238.3	-542.1 ±265.3	-588.2 ±295.4	-639.1 ±328.4	-227.6
	160	-120.2 ±26.9	-131.3 ±37.2	-136.3 ±41.4	-141.7 ±46.3	-148.3 ±52.8	-157.0 ±61.1	-171.3 ±74.7	-51.2
Junkerwerder 1 - August 2020									
	Depth (cm)	06. August	07. August	08. August	09. August	10. August	11. August	12. August	Change over the week
Ψ (hPa)	10	-1360.2 ±364.7	-1373.7 ±359.1	-1378.8 ±351.9	-1399.8 ±347.6	-1443.1 ±356.1	-1501.3 ±370.8	-1531.6 ±363.6	-171.4
	30	-1051.9 ±541.2	-1066.2 ±547.3	-1084.7 ±556.0	-1104.9 ±565.1	-1124.5 ±571.5	-1141.2 ±572.6	-1157.6 ±573.4	-105.7
	60	-425.2 ±152.8	-472.2 ±156.7	-523.1 ±160.1	-559.7 ±181.5	-596.6 ±201.3	-624.1 ±213.4	-650.5 ±225.6	-225.3
	100	-1240.1 ±587.1	-1266.4 ±598.7	-1289.2 ±610.2	-1296.3 ±613.7	-1303.6 ±617.3	-1311.2 ±621.0	-1317.4 ±624.0	-77.4
	160	-628.8 ±474.6	-660.9 ±504.5	-695.3 ±538.5	-718.3 ±561.4	-720.6 ±562.6	-723.6 ±563.0	-726.3 ±564.0	-97.5

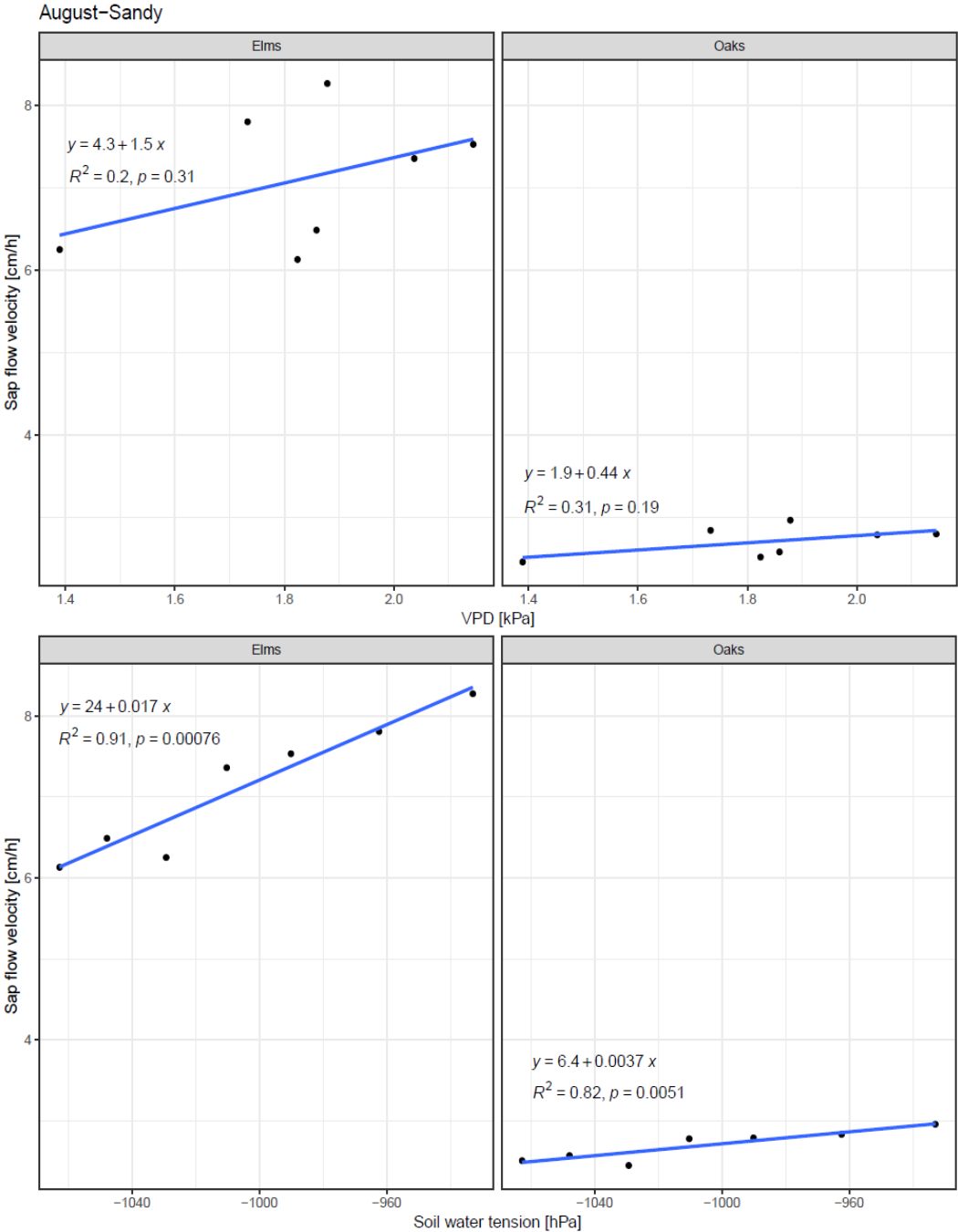
## Appendix E

Linear mixed effect model result:

```
modsap <- lme4(meansap~ Species*Site*Month + (1|PosID) +(1|Date), data=groupind1)
```

	Df	Sum Sq	Mean Sq	F value	Pr(>F)	
Site	1	717.7	717.7	222.499	< 2e-16	***
Species	1	1739.9	1739.9	539.438	< 2e-16	***
Month	1	31.5	31.5	9.754	0.00193	**
Site:Species	1	12.2	12.2	3.786	0.05244	.
Site:Month	1	21.2	21.2	6.578	0.01072	*
Species:Month	1	86.4	86.4	26.775	3.76E-07	***
Site:Species:Month	1	12.1	12.1	3.758	0.05332	.
Residuals	370	1193.4	3.2			
Signif. codes: 0 '***' 0.001 '**' 0.01 '*' 0.05 '.' 0.1 ' ' 1						

Appendix F Linear regressions between abiotic factors (VPD upper row and  $\Psi$  lower row ) and sap flow velocity of oaks and elms in the sandy site during a week in August.



## Acknowledgements

This journey has taken not only some time (5 years and 2 months), but also a lot of support from many people without whom reaching this day would have not been possible. The list is long.

Thank you Annette, for giving me the opportunity to be part of your working group. Thanks for supporting my whole journey from Ecuador and helping me settle in Hamburg. Thanks for always having an open door to discuss scientific topics, without forgetting that there is more to life than that. Thanks for your supervision during this 5 years and for always knowing that I will make it, even when I doubted it. Thanks for your patience, for caring at a personal level and for making possible that I continue this scientific journey until the closure of the MediAN project in the IfB, I am happy to be part of it.

Thank you Kai for your co-supervision and for the discussions we had during the panel meetings and MediAN project meetings. Your input was always appreciated. Thanks Alex G. for the support and for sharing with me all your knowledge about the Elbe floodplains.

Thank you Volker, not only for all the support I got from you in the fieldwork phase and for how amazing was to learn from you about sensors, tools, plants and the Elbe, but for being my friend and for being always there for me. I value deeply our friendship.

Thank you Joscha for all the support. I will never forget the first two-hour meeting I had with you, I explained how confused I was, and then you, with a couple of graphs in the whiteboard cleared my mind and somehow the first paper was there. Literally, you made me believe that this was possible. Thanks for your friendship, for the rum to celebrate small and big steps and for always showing your passion for science.

Thank you Simon and Henrik for the support and nice work together in the sap flow project. It was great to count with your expertise and enthusiasm, Simon, and to count on you Henrik by supervising your Master Thesis (You did a great job!).

Thanks Adrian, Kiri and Mathi for being the best büro-gang and brunch team, for being amazing friends, for almost being the dream-traveling team for the trip to Ecuador that didn't happen, but some day will. It was always and still is (Kiri) a pleasure to share the office with you. Thanks for being there for me and share the good and bad times.

Thanks Alex S. for being such a nice office neighbor and friend. Thanks for all the nice and long talks about life, soil hydrology, trees, and thanks for the parties and good times. Thanks Lutz and Leo for the friendship, the coffee and the long existential conversations about PhD life.

Thank you Rike, Elisa, Johanna, Maria, I could not ask for better working group friends. Thank you especially for all the good energy and support through these last days. I look forward to keep working with you, and having fun in and out of the Uni.

Thanks to all the MediAN project team, it has being fun to work with people that are genuinely interested in the conservation of floodplains and floodplain forests. It was always great to meet you and get motivation, inspiration and knowledge from all of you. Thanks particularly to Heather A. Shupe, Anastasia Leonova, Timo Hartmann, Kristin Ludewig.

Thanks Deborah for your support organizing and performing laboratory analyses. Thanks Lewis Sauerland, Christina Moor, Tiffanie Sarino, Jessica Hamm, Janis Grozinger, Peter Klink, Simone Koller and all other HiWis for your support in the field as well as in the lab.

Gracias Chepito, Rommelpat, Marieli, Ale for our long friendship and for always being there despite the distance. I look forward to have more time to catch up and visit you. Les quiero!

Gracias a mi hermosa familia por su amor, por siempre estar pendientes y por aceptar esta lejanía que sé cuanto cuesta. Les amo Kari, Alex, Pancho, Cachito, Cachita, Tío Cacho. Ahora sí a celebrar!

Finally, you Jogi, THANKS my Love! I did it! I cannot imagine another person that will share with me the same amount of happiness by ending this process, as you will. Let's see what life has for us outside the PhD era. I'm looking forward.

This study was funded by the German Federal Ministry of Education and Research (BMBF) as an initiative for the Research for Sustainable Development (FONA) (FKZ: 01LC1601A), and the German Research Foundation (DFG) under Germany's Excellence Strategy – EXC 2037 'CLICCS - Climate, Climatic Change, and Society' – Project Number: 390683824.